



3

This is to certify that the

dissertation entitled

AN EXPERIMENTAL STUDY OF INCOMPRESSIBLE CHANNEL ENTRANCE FLOW

presented by

Jack Wayne Backus

has been accepted towards fulfillment of the requirements for

Ph. D. degree in Engineering

Major professor

Date August 2, 1993

LIBRARY Michigan State University

PLACE IN RETURN BOX to remove this checkout from your record. TO AVOID FINES return on or before date due.

DATE DUE	DATE DUE	DATE DUE

MSU Is An Affirmative Action/Equal Opportunity Institution c:\circ\detedue.pm3-p.1

AN EXPERIMENTAL STUDY OF INCOMPRESSIBLE CHANNEL ENTRANCE FLOW

Ву

Jack Wayne Backus

A DISSERTATION

Submitted to
Michigan State University
in partial fulfillment of the requirement
for the degree of

DOCTOR OF PHILOSOPHY

Department of Mechanical Engineering

1991

en:

en

are

flo

inc

The

con str

ABSTRACT

AN EXPERIMENTAL STUDY OF INCOMPRESSIBLE CHANNEL ENTRANCE FLOW

Ву

Jack Wayne Backus

An understanding of the entrance flow in a rectangular channel is of significant importance for the design of flow inlets in numerous devices as well as the fundamental understanding of the fluid flow itself. Before an established flow occurs in a channel it must have originated from an entrance. This study focuses on the incompressible flow of air in the entrance region of a rectangular channel. Both turbulent and laminar flows are investigated. In addition, the transition from laminar to turbulent flow is studied.

The study was carried out in a sixteen foot long, three foot wide, and 3/4 inch high channel. The settling chamber upstream of the two-dimensional contraction contained a one inch thick hogs hair filter, a section of straws, followed by four screens. Pressure measurements were made with a

1

c 1 d

10

Decker differential pressure transducer, and Thermo Systems hot-wire anomometers with specially designed probes, were used for velocity measurements.

The turbulent flow entrance region was found to include an inviscid core length, a transition length and an established turbulence length. At the low Reynolds numbers (below 18,000) of this study, turbulence was found to initiate somewhat downstream of the channel inlet. For Reynolds numbers below 12,000 turbulence initiates downstream of the inviscid core region. For a Reynolds number of about 16,000 the pressure gradient is constant throughout the entrance region and is equal to that of the developed flow. For Reynolds numbers less than 16,000 the pressure in the entrance region is less than that of the extrapolated developed flow.

The laminar flow entrance region was found to be composed of an inviscid core region followed by a profile development region. The inviscid core length was found to be equal to about 50 channel heights; the profile development length, which was 15 channel heights at a Reynolds number of 1000, linearly increased to 180 channel heights at a Reynolds number of 6000.

t F

Ro

ACKNOWLEDGEMENTS

The author wishes to thank Dr. M. C. Potter for his assistance throughout the course of this study. Thanks are also due to Dr. R. E. Falco, Dr. M. C. Smith, and Dr. C. Y. Wang for serving as members of the guidance committee.

A special note of thanks is extended to Mr. Brian Agar, Mr. Robert Rose and Mr. Anthony Skeltis for their special assistance in completing this study.

TABLE OF CONTENTS

			Page
1.	EXPE	RIMENTAL FACILITY AND INSTRUMENTATION	. 1
	1.1	Flow System	
	1.2	Instrumentation - Commercially Available	. 2
	1.3	Instrumentation - Custom Equipment	. 3
2.	TURB	ULENT ENTRANCE FLOW	. 5
	2.1	Introduction	. 5
	2.2	Background	. 5
	2.3	Characteristics of Flow	. 11
	2.4	Experimental Facility and Instrumentation	. 14
	2.5	Preliminary Measurements	. 16
	2.6	Results	. 16
	2.7	Conclusions	. 19
	2.8	Recommendations for Further Research	. 21
3.	LAMI	NAR ENTRANCE FLOW	. 23
	3.1	Introduction	. 23
	3.2	Background	. 24
	3.3	Experimental Facility and Instrumentation	. 30
	3.4	Velocity Development	. 31
	3.5	Entrance Region	. 32
	3.6	Pressure Development	. 34
	3.7	Conclusions	. 37

BI

4.	BURS	TING AND BOUNDARY LAYER GROWTH
	4.1	Introduction
	4.2	Background
	4.3	Experimental Facility and Instrumentation
	4.4	Transition Process Characteristics
	4.5	Results
	4.6	Sidewall Boundary Layer
	4.7	Conclusions
BIB	LIOGR	APHY 48

LIST OF FIGURES

- Figure 1. Experimental Channel Facility Top View
- Figure 2. Experimental Channel Facility Side View
- Figure 3. Flow System Floor Plan
- Figure 4. Details of Contraction
- Figure 5. Channel Gapping Instrument
- Figure 6. Channel Gapping Instrument Electrical Schematic
- Figure 7. Experimental Equipment System
- Figure 8. Sidewall Layer Hot-Wire Probe
- Figure 9. Specially Designed Probe
- Figure 10. Hot-Wire Traversing Rig
- Figure 11. Motorized Hot-Wire Probe
- Figure 12. Definition of Turbulent Entrance Lengths
- Figure 13. Variation in Pressure with Changes in Reynolds Number
- Figure 14. Motorized Probe Induced Flow Effects
- Figure 15. Turbulence Initiation Length, L_{t} , vs. Re
- Figure 16. Inviscid Core Length, L, vs. Re
- Figure 17. Established Turbulence Length, L_{st} , vs. Re
- Figure 18. Profile Development Length vs. Re Turbulent Flow
- Figure 19. The distance, L_p , at which the Pressure Gradient attains its fully developed value vs. Re
- Figure 20. Entrance Length, L_{e} , vs. Re
- Figure 21. Schematic of Inviscid Core Region Re = 16000

- Figure 22. Inviscid Core Centerline Streamwise Intensity Variation Re 16000
- Figure 23. Ratio of Entrance Region Wall Shear Stress to Fully Developed

 Region Wall Shear Stress Re = 16000
- Figure 24. Streamwise Velocity Profile Development Re 16000
- Figure 25. Streamwise Pressure Distribution for Re 4000
- Figure 26. Streamwise Pressure Distribution for Re = 6000
- Figure 27. Streamwise Pressure Distribution for Re 8000
- Figure 28. Streamwise Pressure Distribution for Re 10,000
- Figure 29. Streamwise Pressure Distribution for Re 12,000
- Figure 30. Streamwise Pressure Distribution for Re = 14,000
- Figure 31. Streamwise Pressure Distribution for Re = 16,000
- Figure 32. Streamwise Pressure Distribution for Re = 18,000
- Figure 33. Streamwise Pressure Distribution Low Re, Medium Re, High Re.

 All Re nondimensionalized by U for Re = 18,500
- Figure 33. Experimental Channel 3-D View
- Figure 34. Laminar Flow Entrance Region
- Figure 35. Velocity Profile Development
- Figure 36. Velocity Profile Development
- Figure 37. Spanwise Velocity Profile
- Figure 38. Inviscid Core Length vs. Re
- Figure 39. Profile Development Length vs. Re
- Figure 40. Laminar Entrance Length vs. Re
- Figure 41. Streamwise Pressure Distribution for Re = 5000
- Figure 42. Percent Intensity vs. Critical Reynolds Number Laminar Flow

- Figure 43. Spanwise Intensity Variation
- Figure 44. Spanwise Variation of Bursting
- Figure 45. Possible Burst Model
- Figure 46. Channel Spanwise Velocity Profile for Re = 4000, x/h = 262.4
- Figure 47. Sidewall Boundary Layer Velocity Profile for Re 1000, x/h 252.0
- Figure 48. Sidewall Boundary Layer Velocity Profile for Re 5250, x/h 252
- Figure 49. Sidewall Boundary Layer Velocity Profile for Re 8500, x/h 252.0
- Figure 50. Sidewall Boundary Layer Thickness vs. Re

LIST OF TABLES

		Page
Table 1	Entrance Length Comparisons	. 33

f Н

I

L L L

L_s

N

P

Δp Re t

U

บ น'

NOMENCLATURE

dp/dx Pressure gradient E(t) Instantaneous voltage f Friction factor Н Channel gap separation Ι Free-stream fluctuation intensity L Channel length Entrance length Li Inviscid core length Constant pressure gradient length Lpd Profile development length Lst Established turbulent length Lt Transition length N Coordinate perpendicular to channel side wall Static pressure Р Δр Pressure Drop $Re - UH/\nu$ Reynolds number t Time U Average velocity at x/H = 0U_{c1} Centerline velocity u' Velocity perturbation in x-direction Time average velocity in x-direction u_b laminar flow velocity in x-direction u_b Bulk velocity $u_\tau = \sqrt{\frac{\tau_w}{\rho}}$ Friction velocity x, y, z Streamwise, transverse, spanwise coordinates W Channel width β Frequency δ Sidewall boundary layer thickness λ Dimensional wave length

Kinematic viscosity

φ Amplitude function

Y Stream function

ρ Density

τ Wall shear stress

CHAPTER 1

EXPERIMENTAL FACILITY AND INSTRUMENTATION

1.1 Flow System

All of the experiments in this study were performed in a rectangular, parallel-sided channel. The entire channel assembly, as shown in Figures 1 and 2, consisted of an entrance, settling chamber, plenum, contraction and parallel plate test section. This facility occupied two separate rooms in the laboratory as shown in Figure 3. A sealed locking door provided access between the two rooms. This arrangement was used because it eliminated the detrimental effects of:

- 1) leakage into the test section with the fan located downstream.
- 2) fan noise induced flow instabilities with the fan located upstream.

In effect, this setup provided a pressurized test section with a fan located downstream. The facility was shock mounted with felt strips where it pierced the wall dividing the two rooms and where it rested on the laboratory floor to isolate it from building vibration.

The entrance and settling chamber consisted of a smooth twodimensional inlet, one inch thick hogs hair filter, honeycomb section filled with 7.5 inch long, 0.25 inch diameter plastic straws and four stainless steel screens. The screens were eight inches apart with mesh sizes of 18, 44, 60, 80, respectively, and had open areas of 59.5%, 57.8%, 57.4% and 49.6%, respectively.

The plenum was 48 inches long and constructed of plywood. It had a locking resealable door on one side for access to the upstream end of the test section. The two-dimensional contraction began at the downstream end of the plenum. It was constructed of styrofoam blocks, clear acrylic plastic sheets and plywood. The styrofoam blocks were cut to fit a beam deflection curve shape shown in Figure 4 and covered with linoleum.

The experimental test section top consisted of two 4 feet wide by 8 feet by 0.75 inch long clear acrylic plastic sheets. The bottom of the test section consisted of two 4 feet wide by 8 feet long 0.25 inch thick polished aluminum plates covered with a single sheet of linoleum, spray painted flat black and wet sanded smooth. The four sidewall sections were clear acrylic plastic strips 0.75 inch by 0.75 inch by 96 inches long. Nine supporting members consisting of aluminum bars 1 inch by 1 inch by 48 inches were fastened at intervals of 23 inches across the width of the top plate. They insured that the top and bottom plates were kept at a uniform distance apart. The top plate could be displaced up and down by adjusting the bolts in these supports. The gap between the upper and lower plates was adjusted to 0.75 inch ± 0.005 inch utilizing a specially designed strain gauge gapping instrument shown in Figures 5 and 6.

1.2 Instrumentation - Commercially Available

The following commercial instruments were utilized. Together with the subsequently described custom equipment they formed the data acquisition system used in this study. A schematic is shown in Figure 7.

- Pressure measurements including hot-wire calibration were taken with the following instruments:
 - a) Decker Delta 308 differential pressure instrument with a 0.3 to 3.0 inch H₂0 transducer.
 - b) Validyne CD15 pressure measuring instrument with a 53790 transducer.
- 2) Velocity measurements were taken with three Thermo System Incorporated 1054B constant temperature hot-wire anemometers having built-in linearizers.
- 3) Signal conditioning was accomplished by a Thermo Systems
 Incorporated 1057 high/low pass filter unit.
- 4) Time mean pressure and velocity were obtained using a Thermo

 Systems Incorporated 1047 Averaging Circuit module.
- 5) Intensity measurements were made using R.M.S. and mean square output of a D15A55D35 True R.M.S. voltmeter.
- 6) Output display of time mean pressure and hot-wire outputs were available on three Keithley 169 voltmeters.
- 7) Visual and hard copy display were done using:
 - a) Tetronix 564B fast writing storgage oscilloscope coupled with a Tektronix C-40 camera.
 - b) Hewlett Packard X-Y plotter.

1.

ga: di: sho

wit

z(s

tra

me o

cha

1.3 Instrumentation - Custom Equipment

Measurements of the time/mean and R.M.S. velocity profiles were gathered using the hot-wire anemometry system described herein. Three different probes were specially designed for this purpose. These probes are shown in Figures 8 and 9. Two of these probes were used in conjunction with the traversing rig shown in Figure 10 to traverse the flow in the z(spanwise) direction. The third probe, shown in Figure 11, was a motorized probe utilizing a radio control positioning system. This probe was used to traverse the flow in the y (vertical) direction. A special slide pin mechanism in conjunction with a miniature gear and commercially available radio control system allowed the probe to be accurately stepped across the channel gap in thirteen discrete one mm increments.

CHAPTER 2

TURBULENT ENTRANCE FLOW

2.1 Introduction

The study of turbulent entrance flows is important to many engineering applications, including the designs of wind and water tunnels, as well as piping and duct systems. Turbulent inlet flow is characterized by an initial inviscid core region that changes to a profile-development region followed by fully developed flow downstream. The location of a transition region in which turbulence is initiated is dependent on the Reynolds number. Although researchers have developed relations for laminar entrance flows that satisfactorily predict experimental findings, similar success has not been achieved for turbulent flow. It is useful to review the findings of previous researchers.

2.2 Background

Ross and Whippany (1956) provide an analysis of turbulent flow within the first ten pipe diameters length of a pipe. To insure that the transition to turbulent boundary layer occurs as close to the inlet as possible Reynolds numbers are greater than 10^5 . To analyze the flow, the displacement thickness and momentum thickness are used to express the continuity, momentum and energy equations for pipe flow. By assuming that the boundary layer is turbulent, these equations are combined to get

expressions for the growth of the boundary layer, the pressure gradient and energy gradient. To investigate the resulting expressions, the wall shear stress and shape parameter are defined in terms of published data for flat plates and pipes. To confirm the analysis, measurements from model studies in two large water tunnels are used. Calculations for pressure drop agree with the results of experiments for Reynolds numbers in the range of Re = 0.5×10^6 to Re = 3.0×10^6 . At higher Reynolds numbers (Re = 1.0×10^7 to Re = 3.0×10^7) the pressure drop predicted is about 10% below measured values. The authors attribute the discrepancy to the test section design. Results for momentum thickness based on velocity data agree closely with predicted values. Moreover, calculated values for momentum thickness also agree with experiment. In general, the analysis provided is in agreement with experimental findings.

An investigation by Barbin and Jones (1963) is one of the first attempts to describe developing turbulent flow in the entrance region of a pipe. For this study, flow in the inlet is considered to be a transition from boundary layer to fully developed turbulent flow. Moreover, the velocity distribution at the inlet is considered uniform and the boundary layer is very thin. Therefore, the wall shear stress and velocity gradient are large at the entrance. As the boundary layer grows downstream, these values decrease to their values for fully developed flow. After the flow is completely turbulent, the velocity distribution adjusts to a relatively flat profile, characteristic of fully developed flow, due to transverse mixing. The experiments for this study were conducted in a 29-foot long, 8-inch diameter aluminum pipe. Air was the fluid used. Flow straighteners

upstream of the contraction into the test section were used to prevent fluid swirl. Transition to a turbulent boundary layer was promoted with a 1-inch wide strip of sparsely distributed sand grains near the pipe entrance. A splitter of masking tape was added to the hot wire probe to eliminate vortex shedding behind the probes. All the experiments were conducted at Re -388,000 (based on pipe diameter and mean velocity). From the plots of velocity profiles at various distances along the pipe it can be seen that the initially large wall velocity gradients at the pipe inlet decrease as expected. However, fully developed turbulent flow was not attained because the velocity profiles, turbulent intensities and Reynolds stresses were still changing at the end of the test section. The wall shear stress initiated above its fully developed value and decreased to its fully developed value in 15 pipe diameters. A plot of longitudinal velocity fluctuations indicate that turbulent intensities become constant after 25 pipe diameters. Overall, this study provides a good basis for further research.

Bowlus and Brighton (1968) provide an investigation of turbulent flow in the entrance region of a pipe by numerically solving the integral momentum and continuity equations. They use the work of Barbin and Jones as a basis for their study. The unknown quantities in the momentum and continuity equations are the core velocity, boundary-layer thickness, wall shear and static pressure. The one seventh power law model was chosen for the velocity distribution in the boundary layer. This assumption, non-dimensionalization of the equations and the Schultz-Grunow relation for flat plate turbulent skin friction are used to solve the equations for the length

at which the potential core disappears and the length at which the wall shear stress becomes equal to its fully developed value. The results of this analysis are compared with the data of Barbin and Jones; however, insufficient data are available to draw any conclusions about the validity of their analysis.

Salami (1986) begins with a review of previous research in the area of turbulent developing pipe flow. He contends that there are six regimes of flow. These regimes are: 1) a laminar developing boundary-layer flow, 2) transition from laminar to turbulent-boundary layer flow, 3) developing turbulent-boundary layer flow similar to flow over a flat plate, 4) transition from flat-plate flow to pipe flow, 5) free mixing after the inviscid core disappears, 6) fully developed flow. Experiments were conducted in a 50.8-millimeter diameter pipe with water as the fluid. Based on the data from the experiments, mathematical models for regimes 3, 4 and 5 were developed. These models employ a power-law representation of the velocity profile, and the definition of displacement thickness and momentum thickness to predict when the inviscid core disappears. The assumption of a power-law representation for the velocity profile is supported by experimental results. Predictions of when the inviscid core disappears also agree well with the data. In general, this paper provides a good basis for further research.

Klein (1981) uses the blockage factor as the measure of flow development. The blockage factor can be defined in two ways. One definition states that the blockage factor is the ratio of the axisymmetric displacement thickness to the pipe radius. An alternative definition gives

the blockage factor as the ratio of the centerline velocity to the spatial mean velocity. From plots of blockage factor versus distance along the pipe, using the data of previous researchers, it can be seen that the maximum values for the blockage factor occur at 40 pipe diameters.

Moreover, plots of the same data employing both definitions of blockage factor lead to different curves. Klein states that these discrepencies may occur because truly symmetric pipe flow does not exist. Further analysis of past research led the author to conclude that flow development is largely dependent on inlet conditions. Klein states that turbulent energy is dissipated axially in natural flow. However, trip rings result in a greater amount of radial momentum which results in slower turbulent development. From his analysis, Klein concludes that inlet effects are not fully understood and that profile development is dependent on upstream conditions. Moreover, he states that the distance required to obtain fully developed turbulent flow may exceed 140 pipe diameters.

Wang and Tullis (1974) discuss the characteristics of turbulent flow in the entry region of a rough pipe. Before beginning their analysis, a review of past studies of turbulent entrance flow in a smooth pipe is provided. Five independent equations are used to provide a mathematical model of flow in the entry region. The equations required are developed by:

1) employing a logrithmic model for the velocity distribution in the boundary layer, 2) assuming potential flow outside of the boundary layer,

3) using data from experiments to express the wall shear stress, 4) applying the momentum and continuity equations. These equations are solved numerically to provide the model required. The test section was 200 feet

long and 12 inches in diameter. Two commercial steel pipes of different roughness were used. Water was the fluid used and Reynolds numbers ranged from Re = 7.0×10^5 to Re = 3.7×10^6 . From the velocity distribution plots it is shown that the logrithmic equation for the velocity distribution agrees with the data for most of the boundary layer and its applicability improves as the distance along the pipe increases. Fully developed flow was not attained in 49.5 pipe diameters. Predicted and experimental results for boundary-layer thickness, core velocity and pressure coefficient agree very well within the first 12 diameters of the test section. Beyond the first 12 pipe diameters, it is stated that the analysis breaks down due to small errors in measurement of the displacement thickness and the invalidity of the assumption of a potential core beyond that point. The wall shear thickness reduces to its fully developed value in 15 pipe diameters of length. The potential core disappeared at approximately 30 pipe diameters. In general, the mathematical model presented is supported by experimental results near the pipe entrance.

Cebeci and Keller (1974) present a method for solving the boundary-layer equations in duct flows for laminar and turbulent flows. The boundary-layer equations are the continuity and momentum equations, where the shear stress term in the momentum equation for turbulent flow has been replaced with an eddy-viscosity term and a flow index, k, which is unity for axisymmetric flow and zero for two dimensional flow. These equations are transformed into a dimensionless form using a Mangler transformation. After the equations are dimensionless, a stream function is introduced and a Faulkner transformation is executed. If there is a pressure change, the

rest

fin

cal ent

als

con

reg equ

est

tur

to the

dei

ana

edo Vi

Sto

sho

ap

5

resulting set of equations requires the use of the conservation of mass equation, transformed as the continuity and momentum equations were. The final set of equations is then solved by Newton's method. Comparisons of calculated and experimental values for turbulent velocity profiles in the entrance region of a pipe show good agreement. Moreover, good agreement is also found for pressure drop and centerline velocity for laminar flow conditions.

Shcherbinin and Shklyar (1980) investigate the hydrodynamic entrance region of turbulent flow in a plane channel by solving the Navier-Stokes equations with various turbulence models. A uniform entrance flow and established flow at the exit are assumed. Moreover, it is also assumed that the boundary layer is turbulent at the channel entrance. The first turbulence model uses the mixing length and longitudinal velocity gradient to solve the Navier-Stokes equations. For this approach it is assumed that the boundary layer develops the same way as in flow over a flat plate. Two definitions of mixing length are used and the resulting equations are analyzed by numerical methods. The second turbulence model incorporates the eddy viscosity in the kinetic energy and its dissipation. The turbulent viscosity based on this model is solved simultaneously with the Navier-Stokes equations. Although calculations are easier when employing the mixing length model, comparisons of calculated and predicted velocity fields show that the eddy-viscosity model provides better agreement.

Even though a great deal of research has been conducted, there appears to be little data at low-to-intermediate Reynolds numbers (4000 \leq Re \leq 18,000) for entrance flows. Moreover, data over the entire inlet region

to determine the entrance length for fully developed turbulent flow is lacking. Therefore, the purpose of this study is to investigate turbulent entrance flows for low-to-intermediate Reynolds numbers in a smooth channel, with attention given to the entire inlet region.

2.3 Characteristics of Flow

Simplified models of turbulent entrance flows depict the flow as a growing turbulent boundary layer that eventually fills the entire channel. Often, the entrance length is defined as the distance for the inviscid core to disappear and the flow is considered fully developed beyond that point. However, the flow changes considerably beyond the disappearance of the inviscid core before reaching its fully developed velocity profile. Moreover, this simplified model does not accommodate turbulent inlet flows in which turbulent bursting does not initiate at the channel entrance. Therefore, to accurately describe flow in the entire entrance region, a more complex model is required.

To provide a more comprehensive description of developing flow, several lengths have been defined and are shown in Figure 12. The distance from the channel entrance to the location where turbulent bursting begins is called the turbulence initiation length, $L_{\rm t}$. The turbulence initiation length is dependent on the Reynolds number and may occur near the channel entrance for high Reynolds numbers (Re $> 10^5$). As noted earlier, the inviscid core length, $L_{\rm i}$, is the distance from the entrance to the location where the inviscid core disappears and the boundary layer fills the pipe.

Th

tul

its

ent dev

the

pro

str

Thi

ful

the

has Prof

deve

stud entr

large Howev

The distance at which the entire flow is turbulent is the established turbulence length, $L_{\rm st}$. The point at which the pressure gradient achieves its fully developed value is denoted $L_{\rm p}$. The distance from the pipe entrance to the location where the velocity profile attains its fully developed shape is the entrance length, $L_{\rm e}$. Finally, the distance between the end of the inviscid core length and the entrance length is termed the profile development length, $L_{\rm pd}$. It may be possible that the turbulent structure has not been completely established at $L_{\rm e}$, as has been suggested. This study did not address that point.

As previously noted, the choice of a velocity profile to represent fully developed turbulent flow varies between researchers. For this study, the one seventh power law velocity profile

$$\frac{\mathbf{u}}{\mathbf{U}_{\max}} - \left(\frac{\mathbf{y}}{\mathbf{h}}\right)^{1/7} \tag{1}$$

has been selected. This equation provides a good estimate for the velocity profile over most of the channel cross section.

In addition to studying the development of the velocity profile, the development of the pressure gradient is also of interest. In earlier studies at higher Reynolds numbers, where turbulent bursts initiate near the entrance of the channel, the pressure gradient decreased from a relatively large gradient near the entrance to its fully developed value downstream. However, for lower Reynolds number flows the pressure gradient should behave

diff

rela

stre

flow. burst

The w

region

develo

increa

profil

flow.

greate

depict: Variou:

2.4 Ex

Paralle

differently. For steady developed flow, the pressure gradient is directly related to the wall shear stress, $\tau_{\rm w}$ by $\frac{{
m d} \bar {
m p}}{{
m d} {
m x}} = \frac{2}{r_{\rm o}} \bar {
m r}_{\rm w}$. Furthermore, wall shear stress relates to the velocity profile near the wall by

$$\bar{\tau}_{W} - \mu \left| \frac{\partial \bar{u}}{\partial y} \right|_{W} \tag{2}$$

The wall velocity gradient for laminar flow is less than that of turbulent flow. For low Reynolds numbers, the flow is initially laminar and turbulent bursts begins downstream of the channel entrance in the profile-development region. Consequently, the pressure gradient at the inlet may be less than the gradient for fully developed turbulent flow and increase to its fully developed value relatively far downstream. As the Reynolds number is increased, the pressure gradient approaches its fully developed value nearer the inlet. Surprisingly, for some intermediate Re, the pressure gradient profile approximates its fully developed value throughout the entire inlet flow. For high Reynolds numbers, the pressure gradient will initially be greater than its fully developed value, as noted previously. Figure 13 depicts the expected changes in pressure gradient corresponding to the various Reynolds numbers.

2.4 Experimental Facility and Instrumentation

The experiments for this study were conducted in a rectangular, parallel sided channel. The channel assembly (shown in Figure 1) consisted

of an plate reduce channe sealed prever downst

The ple

one-in

0.25 i

test se

feet lo

consist

instrum differe

Velocit

constan

conditio

of an entrance, a settling chamber, a plenum, a contraction and a parallel plate test section. A fan was located downstream of the test section to reduce any flow instabilities associated with an upstream fan location. The channel occupied two rooms so that the entrance could be in a separate room sealed from the test section. This allowed a pressurized test section that prevented leakage into the test section as results in a test section with a downstream fan location for a single room arrangement. The entire assembly was shock mounted to isolate it from building vibrations.

The entrance and settling chamber consisted of a smooth inlet; a one-inch hog-hair filter; a honeycomb section filled with 7.5 inch long, 0.25 inch diameter plastic straws; and four stainless steel screens 8 inches apart with screen meshes of 59.5%, 57.8%, 57.4% and 49.6%, respectively. The plenum was 48 inches long and made of plywood. The two dimensional contraction was formed from a styrofoam block (cut to the dimensions in Figure 4) and covered with linoleum. The experimental test section was 16 feet long by 4 feet wide, with a 0.75 ± 0.005 inch wide gap. The top of the test section was constructed of acrylic sheets. The bottom surface consisted of aluminum plates covered with a sheet of linoleum, spray painted black and wet sanded smooth.

Most of the data was collected with commercially available instruments. The pressure measurements were taken with a Decker Delta 308 differential pressure instrument with a 0.3 to 3.0 inch H₂O transducer. Velocity measurements were taken with three Thermo System Incorporated 1054B constant temperature hot-wire anemometers with built-in linearizers. Signal conditioning was incorporated employing a Thermo Systems Incorporated 1057

high/ using

and h

Y plo

These the tr

measur

positi

2.5 P

perform flow.

numbers

the cha

determi

pressur

signifi flow.

•

2.6 Re

high/low pass filter unit. Time mean pressure and velocity were obtained using a Thermo Systems Incorporated 1047 Averaging Circuit module. Visual and hard-copy displays were done using a Tektronix 546B fast-writing storage oscilliscope, coupled with a Tektronix C-40 camera, and a Hewlett Packard X-Y plotter.

Special probes were used to acquire the data for this investigation. These probes are shown in Figure 8 and 9 and were used in conjunction with the traversing rig shown in Figure 10 for spanwise (z-direction) measurements. For streamwise measurements, a motorized radio controlled positioning system was used in conjunction with the probes.

2.5 Preliminary Measurements

Before conducting extensive turbulent flow experiments, a study was performed to determine the effects the motorized probe would have on the flow. The streamwise static pressure distribution was measured for Reynolds numbers ranging from 4000 to 18,000 at various streamwise locations along the channel centerline. From this analysis, see Figure 14, it was determined that the motorized probe had a minimal effect on the streamwise pressure distribution. Consequently, the motorized probe should not significantly affect the velocity profile measurements in the undisturbed flow.

2.6 Results

develo initia length

gradie veloci

number.

measur(

transve length

will in

shows t

that a applica

Would 1

12,000,

core re

distribu turbule:

Figure 1

To provide a comprehensive description of turbulent flow development, experiments were conducted to determine the turbulence initiation length, the inviscid core length, the established turbulence length, the profile development length, the length at which the pressure gradient achieves its fully developed profile, and the fully developed velocity profile length. These experiments were conducted for Reynolds numbers ranging from 4000 to 18,000.

The turbulence initiation length, $L_{\rm t}$, is plotted in Figure 15. The measurements to determine $L_{\rm t}$ were taken along the channel centerline in the transverse direction. As shown in Figure 15, the turbulence initiation length decreases as the Reynolds number increases. Eventually, turbulence will initiate at the channel entrance at high Reynolds numbers (Re $> 10^5$).

The inviscid core length, L_{i} , is plotted in Figure 16. This plot shows that L_{i} decreases as the Reynolds number increases. This indicates that a relation of the form derived by Bowlus & Brighton (1968) is not applicable for the conditions studied because the equation they proposed would lead to an increasing L_{i} with increasing Reynolds number. For Re < 12,000, the initiation of turbulent bursts occurs downstream of the inviscid core region. Therefore, the velocity profiles and static pressure distributions for Re < 12,000 should resemble laminar flow conditions until turbulence initiates downstream.

Data for the established turbulence length, $L_{\rm st}$, is presented in Figure 17. After the distance $L_{\rm st}$ the flow is fully turbulent; however, the

veloci charac

length

develo

distar

change as wit

215 ct

could

Barbin

that s

on fla

Present The c

Wall

in Fi

using Reyno

into

velocity profile has not reached its fully developed velocity profile as characterized by the one-seventh power law model. The profile development length is then determined and plotted in Figure 18.

The distance, L_p , at which the pressure gradient attains its fully developed value is provided in Figure 19. The pressure gradient development will be discussed later.

The entrance length, $L_{\rm e}$, is plotted in Figure 20. Unlike the other distances measured, $L_{\rm e}$ increases with the Reynolds number. Moreover, changes in the Reynolds number do not affect values for $L_{\rm e}$ as significantly as with the other distances measured. Because $L_{\rm e}$ is in the range of 190 to 215 channel heights, the conclusions of Klein (1981), that entrance lengths could exceed 140 pipe diameters, would tend to be supported over those of Barbin & Jones (1963) or Wang & Tullis (1974). This would further indicate that some past experiments for fully developed flow were actually conducted on flows that were not yet developed.

Details of the entrance flow at a Reynolds number of 16,000 are presented in Figures 21-24. The inviscid core region is shown in Figure 21. The centerline streamwise intensity variation is shown in Figure 22. The wall shear stress is plotted in Figure 23, and velocity profiles are plotted in Figure 24.

Experimental streamwise static pressure distributions were measured using the taps in the channel sidewall. The results of ten trials at each Reynolds number were averaged. The measured distributions can be divided into three categories.

as low
Figure
core b
this c
charac
pressu
fully

distr disap

in Fi

Reyno devel

As Re

press

entin occun

- 16

numb

cate

othe

The first category of static pressure distributions are designated as low Reynolds number distributions. These flows are illustrated in Figures 25-28 and are characterized by the disappearance of the inviscid core before the first turbulent bursts are detected (i.e., $L_{\rm i} < L_{\rm t}$). For this category, the pressure gradient initially follows a gradient characteristic of laminar flow. After turbulent bursts initiate, the pressure gradient deviates from the laminar gradient and approaches that of fully developed turbulent flow.

The second category of static pressure distributions are presented in Figures 29-31 and are designated as intermediate Reynolds number distributions. For this case, the turbulent bursts initiate prior to the disappearance of the inviscid core (i.e., $L_{\rm t} < L_{\rm i}$). As with the low Reynolds number flows, the pressure gradients start below their fully developed profiles; however, they are above the values for laminar flows. As Reynolds numbers increase there will eventually be a value for which the pressure distribution remains at its fully developed value throughout the entire flow. Although the exact value of the Reynolds number at which this occurs is unknown, the available data indicates that it is slightly above Re = 16,000.

The final category of pressure distributions is the high Reynolds number distributions. For this case, the pressure gradient at the entrance to the channel is initially greater than its fully developed value. This category is illustrated in Figure 32 and was similar to results found by other researchers at high Reynolds numbers.

This

press

2.7

concl

51100

The three categories are plotted on the same graph in Figure 33.

This provides a good comparison for the magnitude of the dimensionless pressures.

2.7 Conclusions

Based on the results of this investigation, the following conclusions can be made for turbulent flow in the entrance region of a smooth channel.

1. The inviscid core length, L_i , decreases with increasing Reynolds number. It can be approximated by the relationship

$$\frac{L_{i}}{H}$$
 - - 0.00156 Re + 68.6

2. The turbulence initiation length, L_{t} , decreases with increasing Reynolds number and can be approximated by the relationship

$$\frac{L_t}{H}$$
 = -0.00725 Re + 139.5

3. The established turbulence length, $L_{\rm st}$, decreases with increasing Reynolds number. It can be approximated by the relationship

$$\frac{L_{st}}{H} = 6.8476 \times 10^{-8} (Re)^2 - 0.00800 Re + 168$$

4. The distance from the channel entrance to the location where the pressure gradient attains its fully developed value, L_p , decreases with increasing in Reynolds number for Re \leq 16,000 and can be approximated by the relationship

$$\frac{L_p}{H} = 6.8840 \times 10^{-8} (Re)^2 - 0.0098732 Re + 221$$

For Re > 16,000 the value for $L_{\mbox{\scriptsize p}}$ increases with increasing Reynolds number.

5. The entrance length, $L_{\rm e}$, for the velocity profile to attain its fully developed form increases with Reynolds number and exceeds 190 channel heights. It can be approximated by the relationship

$$\frac{L_{e}}{H}$$
 - 0.00104 Re + 192

- 6. There are three categories of turbulent flows that are designated as follows:
 - a.) Low Reynolds number turbulent flows for which $L_{\rm i} < L_{\rm t}$. In this category, Re < 10,000 and the initial pressure

2.8

fino

exan

near

< 40

bear inve

deve

thos

- gradients are less than the pressure gradient associated with fully developed flow.
- b.) Intermediate Reynolds number turbulent flows for which $0 < L_{\rm t} < L_{\rm i}$. In this category, $10,000 < {\rm Re} < 18,000$ and the pressure gradients initiate above their laminar form, but below their fully developed turbulent values. This category includes a flow, with Re = 16,000, for which the pressure gradient retains its fully developed value throughout the entire inlet region.
- c.) High Reynolds number flows for which $L_t = 0$. In this category, Re > 18,000 and the pressure gradients initiate above their fully developed value and reduce monotonically to their fully developed value downstream.

2.8 Recommendations for Further Research

Even though the present investigation resulted in many significant findings, it also points to the need for further investigation. For example, it is worthwhile to note that for Re = 4000 the value for L_p is nearly equal to that of $L_{\rm st}$. An investigation of profile development for Re < 4000 would help determine if the relation between L_p and $L_{\rm st}$ has any bearing on whether turbulent flow develops. Furthermore, such an investigation could provide a link between studies of laminar flow and developing turbulent flow. Just as flows at Reynolds numbers lower than those studied here are of interest, flow at higher Reynolds numbers would

pro Re

and

hig

to Rey

fur

of

pre

int

Ъe

res

tur

provide a greater understanding of developing turbulent flow. Research for Re > 18,000 would provide continuity between the information presented here and that presented by previous researchers. Moreover, further study at higher Reynolds numbers should be conducted in channels of sufficient length to obtain fully developed flow. In addition to the need for research at Reynolds numbers outside the range (4000 < Re < 18,000) of this study, further investigation within this range is required to pinpoint the location of certain events. For example, the Reynolds number at which the static pressure gradient remains constant throughout the entire flow is of interest. Similarly, occurrences of other events in the flow history could be tracked more closely to changes in Reynolds number. In general, the results of this investigation provide a solid basis for further research of turbulent entrance flows.

3.1

the

entr

sha

fol

div

des

de

st

.

CHAPTER 3

LAMINAR ENTRANCE FLOW

3.1 Introduction

Laminar flow in a channel can be represented by simplification of the momentum, energy, and continuity equations. The flow commences in an entrance region with variables shown in Figure 33A and continues until the flow becomes developed where the velocity profile has attained a parabolic shape. The shape maintains itself downstream unless bursting occurs followed by transition to turbulent flow. The laminar entrance region is divided into two areas as shown in Figure 34. The entrance region length, designated $L_{\rm e}$, is split into an inviscid core length $L_{\rm i}$, and a profile development length $L_{\rm i}$.

The Navier-Stokes equation pertaining to this experiment for the steady, fully-developed flow in a channel is

$$\frac{d^2u}{dy^2} - \frac{1}{\mu} \frac{dp}{dx} - constant \tag{3}$$

The solution to this equation is

$$u(y) = \frac{-4U_{\text{max}}}{H} (y^2 - Hy)$$
 (4)

The

syst

subs

at t

Equa

from

rev

3.2

inc

bei

si.

٥f

st 75

7

i. e

7

The solution for the velocity in the above equation was found using the boundary conditions u=0 at y=0, and u=0 at y=H where the coordinate system can be found in Figure 33a. Noting that the maximum velocity occurs at the center of the channel (y=H/2), the resulting U_{max} can be found and substituted into the original velocity equation to obtain the constant in Equation 3. The resulting velocity profile is parabolic.

In the entrance region the velocity profile undergoes a transition from the relatively uniform inlet profile to the developed profile presented above. This study is aimed primarily at this entrance region. Let us first review the literature that relates to the laminar flow entrance region.

3.2 Background

Feliss, Smith and Potter (1977) present experimental results for incompressible flow in a channel near the transition from laminar to turbulent channel flow. The two paths of the investigation involve the behavior of the flow before and after the onset of turbulent bursting. The side wall boundary layer development and its effect on the mean flow, the laminar entrance length as a function of Reynolds number, and the variation of laminar flow in the entrance and developed regions are discussed. The study continues with the bursting phenomenon. A critical Reynolds number of 7500 was achieved. The authors stated that the linear theoretical number of 1700 at instability onset was found by extrapolation of the data for an intensity disturbance approaching zero. A linear relationship between the entrance length and Reynolds number was given. The data compared favorably to the calculated values of Schlichting (1960). The authors note initial

bu ob:

di:

Ъe

bo:

reg

ve?

exp Rey

pro

ent

de

Va:

le

re:

the re:

pr

wh

bursting at Re - 700 and at a distance of x/D - 500. No bursting was observed at lengths less than 200. Also the point of the first burst could be monotonically increased by decreasing the intensity level of the disturbances in the channel. The boundary layer thickness was plotted and noted to have a negligible effect on the mean velocity. The increase in boundary layer thickness above Re - 2500 was attributed to the increase in disturbance intensity. The sudden growth of disturbances in the viscous regions was suggested to be due to boundary layers undergoing transition to turbulent flow before the formation of the parabolic velocity profile, for velocities exceeding the critical Reynolds number. The paper provides good experimental support for the linear relationship of entrance length to Reynolds number and a detailed examination of the bursting phenomenon. It provides many suggestions for further experimental pursuit.

Sparrow, Hixon and Shavit (1987) studied by experiment the development of the laminar velocity and pressure fields in the hydrodynamic entrance region of rectangular ducts with 5:1 and 2:1 aspect ratios. Air was the working fluid and the Reynolds numbers were in the range of 1000 to 5000. The static pressure distributions compare very favorably for the length of the duct with the theoretical pressure distributions. A relatively large pressure gradient occurs in the entrance region. This is due to a combination of wall shear stress and to the increase of momentum in the entrance region. The pressure gradient continues to decrease until reaching the constant value corresponding to fully developed flow. The pressure entrance length is represented by $L_{\rm p}/D_{\rm e}$ = 0.02 Re for the ducts, where $D_{\rm e}$ is an equivalent diameter. The velocity profile along the

symme duct.

becom

It wa

1

narro

lower

flow with

> expe rela

> > undi

damp

joir

of 1

Wit

num

dis

ca]

th: lo

am

Re

٥f

symmetric cross section showed a more rapid flow development for the larger duct. The boundary layers developed along the wall as the velocity profile becomes rounded due to mass conservation resulting in increased core speed. It was also noted that the boundary layer played a greater role in the narrow axis. An interesting phenomenon was the higher velocity seen in the lower half of a duct compared with the upper half.

Leite and Kuethe (1955) investigated the stability of Poiseuille flow in a pipe with and without heat addition and the results were compared with theoretical predictions. This investigation was the first quantitative experimental study of the stability of fully developed laminar flow in relation to small disturbances. One major finding was the attainment of undisturbed laminar flow at a high Reynolds number. Precautions of adequate dampening screens in the settling chamber, a well rounded inlet, and smooth joints contributed to the attainment of laminar flow at the maximum capacity of this system near Re - 20,000. The authors stated that such values concur with Prandtl's theory that no definite upper limit for the critical Reynolds number exists and that higher values can be obtained by reduction of initial disturbances. The velocity profile data compares well to that predicted by theory. Also, the length of transition was approximated and compared with calculated results of Bousinesq. Bousinesq's formula gave lengths longer than those observed in the experiment, however good correlation was found at low Reynolds numbers. Other points of interest were that the maximum amplitude of disturbances that allowed flow stability decreased as the Reynolds number increased. Also, the data for the rate of decay and speed of propagation of disturbances agreed well with theoretical predictions.

Lundgren. Sparrow and Starr (1964) used an analytical method to determine the pressure drop in the entrance region of ducts of various cross sections. The difficulty of the nonlinear behavior of the inertia terms found in the equations of motion have prevented past analyses from obtaining an exact solution. This analysis avoided using the inertia terms. Instead a knowledge of the fully developed velocity profile was used with the momentum and continuity equations or with the mechanical energy equation substituted for continuity. The pressure drop was developed using the momentum and continuity equations with a correction term. The correction term is needed due to the momentum change between the entrance section and the downstream section and secondly due to the accumulated increment in wall shear between a developing and fully developed flow. Several applications of this theory were presented for circular tubes, elliptical, rectangular, triangular, and annular ducts. Their results were compared with other analytical studies and experimental data. The study compares reasonably well with other studies; however, there is a lack of comparison regarding the triangular and annular ducts.

Bhatti and Savery (1979) used a generalization of the fully developed velocity profile in a channel and application of mass balance and energy equations to develop simple analytical expressions for the velocity profiles, pressure drop, and friction coefficients. The idealized flow consisted of a viscous boundary layer and an inviscid core. The flow was also assumed to be imcompressible, two-dimensional, steady-state, and laminar involving Newtonian fluids with constant properties; the transverse velocity is small and consequently the pressure gradient is independent of

the cross section; in the boundary layer the transverse convection term is negligible and there are no body forces. The steps taken were to use an approximate velocity distribution. The pressure gradient and boundary layer thickness were found in terms of the velocity using a mass balance. And finally the improved velocity distributions were determined by solving the mechanical energy equation. The entrance length at which the velocity was 99% of its ultimate value was found to be $L_{\rm e}/a=0.1674$ Re. However, comparison to experimental data was not done, making a judgement of accuracy difficult.

Wang and Longwell (1964) presented a numerical study of laminar flow in the inlet section of parallel plates. Most authors study this topic by using boundary layer theory. These authors agreed that this is a powerful tool, yet it is also known that its assumptions are not valid in the vicinity of the leading edge of the plate. In this region the second derivative of velocity in the x-direction is not negligible relative to the y-direction. Also the pressure gradients in the y direction are not necessarily small enough that the momentum equation for y-direction velocity is negligible. The numerical technique did not make these assumptions and therefore was more exact. Two cases were treated. In Case I, a flat velocity distribution at the entrance was assumed. For Case II, the velocity distribution at the entrance was unknown and the flat distribution occurs further upstream of the entrance. The velocity from these two cases was compared along the plate to results obtained by Schlichting. They agreed better at large x and diverged closer to the entrance. The center line velocity was also compared to other authors. Finally the pressure

grad.

conc

near

for entr

plat

term

post

sect

The the

laye

flow

the

dire This

Comp

Prof

пише

entr

gradients were compared in graphical form. The graphs showed that the pressure gradient was not negligible in the entrance region. The authors conclude that a numerical solution must be used in place of a boundary layer solution if one is seeking velocity distributions and pressure gradients near the entrance region.

Sparrow, Lin and Lundgren (1964) presented a new analytical method for analyzing laminar flow and the corresponding pressure drop found in the entrance region. Entrance regions in a circular tube and in a parallel plate channel were studied. The problem of the nonlinearity of the inertia terms found in the equations of motion was approached by linearizing these inertia terms. By this method, the boundary layer model does not need to be postulated. The velocity profiles obtained are continuous over the cross section and along the length from the entrance to fully developed region. The resulting derivation for velocity between the parallel plates suggested the presence of an inviscid core which gradually shrinks due to the boundary layer development along the channel wall.

Wiginton and Dalton (1970) analyzed the entrance region of laminar flow in a rectangular duct by linearization of the inertia terms found in the equations of motion. They used a stretched coordinate in the flow direction as presented in the earlier work by Sparrow, Lin, and Lundgren. This analysis concentrated on ducts of four different aspect ratios. Comparison was done for both the pressure drop results and the velocity profiles across the duct. Velocity profiles showed a close proximity to the numerical and analytical solutions, and the experimental data. Also the entrance length compared favorably. The authors noted in each case that the

pre:

deve dif:

bou

ups

ent

met alt

sol

cir

sta

fin

alg

Wei

соп

ful abo

bel

rea

pressure distribution reached a fully developed state in about half the distance of the velocity profile development.

Collino and Schowalter (1962) examined laminar flow velocity profile development between two parallel semi-infinite planes using a finite difference method. A comparison was made between these results and the boundary layer solution of Schlichting. This work stated that the use of six terms in the downstream velocity solution and three terms in the upstream velocity, results in the needed convergence for solution. The entrance length and the velocity profile results compared well to other works.

McDonald, Denny and Mills (1972) presented an improved computational method for solving steady state, two dimensional flow problems. An alternating direction implicit (ADI) algorithm was applied to the numerical solution. Laminar flow in the inlet region of a straight channel and in a circular tube were examined. An important aspect of this study was the stability of the solution offered. The mathematical basis was shown and the final equations were put into the finite difference form. The resulting algebraic system of equations were then solved using the ADI method.

Weighting parameters were also used to stabilize the solution by compensating for the coupling of the equations. The authors noted that the fully developed velocity profile undergoes subtle changes in inflection about the core as the distance increases. They also noted a nonmonotonic behavior of the center line velocity with Reynolds number and cautioned the reader when interpreting the entrance lengths because of this response.

3.3 Experimental Facility and Instrumentation

The experiments for this study were conducted in a rectangular, parallel-sided channel. This channel, as shown in Figure 1, consisted of the entry, settling chamber, plenum, contraction, and parallel plate sections. The air flow was provided by a fan downstream of the parallel plate section at which the test data was taken. This location reduced instabilities generally associated with an upstream fan location. As a further measure of reducing instabilities, the entry section occupied a separate room sealed from the test section. This arrangement allowed a pressurized test section and prevented leakage into the test section as occurs in a single room experiment. In addition, the entire assembly was shock mounted to isolate it from building vibrations.

The entry and settling chamber consisted of a smooth inlet, a one inch hog hair filter; a honeycomb section filled with 7.5 inch long, 0.25 inch diameter plastic straws; and four stainless steel screens 8 inches apart with screen meshes of 59.5%, 57.8%, 57.5%, and 49.6%, respectively. The plenum was 48 inches long and constructed of plywood. The contraction area was made of a styrofoam block covered with linoleum. The parallel plate section measured 16 feet long, 35 inches wide, and 0.75 plus/minus 0.005 inches in height. Acrylic sheets formed the top surface of this section and aluminum plates covered with a sheet of linoleum, spray painted black and wet sanded smooth, formed the bottom surface.

3.4 Velocity Development

The velocity development was examined at the start and throughout the length of the channel. Figures 35 and 36 show the velocity development along the channel normalized for the maximum and average velocity, respectively; the Reynolds number is 5000. The Reynolds number is based on channel height and average velocity. The velocity profile remains flat near the center of the channel within the boundaries of the inviscid core region. The center curvature becomes more pronounced at the start of the profile development region. This curvature continues to form in this development region until attaining the parabolic shape signifying the end of the entrance region. This shape is shown as the solid line in Figure 22. Similar velocity profiles have been found with both experimental and analytical methods used by Wang and Longwell (1964), Sparrow, Lin, and Lundgren (1964), Collins and Schowalter (1962), and McDonald, Denny, and Mills (1972). This study does contradict some findings of Wang and Longwell who found the center profile to be concave rather than flat in the inviscid core region.

Additional study was performed to confirm that the channel did exhibit behavior similar to that of parallel plates. Velocity readings were taken downstream at a sufficient length that the two-dimensional channel behavior was represented. The results in Figure 24 show the insignificance of a spanwise velocity variation in the channel. The width was sufficiently greater than the height so that two-dimensional flow was simulated.

3.5 Entrance Region

dev

fro

for

uni

in

bet

red sh

pr

Fi

co

de

in

Th

au

As stated earlier, the inviscid core length and the profile development length mark the two parts of the entrance region. One can see from Figure 34 that the initial section is the inviscid core. At the entrance of the channel the walls create a drag force on the air flow. The force results in the viscous layer growth along the streamwise direction until the two viscous layers meet. This joining signifies the end of the inviscid core length. This study's experiments included a correlation between this length and Reynolds number. The length is essentially independent of Reynolds number, as shown in Figure 38.

At the end of this inviscid core length additional distance is required for the velocity profile in the channel to become parabolic in shape. This distance is termed the profile development length. This profile development length is dependent on Reynolds number, as shown in Figure 39.

Since the entrance length is comprised of the sum of the inviscid core length and the profile development length, one would expect it to be dependent on Reynolds number. This expectation was confirmed and is found in Figure 40. The linear relationship from Figure 40 is

$$\frac{L_e}{H}$$
 = 0.032 Re + 30 (Re > 1000) (5)

The dependence of the entrance length has also been documented by various authors including Felis, Smith, and Potter (1977), Bhatti and Savery (1979),

and

num

smo ent

ter Kue

ini rea

nun

stu

and Collins and Schowalter (1962). A comparison of these studies and this study has been normalized and summarized in Table 1.

TABLE 1
ENTRANCE LENGTH COMPARISONS

L/H = 0.032 Re + 32 This study
e

L_e/H = 0.034 Re - 45 Feliss, et al (1977)

L_e/H = 0.040 Re This study assuming L_e = 0 for Re = 0

L_e/H = 0.063 Re Bhatti and Savery (1979)

L_e/H = 0.068 Re Collins and Schowalter (1962)

The length of the entrance region is dependent on the Reynolds number, as shown in Figure 40. However each channel has, due to its smoothness and the inherent flow disturbances, an upper limit to the entrance length and the associated Reynolds number. This value is often termed the critical Reynolds number. Prandtl theorized (see Leite and Kuethe) that given a sufficiently smooth channel and the reduction of initial disturbances, subsequently higher critical Reynolds numbers can be realized. In linear stability theory this value of a critical Reynolds number is 7700. However, by the application of Prandtl's principle in this study, and also by Leite and Kuethe, critical Reynolds numbers have been

obtained for laminar flow which exceed 7700. A value of 11,100 was obtained in this study. The length of this channel was insufficient to obtain a fully-developed parabolic flow. Consequently, a nonparabolic profile similar that of the data presented in Figure 35 existed at the end of the channel. The flow remained stable and laminar since no bursting occurred. If the channel were sufficiently long, bursting would have occurred at or slightly below Re = 7700.

3.6 Pressure Development

The pressure gradient is created by wall shear stresses and the increase in the momentum as the flow progresses downstream. The value of this gradient is constant in the development-flow region, as shown previously in Equation 1. In contrast to the linear relationship, the data of this study showed an increase over the linear relationship near the channel entrance. This is due to the larger wall stresses and the increase in momentum experienced from the plenum to the end of the entrance length. Similar results were seen by Leite and Kuethe. A representative streamwise static pressure distribution as a function of channel length for this study is shown graphically in Figure 41. The variation near X/H = 250 was due to the exit of the channel. The magnitude and relationship to Reynolds number of this study compared well to experimental and analytical analysis by Sparrow, Hixon, and Shavit (1987), Lundgren, Sparrow, and Starr (1964), Sparrow, Lin, and Lundgren (1964), and Wiginton and Dalton (1980).

3.7 Conclusions

Based on the results of this investigation, the following statements can be made for laminar flow in a smooth channel.

- A critical Reynolds number equal to that predicted by linear stability theory can be achieved given a channel which is smooth enough with a sufficient reduction of the intensity of the initial flow disturbances.
- 2. The inviscid core length, $L_{\underline{i}}$ is independent of Reynolds number and equal to about 50 channel heights.
- 3. The profile development length, L_{pd} , linearly increases with Reynolds number.
- 4. The entrance length, $L_{\underline{e}}$ being the sum of the above lengths, increases linearly with Reynolds number.
- 5. The velocity profile is flat at the center in the inviscid core region, and finally reaches a parabolic shape at the end of the entrance region.
- 6. The static pressure distribution decreases monotonically in the entrance region. The phenomenon is due to decrease in the momentum change and wall shear stress in the entrance region.

CHAPTER 4

BURSTING AND BOUNDARY LAYER GROWTH

4.1 Introduction

The objective of this chapter is to present the results of two areas of investigation of incompressible flow that were performed in the rectangular parallel sided channel. The first area of investigation deals with the bursting phenomenon in turbulent boundary layer flow. The second involves growth of the sidewall boundary layer for high Reynolds number flows. Before presenting these investigations it is useful to review the findings of past research.

4.2 Background

Elder (1960) investigates turbulent spots and their impact on the theory of hydrodynamic stability. He reviews the assumptions that were made by Emmons in his theory of a transition zone and references experimental work which supports these assumptions, (1) point-like breakdown, (2) a sharp boundary between the turbulent fluid of a spot and the surrounding laminar flow, (3) a uniform rate of spot growth and (4) no interaction between spots. An investigation was performed in order to determine the conditions under which breakdown to turbulence near a wall occurs or a turbulent spot is initiated. In the experiments, the turbulent spots were initiated in a laminar boundary layer by a spark driven pulse that resulted from discharging a condenser across the primary coil of a transformer. The pulse amplitude was controlled by varying the condenser charging voltage. It was

cond

loca

crit

the

flo

as l

fro

fro

ran

sha bac

def

sug

int

the

wir One

dif

des

re:

concluded from this investigation, over the range tested, that the breakdown condition is independent of the Reynolds number and that it is determined by local factors alone. Breakdown to turbulence occurs by the initiation of a turbulent spot at all points at which the velocity fluctuation exceeds a critical intensity. This critical intensity was found to be about 0.2 times the free-stream velocity.

Kim, Kline and Reynolds (1971) used Hydrogen-bubble measurements and hot-wire measurements with dye visualization to study the boundary layer flow of water over a smooth, flat plate. The bursting process is described as being made up of three stages: (1) a lifting up of a low-speed streak from the wall, forming inflexional instantaneous velocity profiles; (2) the growth of an oscillatory motion, which is at first quite regular, following from the inflexional zone; (3) a breakup of the oscillatory motion into more random, chaotic motions with the return of the instantaneous profile to a shape like that of the mean profile and a movement of the low-speed streak back towards the wall. The final stage is intermittent but has a well-defined mean frequency. Although not proven, all of the data presented suggest that turbulence production is primarily associated with a local intermittent instability, with most of the energy transfer concentrated in the part of the motions which have been called 'oscillatory growth'.

Kline and Offen (1971) used two dye injectors and a normal bubble wire to visually observe the turbulent boundary layer over a flat plate. One of the dye injectors was a pitot probe which could be placed at different locations and the other was a standard wall slot. The authors describe in detail their observations of the burst cycle and its relationships with the outer flow. Based on their observations, it appears that each lift-up is associated with a disturbance which originates in the

logar have

be go

invo

diox trig

prov

spot the

stru

numb

tran

flow

and

cen

the

spo

sug

tra

Par cri

val

obs

logarithmic region of the velocity profile. These disturbances generally have a significant velocity component towards the wall and are believed to be generated by the interaction of an earlier burst from further upstream with the fluid motion in the logarithmic region. Thus the complete sequence involves relations at various places over a period of time.

Carlson, Windall and Peters (1982) used 10-20 µm diameter titaniumdioxide coated mica particles for flow visualization of artificially triggered transition in plane Poiseuille flow in a water channel. This proved to be an effective method of revealing the structure of turbulent spots in the flow. The spots were characterized by strong oblique waves at the front of and trailing from the rear tips of an arrowhead-shaped coherent structure, with a spreading half-angle of eight degrees. For Reynolds numbers slightly above 1000, both natural and artificially triggered transitions were observed to occur. At Reynolds numbers above 1000, the flow became fully turbulent. It was found that the front of the spot has a propogation velocity of approximately two-thirds of the centerline velocity and the rear moves at a propogation velocity of about one-third of centerline velocity. The spots were found to expand to a size of 35 times the channel depth (h) at a downstream distance x/h of about 300. Turbulent spots were found to split and form two new spots. Results of this study suggest that wave propagation and breakdown play a crucial role in transition to turbulence in Poiseuille flow.

Feliss, Potter and Smith (1977) investigated flow in a rectangular parallel-sided channel with air as the working fluid. The experimental critical Reynolds number was found to be 7500, approaching the theoretical value of 7700 as the disturbance intensity decreased to zero. Bursting was observed at transition. The velocity profile during the burst process was

found to be the one-seventh power law profile over 70 percent of the burst. It was noted that the change from a turbulent profile to a parabolic profile is significantly slower than the change from a parabolic to a turbulent profile. Disturbances in the wall boundary layers became turbulent bursts in the entrance region for Reynolds numbers from 6400 to 7600. This suggests that the transition to turbulence occurs before the parabolic profile is obtained at Reynolds numbers near the critical Reynolds number of linear stability theory.

Chambers, Murphy and McEligot (1983) measured both fully developed and accelerated flows in order to determine if a preferred form of scaling was apparent. Instantaneous measurements of the wall shear stress were made and analyzed by conditional sampling and by conditional averaging. In this investigation the variable-interval time-averaging technique was used with a wall sensor to avoid the interference effects of probes. The sensor size was fixed for each of 27 flows examined. The apparatus used was a duct with sidewalls that could be adjusted to provide a constant rectangular crosssection or laterally converging duct causing streamwise acceleration of the flow.

The burst pattern found by the wall shear stress was similar to that found previously by other researchers for the streamwise velocity fluctuation. It was found that for fully developed flows the dimensionless bursting frequencies were independent of the Reynolds number when scaled with the inner wall variables but not independent when scaled with outer variables. Sweep times and magnitudes of the conditionally averaged time histories varied with Reynolds number with either scaling. Accelerating flows due to lateral convergence showed a decrease in bursting frequency.

As with non-accelerated flows, variation in accelerated flow characteristics was generally less when presented in terms of inner scaling.

Blackwelder and Haritonidio (1983) reported an attempt to resolve the past differences found concerning the frequency of occurence and the scaling of the bursting structure in bounded turbulent shear flows. Since this lack of agreement is usually attributed to the different detection techniques, the authors used a probe technique to provide better reproducibility as other parameters were varied. The variable-interval time-averaging method (VITA) was used because it could be utilized over the entire Reynolds number range studied ($10^3 < U_\infty \theta/\nu < 10^4$). A closed-return wind tunnel was used in this experiment. The naturally occurring turbulence within the boundary layer was studied and boundary layer trips were also used.

The most significant conclusion of this investigation is that the bursting frequency scales with the inner wall variables instead of the outer wall variables. When scaled with the wall variables, the non-dimensional bursting frequency was found to be constant and independent of Reynolds number. An additional conclusion from this investigation was that the sensor size has as a strong effect on the measured bursting frequency and that only sensors with a spatial scale less than twenty viscous length scales would give consistent results.

Zamir and Young (1970) presented experimental data on the laminar boundary layer in incompressible flow with zero pressure gradients. The work also included some investigation of the transition process of turbulent flow and a limited investigation of the effects of pressure gradient. Air was the working fluid for this investigation. Velocity measurements were

taken in planes normal to the corner line along lines parallel to the bisector of the corner angle. The laminar corner flow with zero pressure gradient showed distinct changes in the velocity profile with distance downstream. These changes were found to be associated with a secondary corner flow. The results of this study suggest that the secondary flow is a flow along the corner walls towards the corner line for laminar flow and away from the corner line in the case of turbulent flow. This flow along the walls is coupled with an outflow from the corner along the bisector of the corner angle for laminar flow and an inflow into the corner in the turbulent case. It was concluded from this investigation that the extent of the corner influence in laminar flow is approximately two boundary thicknesses from the corner. The results of this study also show that a favorable streamwise pressure gradient will delay the transition process and conversely, laminar flow separates readily with an adverse streamwise pressure gradient.

El-Gamal and Barclay (1978) study the flow of air along a rectangular corner. The results are presented in the form of velocity profiles for flow in a slightly favorable streamwise pressure gradient and for flow when the pressure gradient is "practically zero". This experiment was carried out in the same wind-tunnel and with the same plates used by Zamir and Young in their investigation. Velocity measurements were taken in the same manner as those taken by Zamir and Young: in planes normal to the flow direction and along lines parallel to the bisector of the corner angle. The most notable feature of the results of this study is the absence of the distortions in the velocity profiles as compared to those noted by Zamir and Young. The authors attribute this to different leading edge forms used in the investigations. Although there is a significant difference between the

resu:

simil

inves

and t

zero of 0

to ve

great

vici

incre

field

perp

irro

the

subs

иѕед

have

results of this investigation and available theoretical solutions, the experimental results are consistent with the notion of corner layer similarity.

Gessner and Jones (1961) presented the findings of an experimental investigation to determine the effect of free-stream turbulence intensity and to explore the directional turbulence characteristics of corner flow. Measurements were made in a developing boundary layer in order to maintain a zero pressure gradient and over a range of free-stream turbulence intensity of 0.8 to 2.3 percent. As a result of the data taken, the authors were able to verify Prandtl's hypothesis, that the ratio of the turbulence component tangent to an isotach to the component normal to an isotach (w'/v') is greater than unity. Isotach patterns were found to be essentially independent of free-stream turbulence intensity. Data showed that in the vicinity of the bisector of the corner angle the ratio w'/v' increases with increasing isotach curvature but this is not the case elsewhere in the flow field. Finally, it was concluded that the turbulence ratio for two perpendicular directions (in the plane normal to the mean flow direction) is a maximum for directions tangent and normal to an isotach.

Li and Ludford (1980) examined analytically both uniform and irrotational entry flow to determine whether the overshoots found numerically are valid or not. For uniform entry and large Reynolds numbers, the overshoot was found to lie at both the leading-edge and in the subsequent boundary layer. In the case of irrotational flow, the overshoot was found to lie at the edge of the boundary layer. A model equation is used for the irrotational flow case to show that the axial velocity must have an overshoot for all values of Reynolds number.

place pages

A see

4.3

of a

para

The

inst

test

prov

comp

inch

0.25

resp dime

styr

lino

by 0

Plat

- -

Many experimental investigations of turbulent bursting have taken place in order to better characterize the transition process. The following pages present an experimental investigation of spanwise turbulent bursting.

A second area covered by this investigation is the growth of the sidewall boundary layer.

4.3 Experimental Facility and Instrumentation

In this study the experiments were performed in a rectangular, parallel sided channel. The channel assembly, shown in Figure 1 consisted of an entrance, a plenum, a contraction and a parallel plate test section. The channel assembly occupied two rooms with a sealed door between the two. The facility was set up in this manner in order to prevent leakage into the test section with the fan located downstream, thereby eliminating flow instabilities associated with an upstream fan location. This arrangement provided a pressurized test section with a downstream fan location. The complete assembly was shock mounted to isolate it from building vibration.

The entrance and settling chamber consisted of a smooth inlet, a one inch thick hog hair filter, a honeycomb section filled with 7.5 inch long, 0.25 inch diameter plastic straws, and four stainless steel screens that were eight inches apart with screen meshes of 59.5%, 57.8%, 57.4% and 49.6%, respectively. The plenum was 48 inches long and made of plywood. The two dimensional contraction was constructed from a styrofoam block. The styrofoam was cut to the dimensions shown in Figure 4 and covered with linoleum. The experimental test section was 15 feet long with a 34.5 inch by 0.5 inch cross-section. The top of the test section was made of acrylic sheets and the bottom surface was constructed of 0.25 inch thick aluminum plates covered with a sheet of linoleum, spray painted black and wet sanded

smooth. Commercially available equipment was used for most of the data collection. Velocity measurements were taken with a Thermo System

Incorporated 1054B constant temperature hot-wire anemometer with built in linearizer. Pressure measurements were taken with a Decker Delta 308 differential pressure instrument. A Thermo Systems Incorporated 1057 high/low pass filter unit was used for signal conditioning. Time mean velocity was obtained using a Thermo Systems Incorporated 1047 Averaging Circuit module. Voltage measurements were made with a Thermo Systems Incorporated digital voltmeter. A Tektronix 546B fast-writing storage oscilloscope along with a Tektronix C-40 camera and a Hewlett Packard X-Y plotter were used for visual and hard-copy displays. A special hot-wire probe shown in Figure 8 was used in this investigation. This probe was used along with the traversing rig shown in Figure 10 to acquire sidewall, or spanwise (Z direction), boundary layer data.

4.4 Transition Process Characteristics

Laminar channel flow ends with the onset of turbulent flow at or above the critical Reynolds number. Early in the transition process, initial infinitesimal disturbances expand and develop into two dimensional disturbances. Further growth of these disturbances lead to three-dimensional fluctuations resulting in the formation of localized turbulent bursts. As a burst grows, the flow resistance increases causing a decrease in mean velocity as the burst moves downstream. Finally, the burst moves out of the channel and the flow again becomes laminar. With laminar flow the flow resistance drops and the Reynolds number increases until it reaches its critical value. At this point transition begins to occur again and the

process repeats itself. For this investigation, the turbulent bursts were found to occur at Reynolds numbers from 4000 to 6000.

4.5 Results

The critical Reynolds number is dependent on the inlet intensity level of the channel. A study was conducted to experimentally determine the variation of the critical Reynolds number with inlet intensity level. The inlet intensity was varied by placing grids of varying mesh size in the contraction portion of the experimental channel. For each mesh, the intensity level was measured before the onset of turbulence, at X/H = 48. The results of this study are shown in Figure 42 along with results obtained by Feliss, Potter & Smith (1977). The curve monatonically decreased to an intensity level of 0.05% at a Reynolds number of 11,100 without grids in the contraction. This was the natural intensity level of the channel. The theoretical critical Reynolds number predicted by linear stability theory is 7700. The experimental value of 11,100 found in this investigation far exceeds the theoretical value due to the short length of the channel test section. The 16.46 foot test section was not long enough to allow a fully developed flow condition with its parabolic velocity profile at the end of the entrance length. Thus, a viscous nonparabolic velocity profile existed at the exit of the channel and bursting did not occur.

A study was conducted to investigate the two-dimensional nature of turbulent bursting in a plane Poiseuille flow. The study was performed to determine if turbulent bursting occurs uniformly across the channel width or if it is highly variable in the spanwise direction. For this study, a 0.25 inch square mesh wire grid was placed across the contraction at X/H = -4.0, lowering the critical Reynolds number of the channel to 5000. At a critical

Reynolds number of 5000, cycles of turbulent bursting occurred on a regular basis. Spanwise traverses were made at Y/H = 0 using a single hot-wire probe. This was done at X/H = 48.0 and X/H = 90.0. The intensities were calculated and are shown in Figure 43. Next, two hot-wire probes were placed at X/H = 229.5 at a spanwise location of Z/W = -0.125 and Z/W = -0.375. Figure 44 shows the result of the output from the two hot-wire probes. These result were used to obtain two possible models of the spanwise bursting process as shown in Figure 45.

4.6 Sidewall Boundary Layer

A study was conducted to document the velocity profile behavior and boundary layer thickness variation with Reynolds number at a streamwise location of X/H = 252. Initially the channel was checked using the probe shown in Figure 8 in conjunction with the traversing rig of Figure 10 to verify two-dimensional flow. Figure 46 presents the results.

Sidewall velocity profile data taken next. This data was taken at regular intervals over the range of subcritical Reynolds numbers from 500 to 11,300. At a Reynolds number of 11,200, transition occured and the sidewall boundary layer became fully turbulent. Three velocity profiles for Reynolds numbers of 1000, 5250, and 8500 are shown in Figures 47, 48, and 49, respectively. These figures show an overshoot in the velocity profile which became more pronounced with increased Reynolds numbers. The sidewall boundary layer thickness, δ , was determined from the data over the range of Reynolds numbers investigated. Boundary layer thickness was based on $u = 0.99U_{\infty}$. Figure 50 presents the results as sidewall boundary layer thickness versus Reynolds number. As indicated in this figure the boundary layer

thickness decreases at a decreasing rate as the Reynolds number increases from 500 to approximately 5600. After this point the boundary layer thickness increases as the Reynolds number increases until transition occurs.

4.7 Conclusions

The following conclusions can be made based on the results of the present investigation.

- 1. The dependence of the critical Reynolds number on the inlet intensity level of the channel has been shown. However, for Reynolds numbers above the theoretical value of 7700, the channel was not long enough to allow a parabolic velocity profile to develop and therefore bursting did not occur.
- 2. At a critical Reynolds number of 5000, where turbulent bursting occured on a regular basis, the spanwise intensity varied nonuniformly, with a higher intensity occuring downstream. Turbulent bursting does not occur uniformly across the channel width.
- 3. Overshoot was shown to occur in the sidewall boundary layer velocity profile, which became more pronounced at higher Reynolds numbers. The boundary layer thickness drops with increasing Reynolds number up to 5600. At this point sidewall boundary layer thickness increases with increasing Reynolds number until transition.

BIBLIOGRAPHY

- Barbin, A. R., and Jones, J. B., "Turbulent Flow in the Inlet Region of a Smooth Pipe," <u>Journal of Basic Engineering</u>, <u>Trans. of ASME</u>, vol. 85, Series D, March 1963, pp. 29-34.
- Bhatti, M., Savery, C., "Heat Transfer in the Entrance Region of a Straight Channel: Laminar Flow with Uniform Wall Heat Flux", ASME Journal, 79-HT-20.
- Blackwelder, R. F., and Haritonidis, J. H., "Scaling of the Bursting Frequency in Turbulent Boundary Layers," <u>Journal of Fluid Mechanics</u>, vol. 132, 1983, pp. 87-103.
- Bowlus, A., and Brighton, J. A., "Incompressible Turbulent Flow in the Inlet Region of a Pipe," <u>Journal of Basic Engineering</u>, <u>Trans of ASME</u>, vol. 90, Series 3, Sept. 1968, pp. 431-433.
- Carlson, Dale R., Windall, Sheila E., and Peters, Martin F., "A Flow Visualization Study of Transition in Plane Poiseuille Flow," <u>Journal of Fluid Mechanics</u>, vol. 121, 1982, pp. 487-505.
- Cebeci, T., and Keller, H. B., "Flow in Ducts by Boundary-Layer Theory," Proceedings of the Fifth Australian Conference on Hydralics and Fluid Mechanics, Dec. 9-13, 1974, pp. 538-545.
- Chambers, W. F., Murphy, H. D., and McEligot, D. M., "Laterally Converging Flow, Part 2. Temporal Wall Shear Stress," <u>Journal of Fluid Mechanics</u>, vol. 127, 1983, pp. 403-428.
- Collins, M., Schowalter, W., "Laminar Flow in the Inlet Region of a Straight Channel", Appl. Sci. Research, 1962, p. 1122.
- Elder, J. N., "An Experimental Investigation of Turbulent Spotts and Breakdown to Turbulence," <u>Journal of Fluid Mechanics</u>, vol. 9, 1960, pp. 235-246.
- El-Gamai, H. A., and Barclay, W. H., "Experiments on the Laminar Flow in a Rectangular Streamwise Corner," <u>Aeronautical Quarterly</u>, vol. 29, May 1978, pp. 75-97.
- Feliss, N. A., Potter, M. C., and Smith, M. C., "An Experimental Investigation of Incompressible Channel Flow Near Transition," <u>Journal of Fluids Engineering</u>, vol. 99, December 1977, pp. 693-698.
- Gessner, F. B., and Jones, J. B., "A Preliminary Study of Turbulence Characteristics of Flow Along a Corner," <u>Journal of Basic Engineering.</u> <u>Trans. of ASME</u>, vol. 83, December 1961, pp. 657-662.
- Kim, H. T., Kline, S. J., and Reynolds, W. C., "The Production of Turbulence near a Smooth wall in a Turbulent Boundary Layer," <u>Journal of Fluid Mechanics</u>, vol. 50, part 1. November 1971, pp. 133-160.

- Klein, A., "Review of Turbulent Developing Pipe Flow," ASME Journal of Fluids Engineering, vol. 102, June 1981, pp. 243-249.
- Kline, S., J., and Offen, G. R., "Combined Dye-Streak and Hydrogen-Bubble Visual Observations of a Turbulent Boundary Layer," <u>Journal of Fluid Mechanics</u>, vol. 62, part 2, 1971, pp. 223-239.
- Leite, R., Kuethe, A., "An Experimental Investigation of the Stability of Axially Symmetric Poiseuille FLow", University of Michigan Paper 2072-2-F, 1955.
- Li, L. C., and Ludford, G. S. S., "The Overshoot in Entry Flow," Arch. Mech., 32, 5, Warszawa 1980, pp. 747-756.
- Lundgren, T., Sparrow, R., Starr, J., "Pressure Drop Due to the Entrance Region in Ducts of Arbitrary Cross Section", <u>Journal of Basic Engineering</u>, Sept. 1964, p. 620.
- McDonald, J., Denny, W., Mills, A., "Numerical Solutions of the Navier-Stokes Equations in Inlet Regions", <u>Journal of Applied Mechanics</u>, Dec. 1972, p. 873.
- Ross, D., and Whippany, N. J., "Turbulent Flow in the Entrance Region of a Pipe," <u>Transactions of the ASME Journal</u>, vol. 78, Series D, Dec. 1956, pp. 915-923.
- Salami, L. A., "Investigation of Turbulent Developing Flow at the Entrance to a Smooth Pipe," <u>International Journal of Heat and Fluid Flow</u>, vol. 7, Dec. 1976, pp. 247-257.
- Shcherbinin, V. I., and Shklyar, F. R., "Analysis of the Hydrodynamic Entrance Region of a Plane Channel with the Application of Various Turbulence Models," <u>High Temperature</u>, vol. 18, Sept. Oct., 1980, pp. 62-68.
- Schlichting, H., Boundary Layer Theory, McGraw-Hill, Inc., 1960
- Sparrow, E., Hixon, C., Shavit, A., "Experiments on Laminar Flow Development in Rectangular Ducts", <u>Journal of Basic Engineering</u>, March 1987, p. 116.
- Sparrow, E., Lin, S., Lundgren, T., "Flow Development in the Hydrodynamic Entrance Region of Tubes and Ducts", <u>Physics of Fluids</u>, March 1964, p. 338.
- Wang, Jeng-Song, and Tullis, J. P., "Turbulent Flow in the Entry Region of a Rough Pipe," <u>ASME Journal of Fluids Engineering</u>, vol. 96, March 1974, pp. 62-68.
- Wang, Y., Longwell, P., "Laminar Flow in the Inlet Section of Parallel Plats", A.I. Ch.E. Journal, May 1964, p. 323.
- Wiginton, C., Dalton, C., "Incompressible Laminar Flow in the Entrance Region of a Rectangular Duct", <u>Journal of Applied Mechanics</u>, Sept. 1970, p. 854.

Zamir, M., and Young, A. D., "Experimental Investigation of the Boundary Layer in a Streamwise Corner," <u>The Aeronautical Quarterly</u>, vol. 21, November 1970, pp. 313-339.

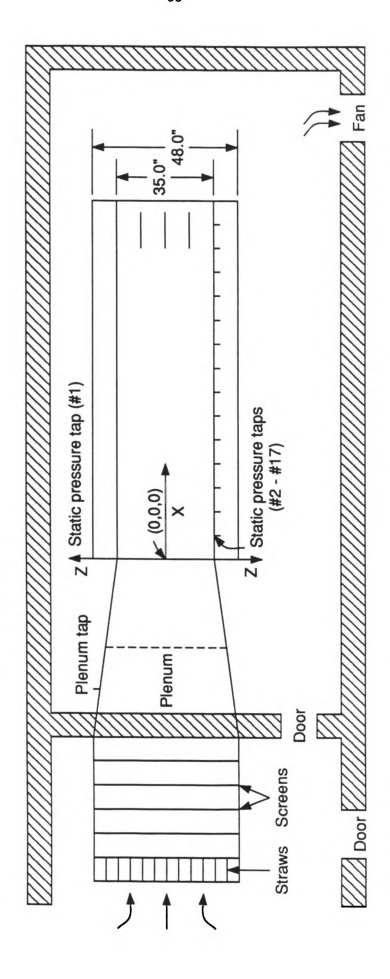


Figure 1. Experimental Channel Facility - Top View

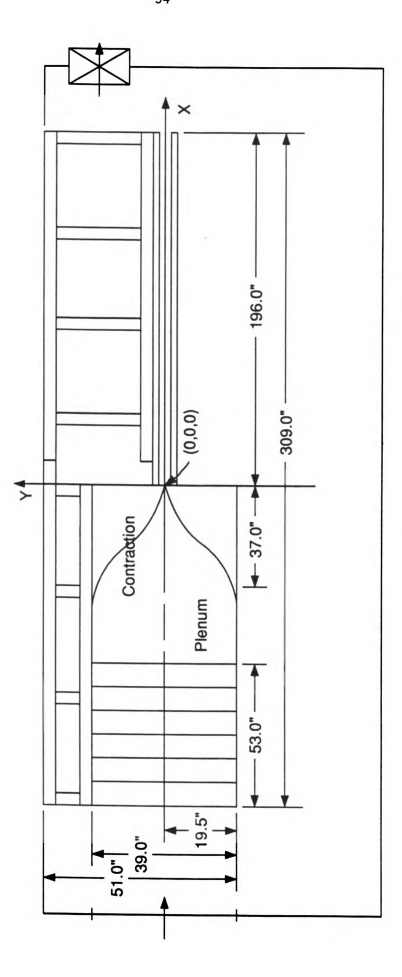


Figure 2. Experimental Channel Facility - Side View

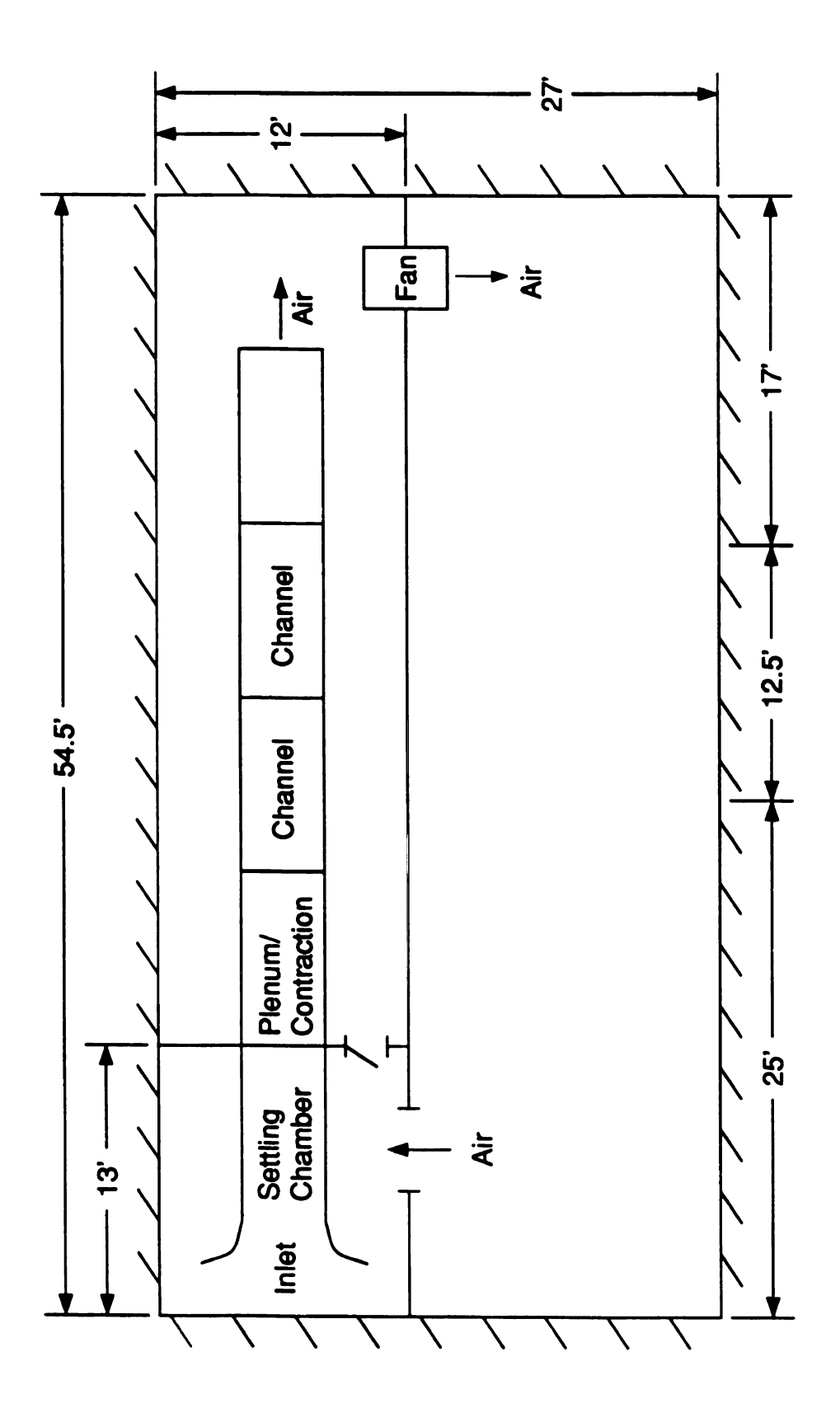


Figure 3. Flow System Floor Plan

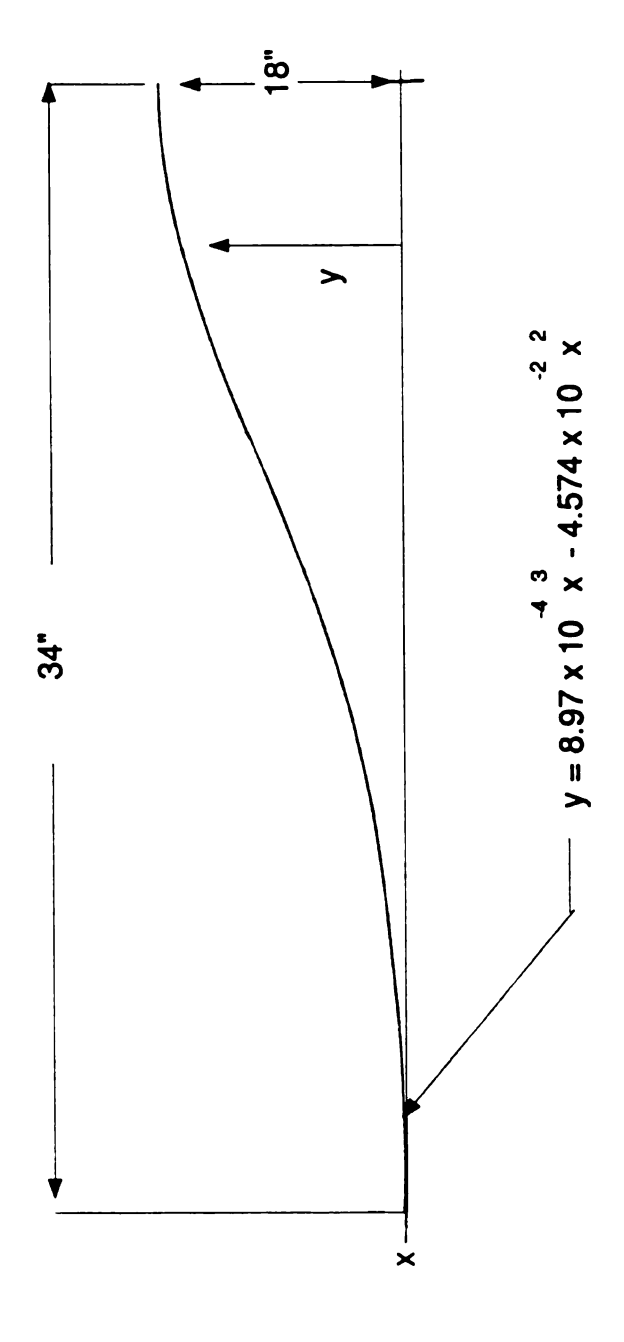


Figure 4. Details of Contraction

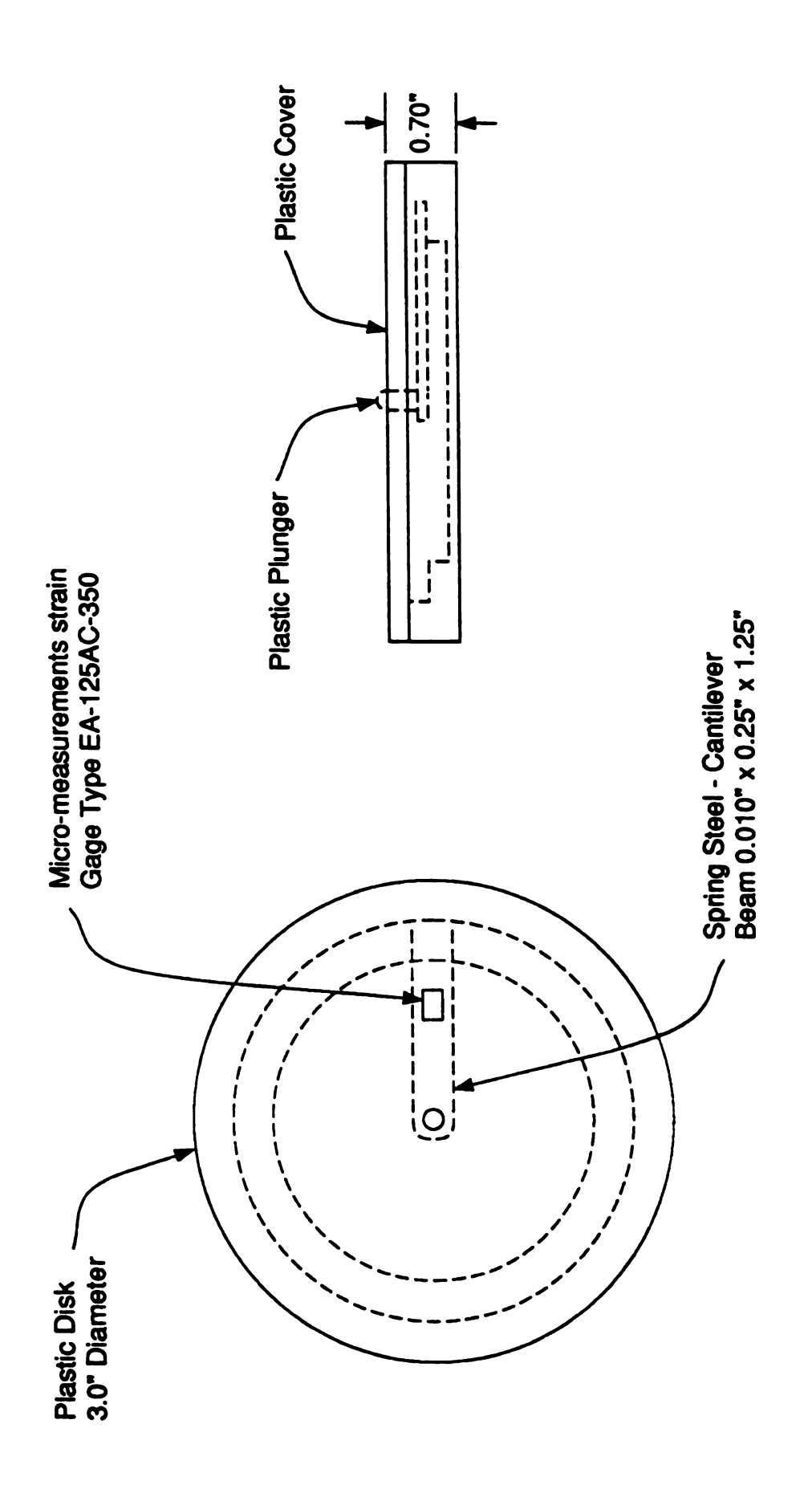


Figure 5. Channel Gapping Instrument

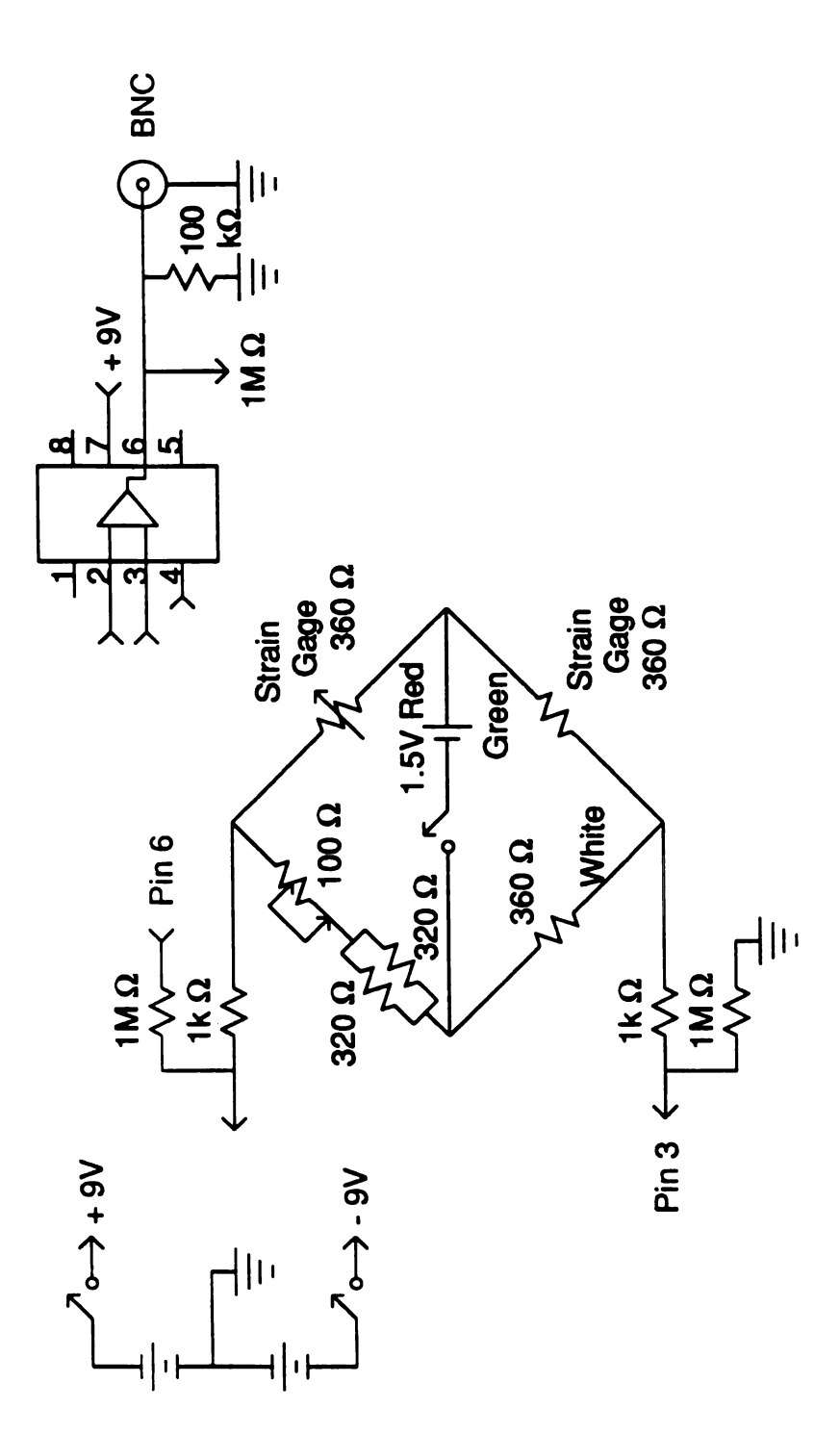


Figure 6. Channel Gapping Instrument Electrical Schematic

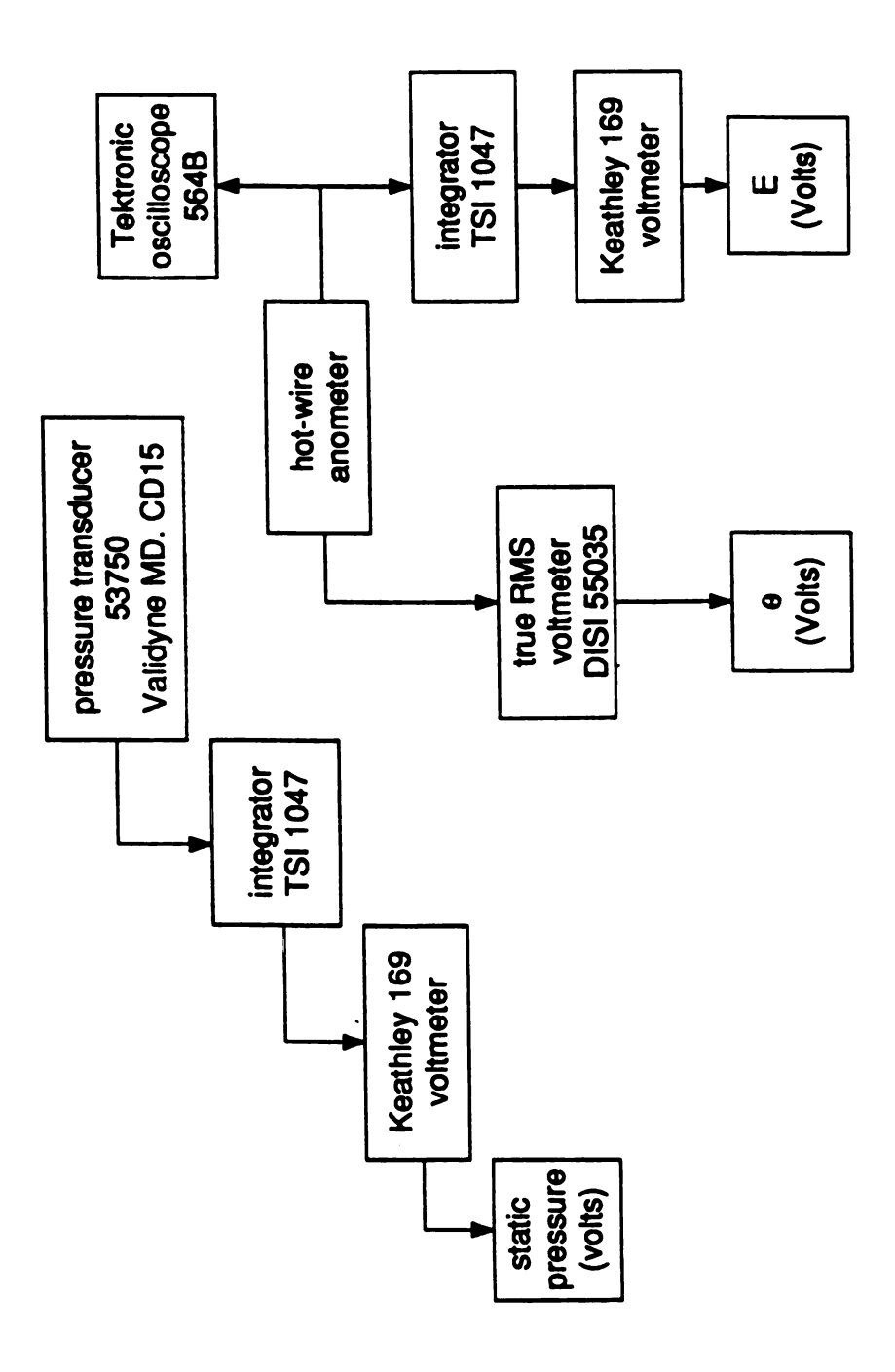


Figure 7. Experimental Equipment System

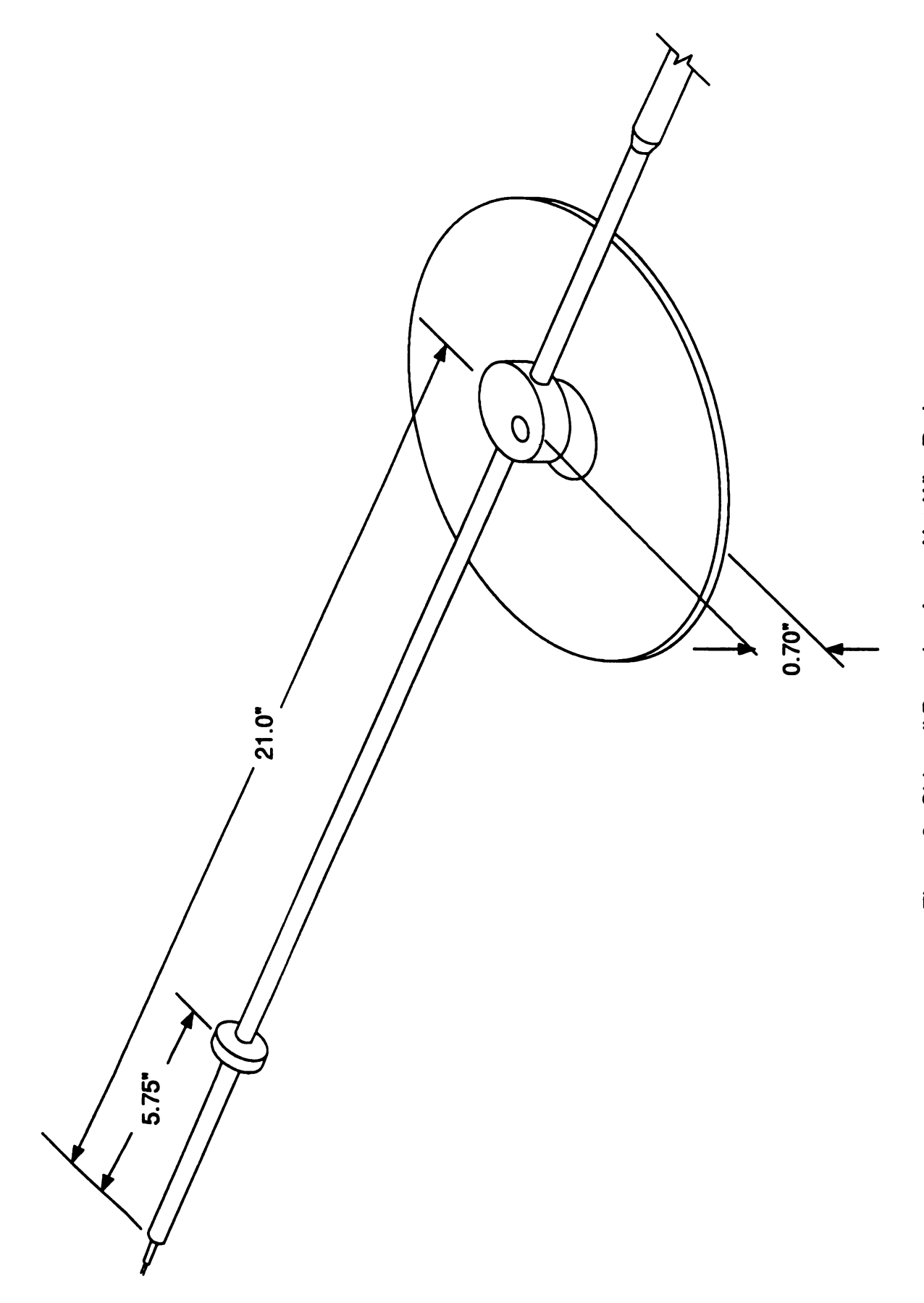


Figure 8. Sidewall Boundary Layer Hot-Wire Probe

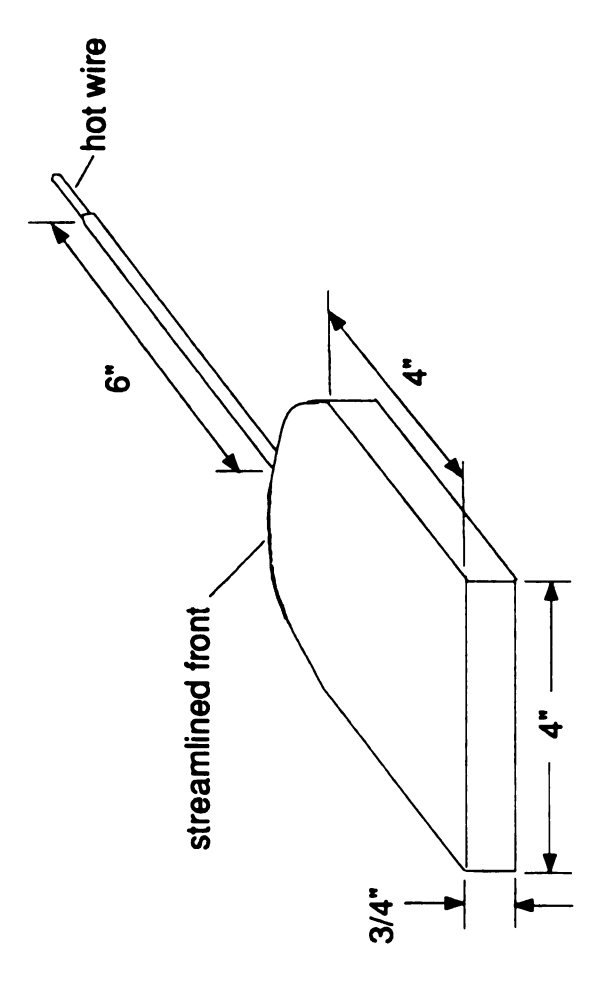


Figure 9. Specially designed probe

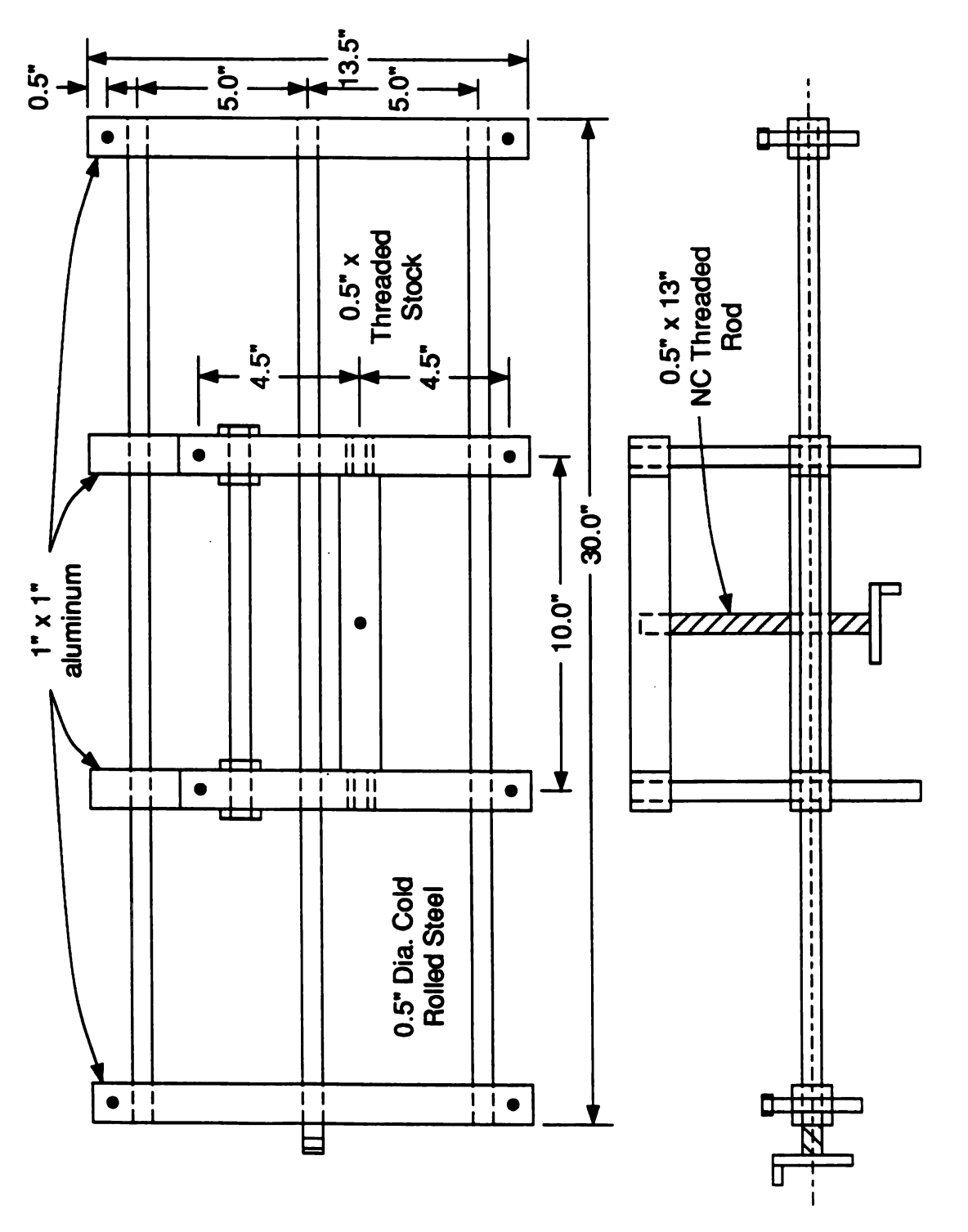


Figure 10. Hot-Wire Traversing Rig

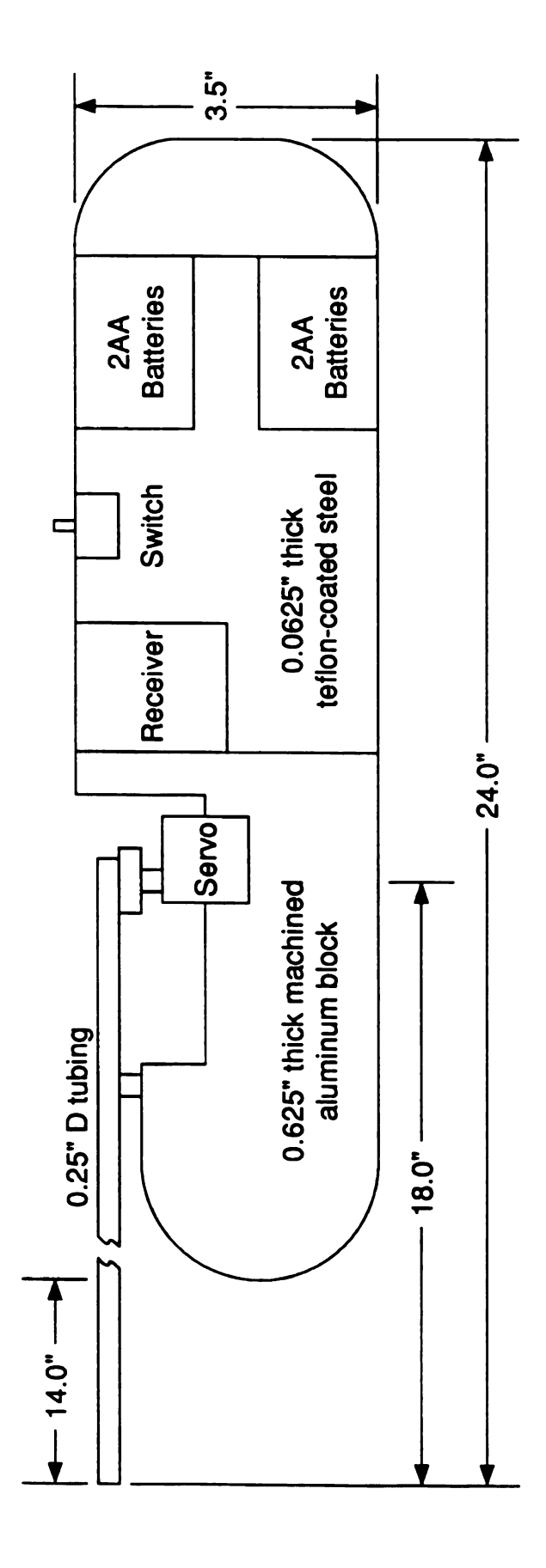


Figure 11. Motorized Hot-Wire Probe

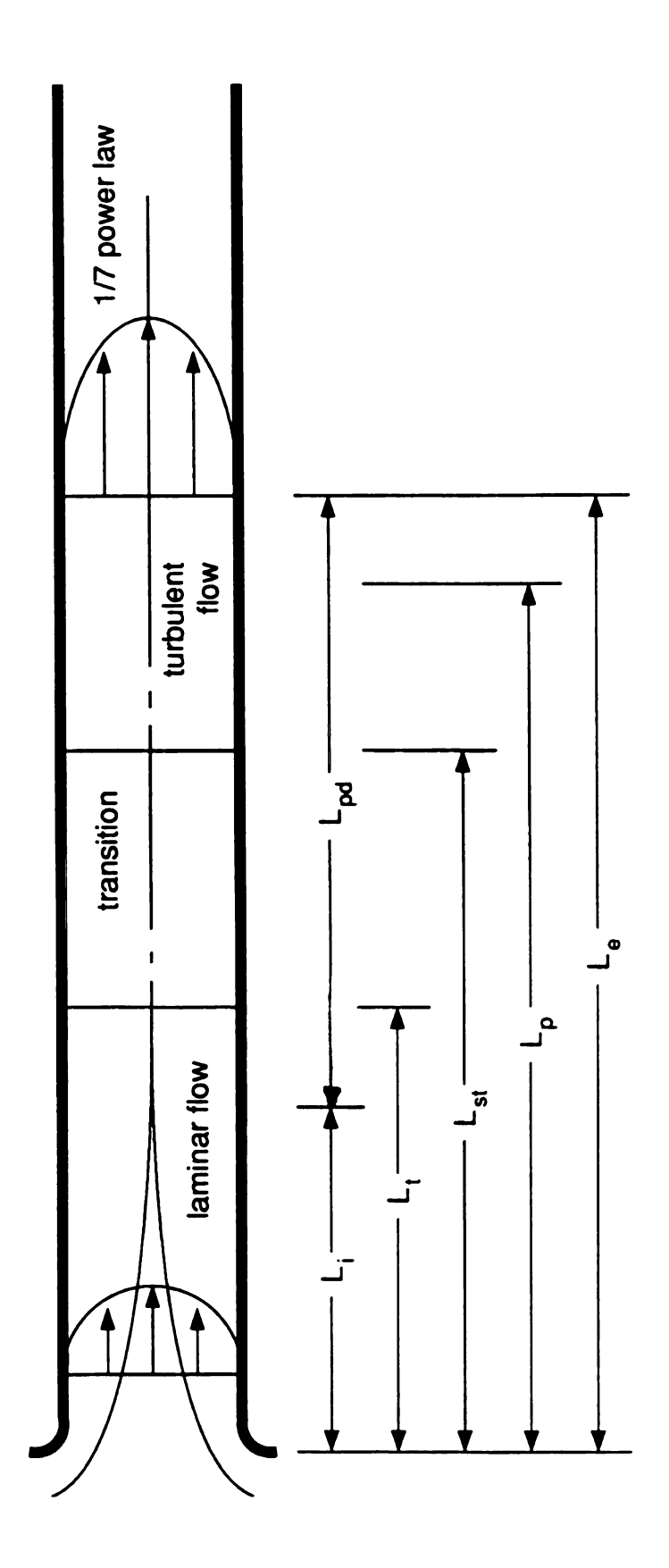


Figure 12. Definition of Turbulent Entrance Lengths

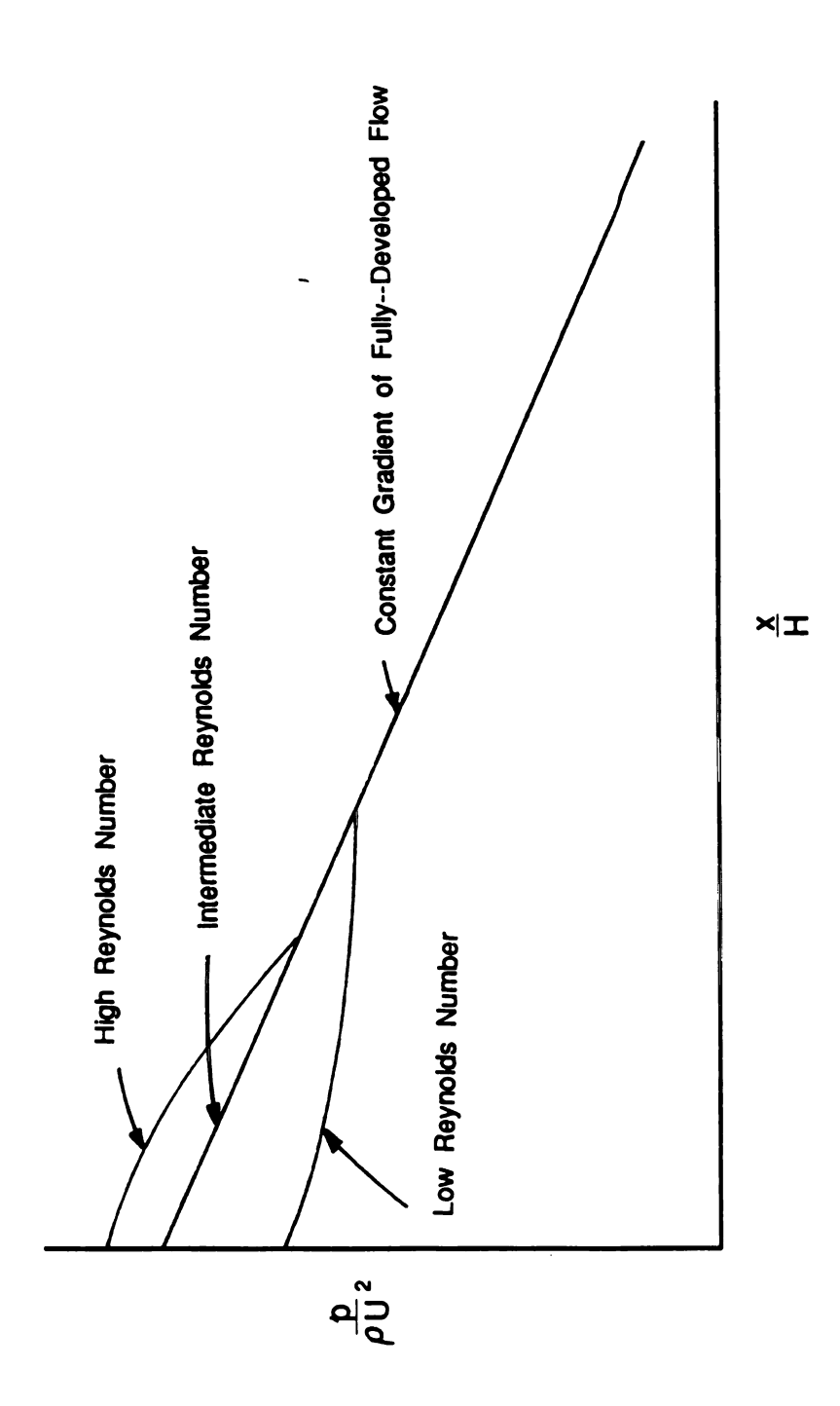


Figure 13. Variation in Pressure Gradient with Changes in Reynolds Number

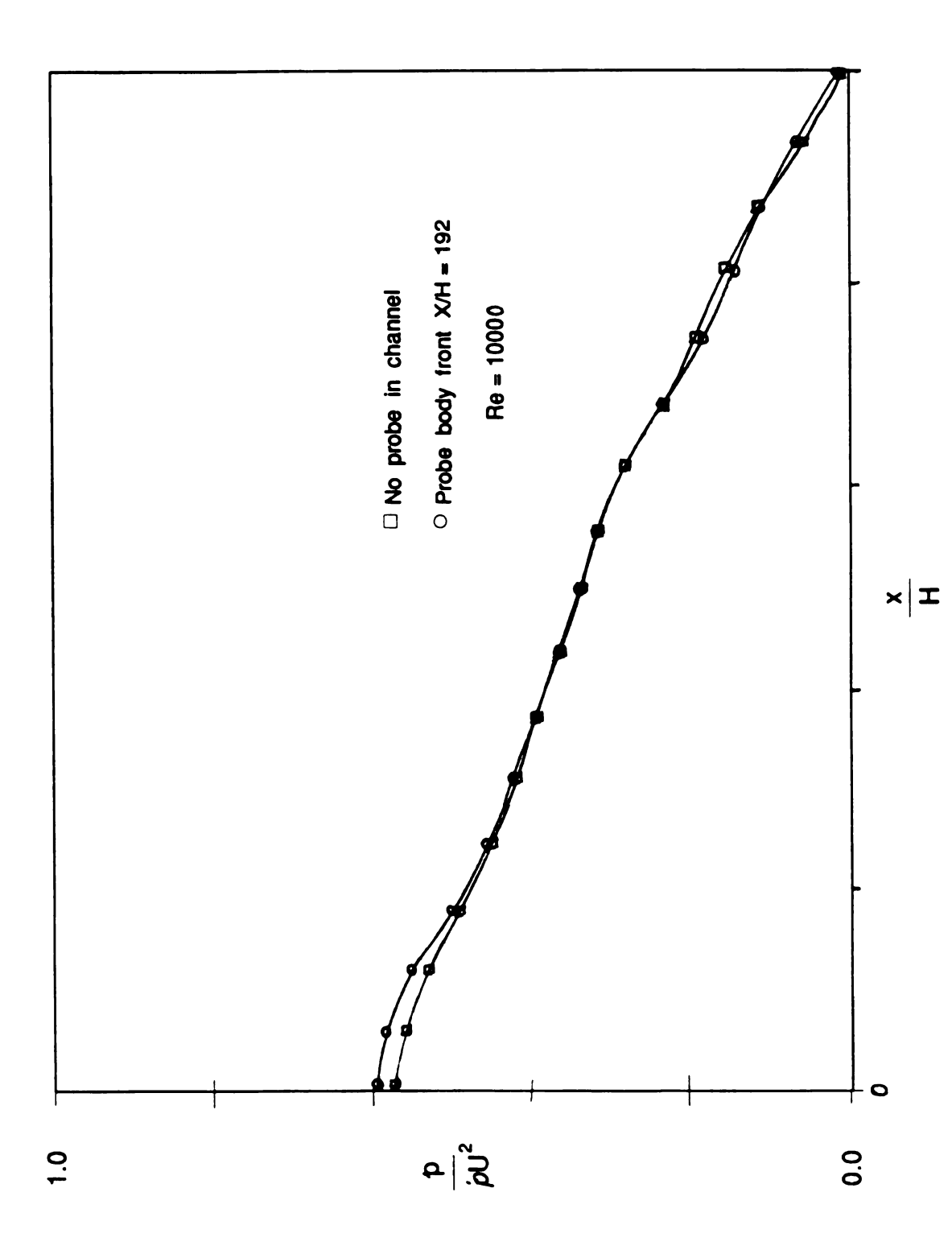


Figure 14. Motorized Probe Induced Flow Effects

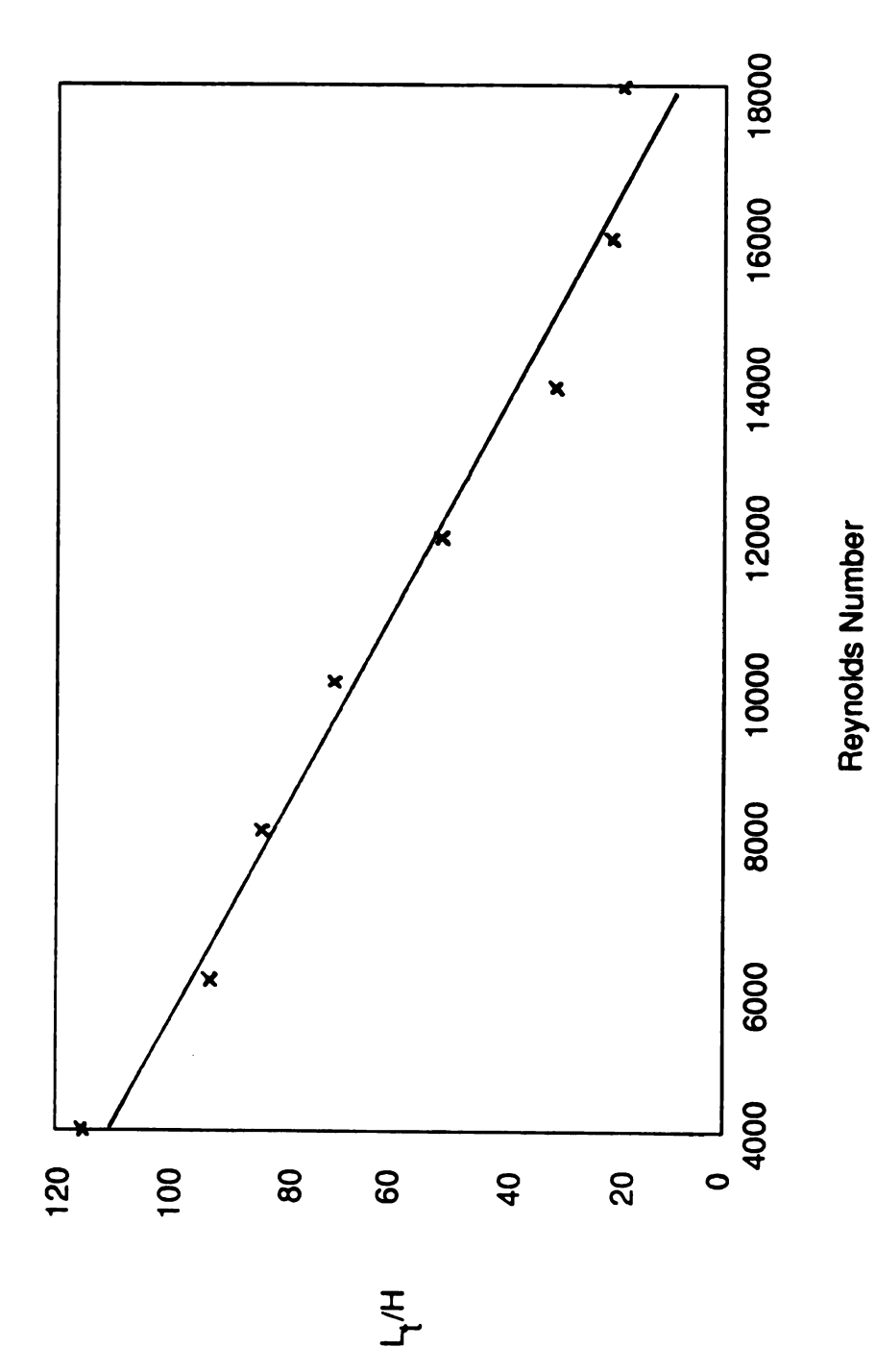


Figure 15. Turbulence Initiation Length, L_t, vs Re

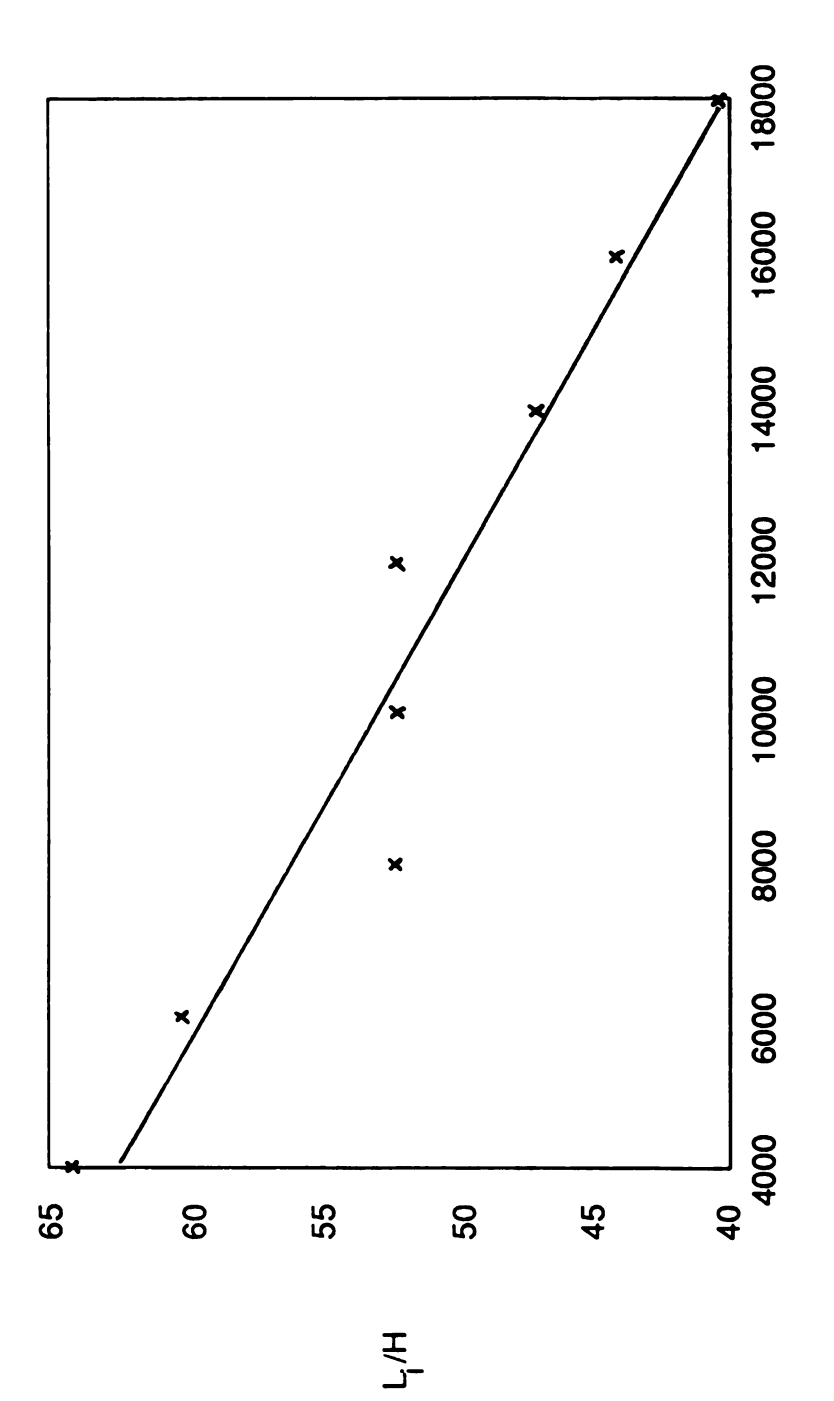


Figure 16. Inviscid Core Length, L, vs Re

Reynolds Number

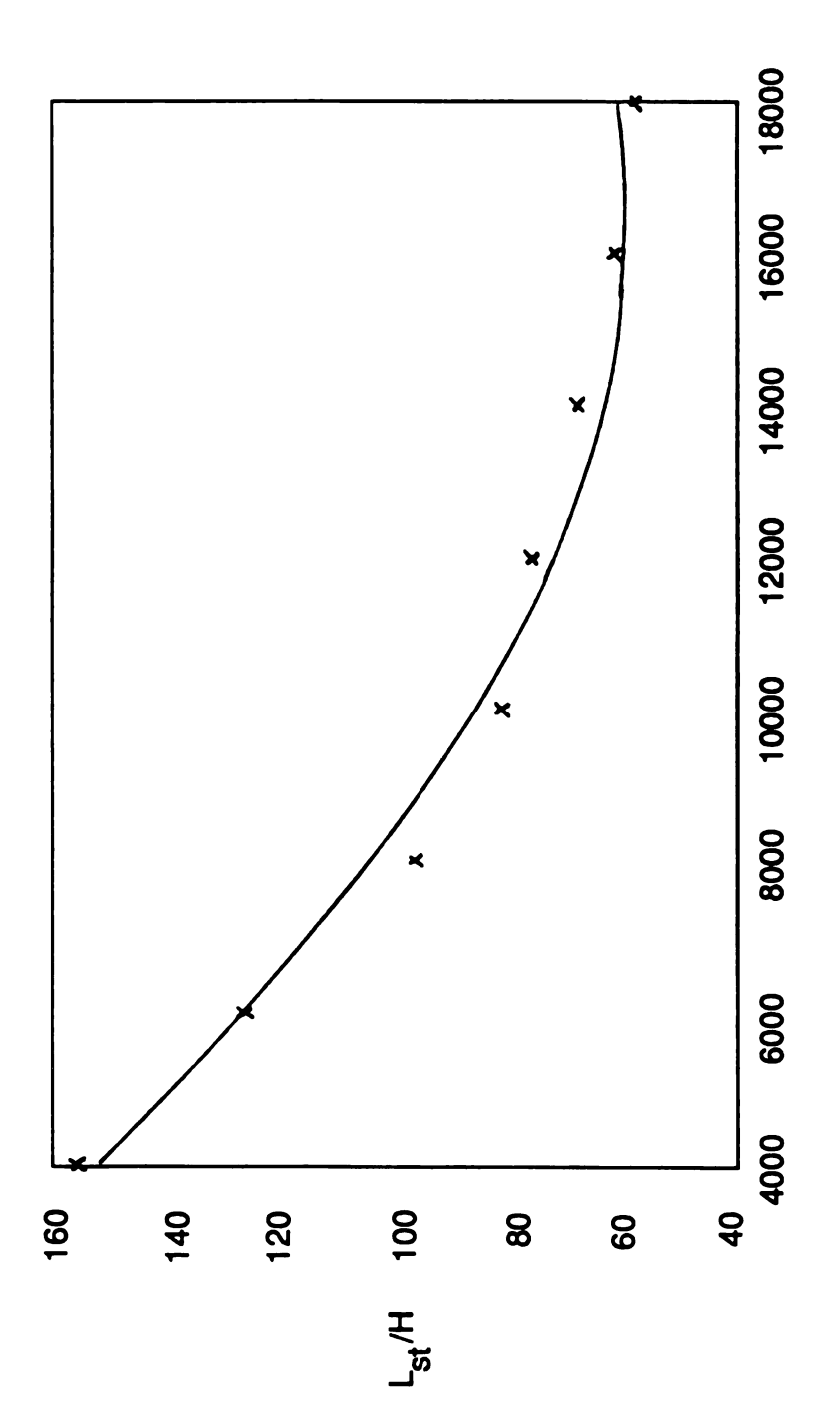
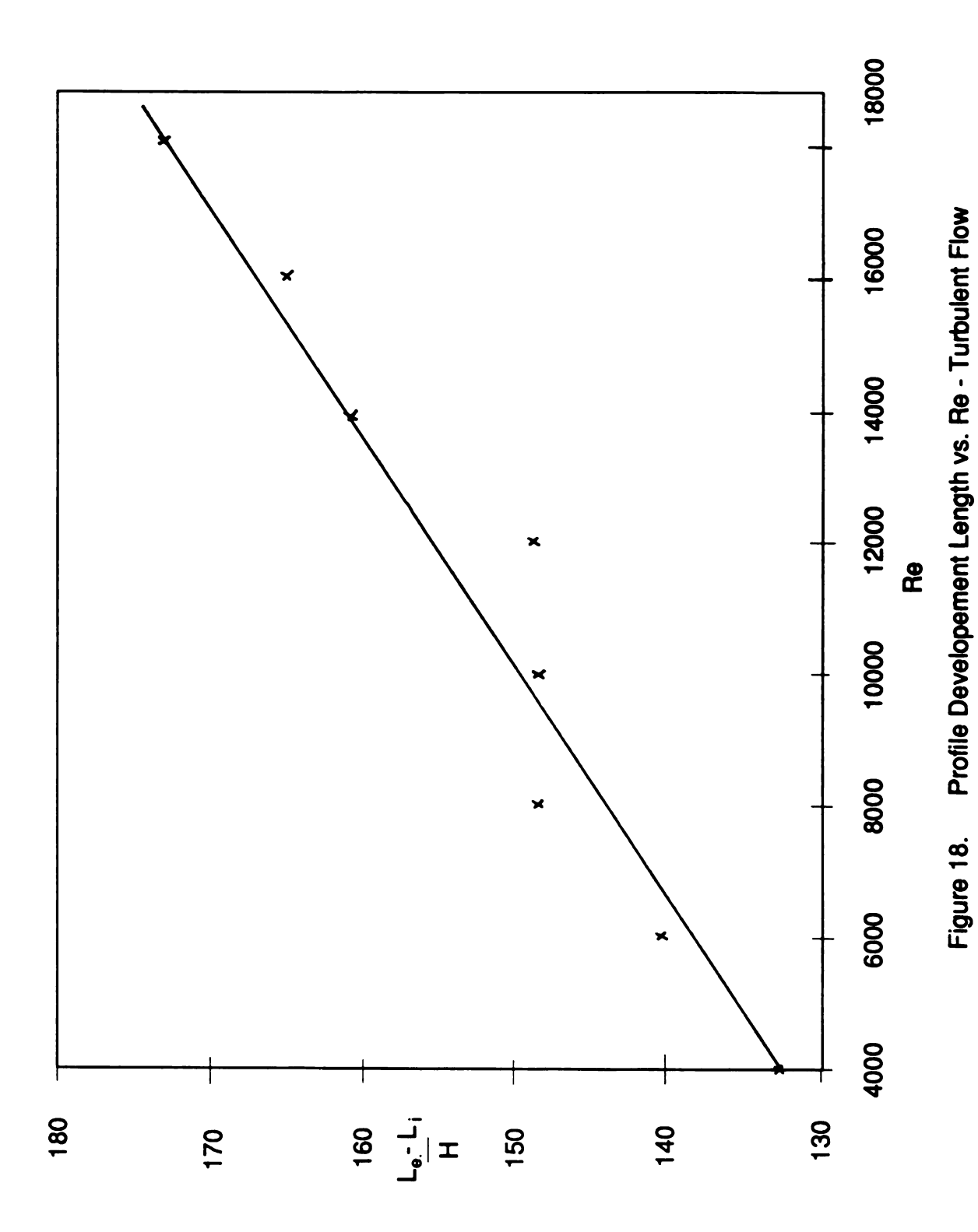


Figure 17. Established Turbulence Length, Lst, vs. Re

Reynolds Number



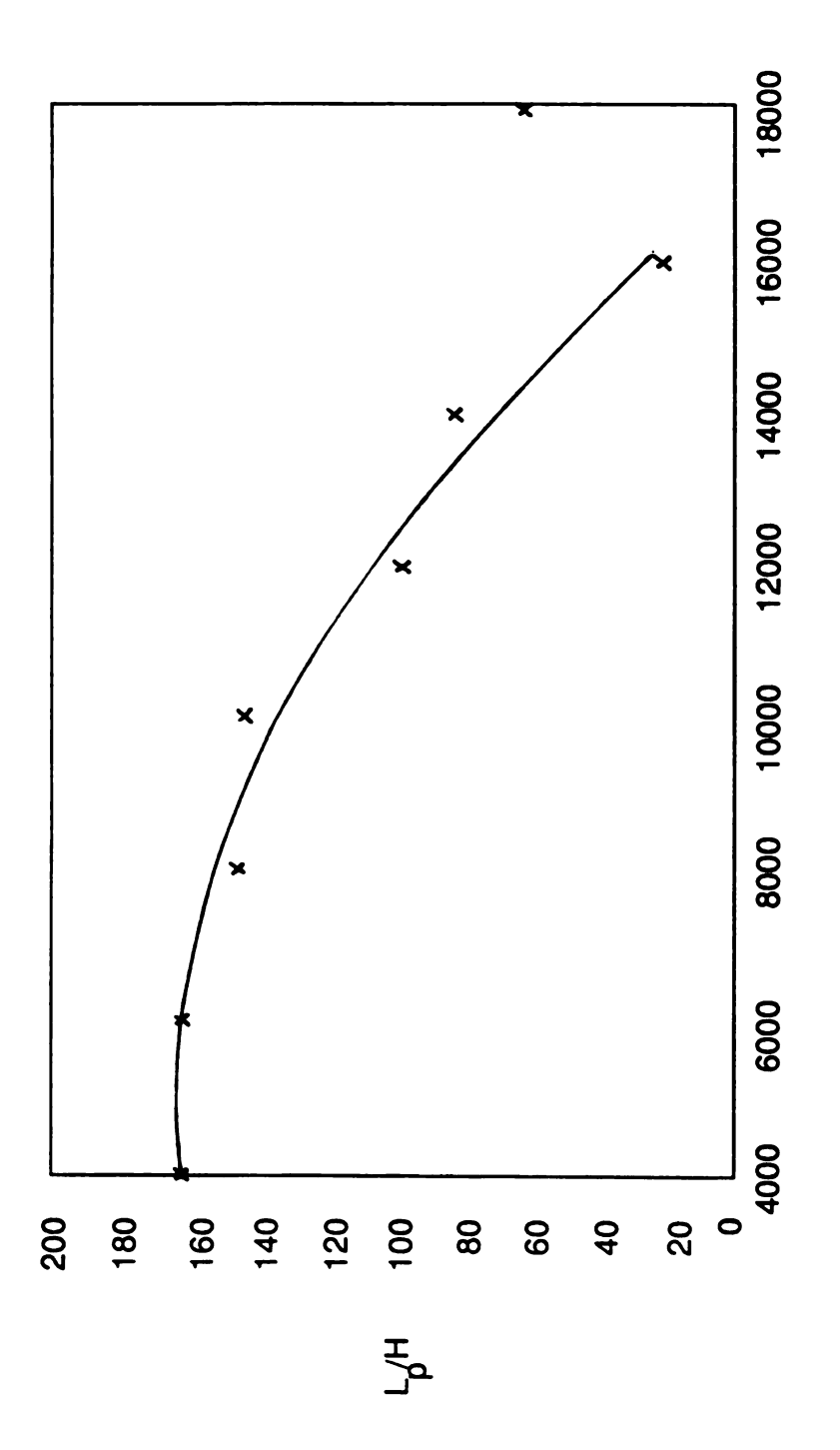


Figure 19. The Distance, Lp, at which the Pressure Gradient attains its fully developed value vs. Re

Reynolds Number

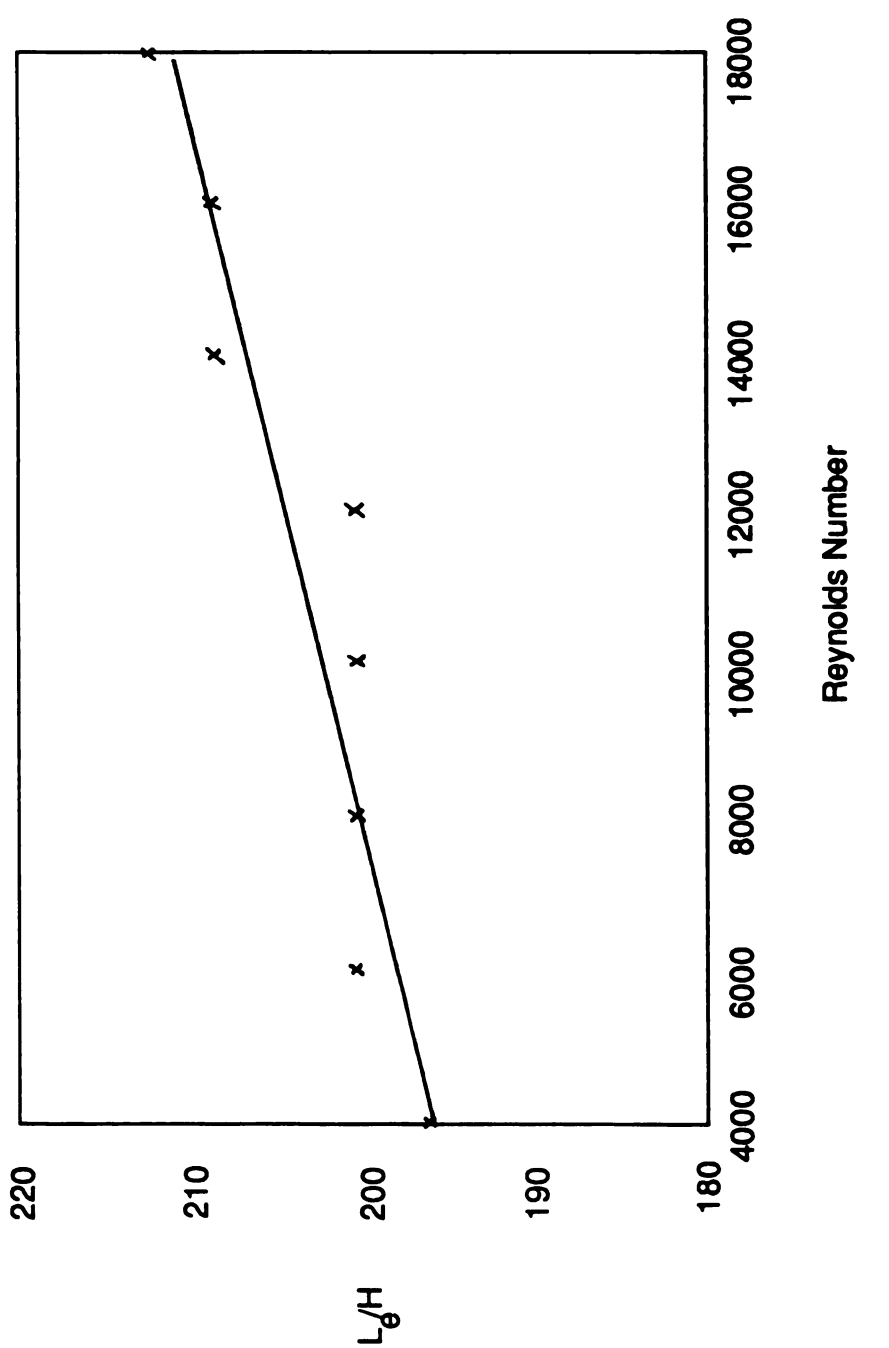


Figure 20. Entrance Length, Le, vs. Re

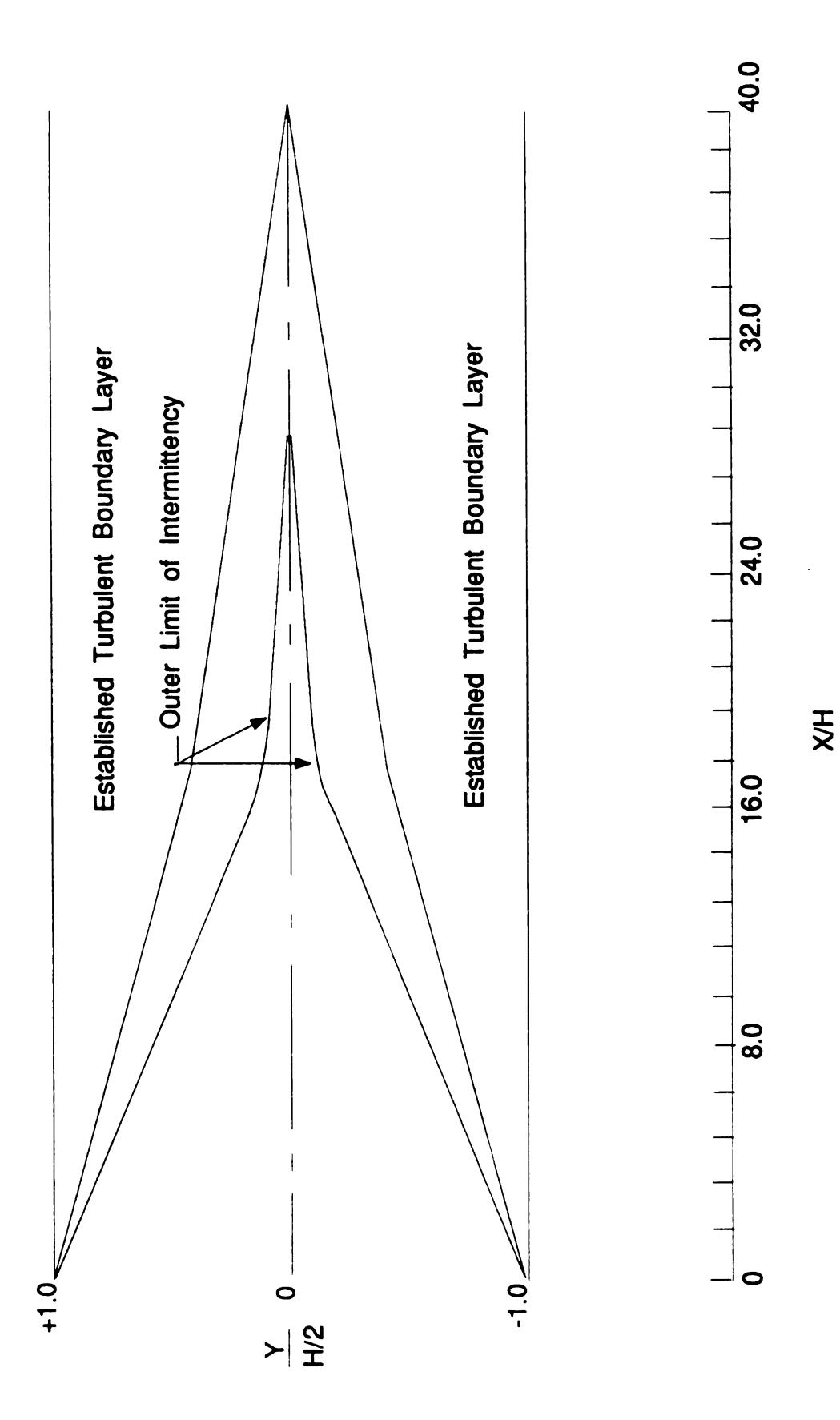
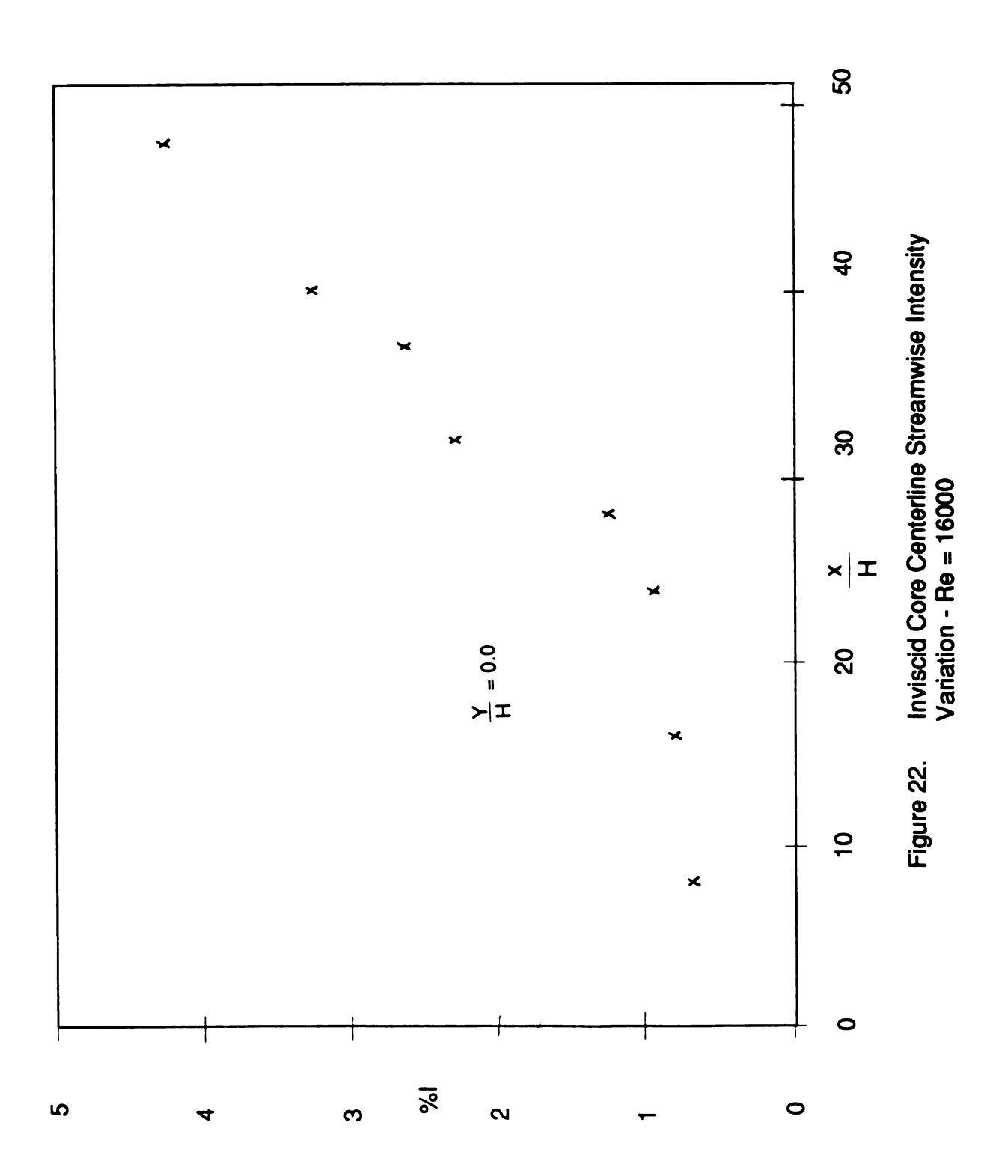
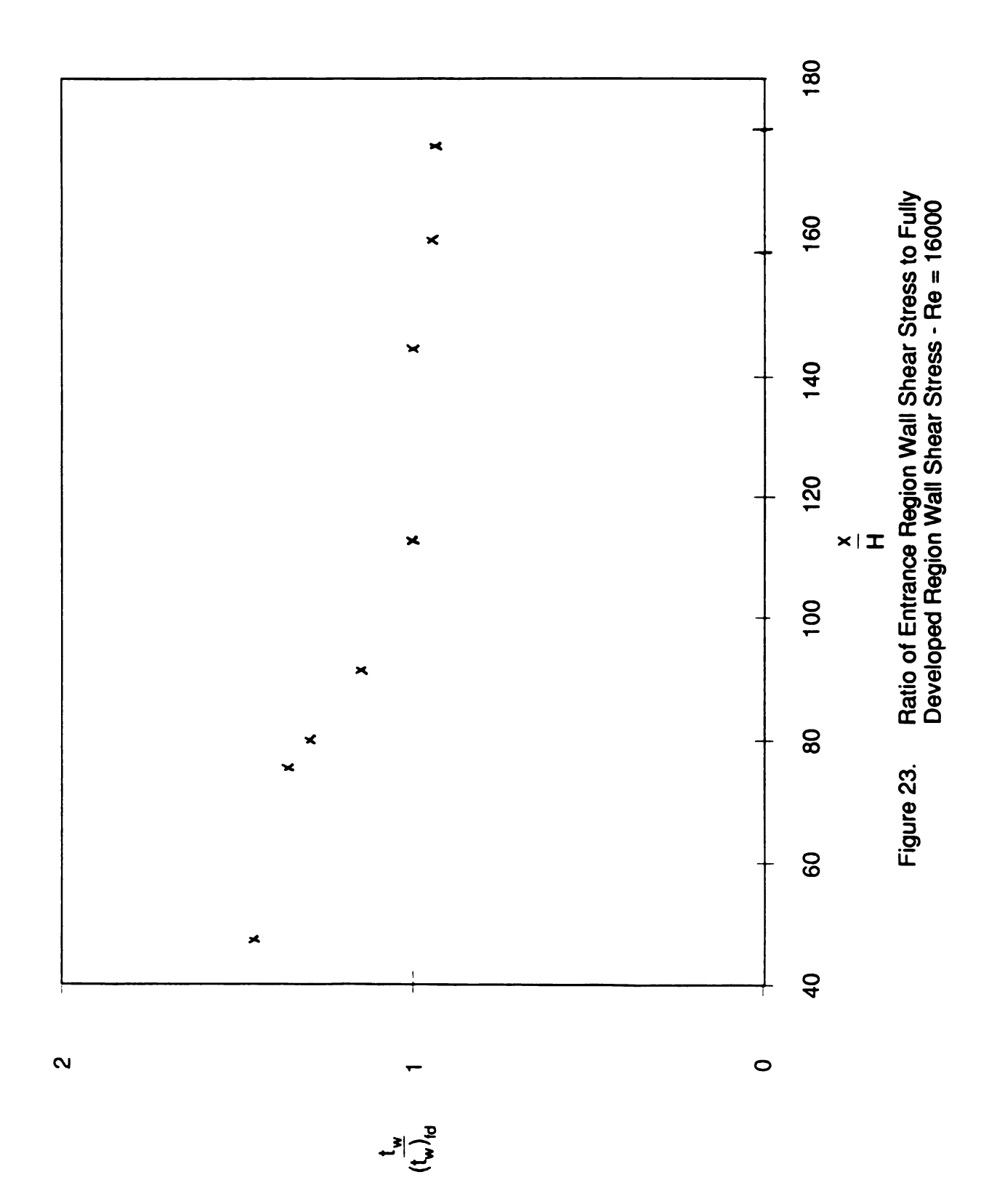


Figure 21. Schematic of Inviscid Core Region - Re = 16000





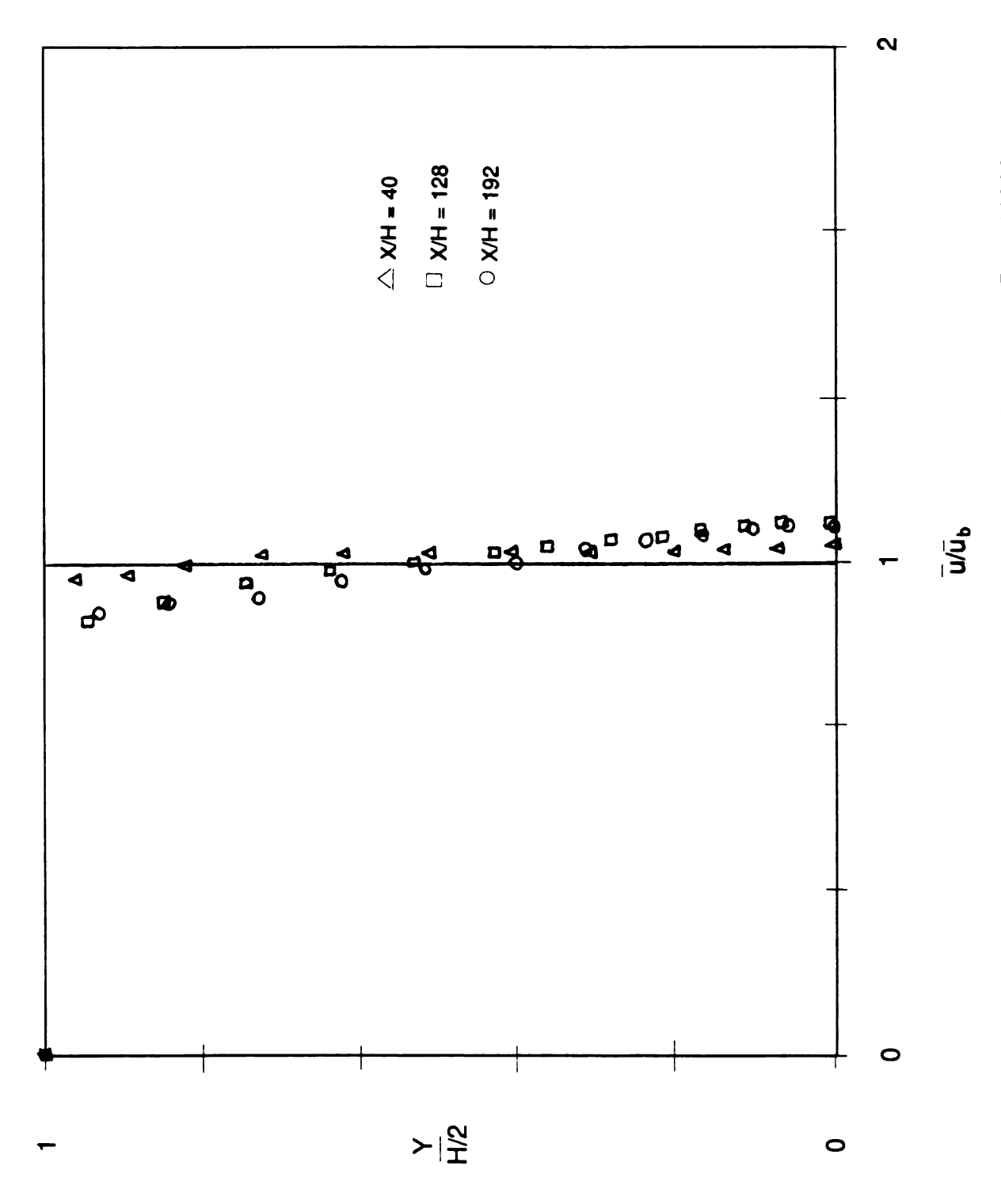


Figure 24. Streamwise Velocity Profile Developement -Re = 16000

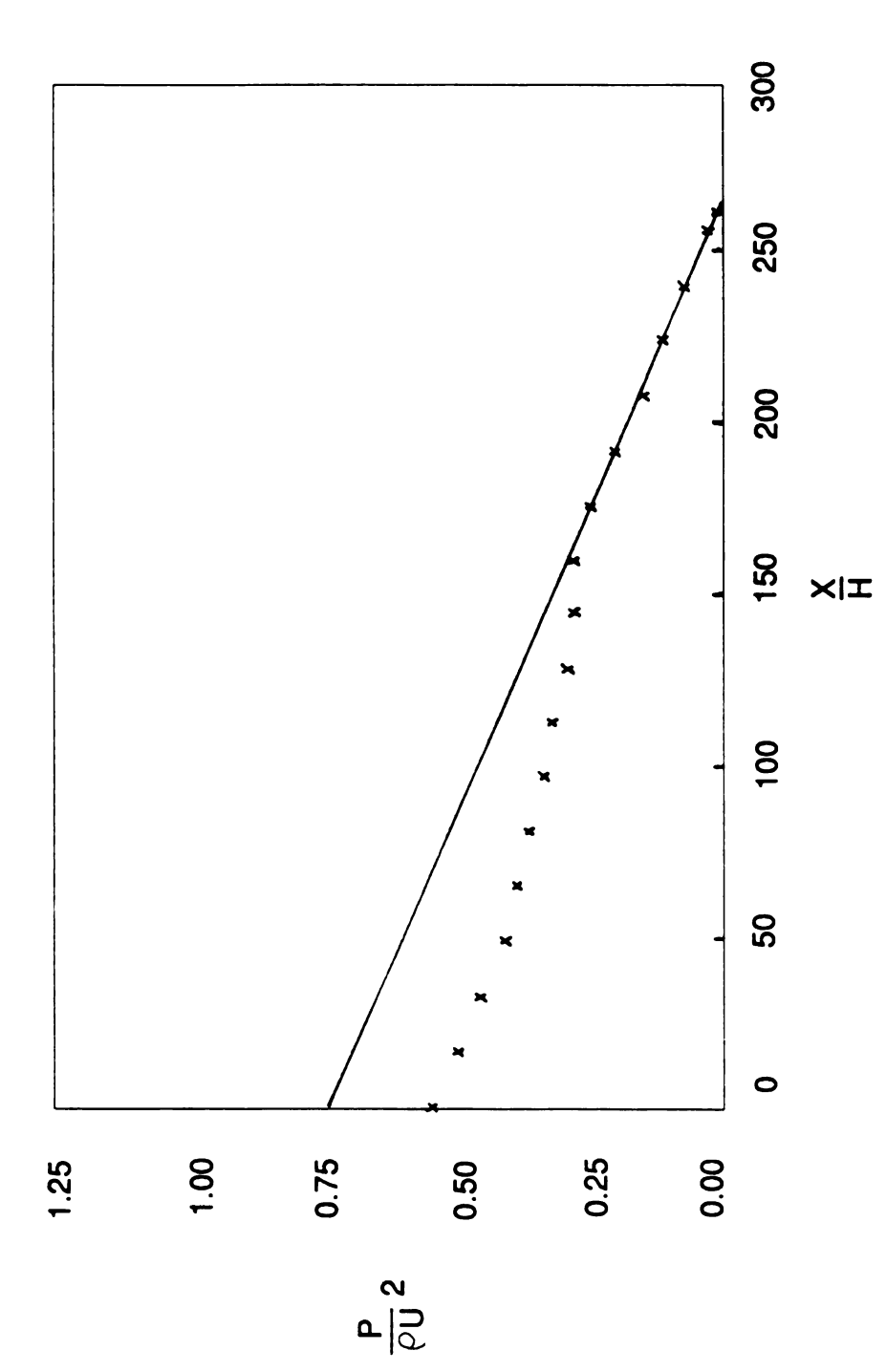
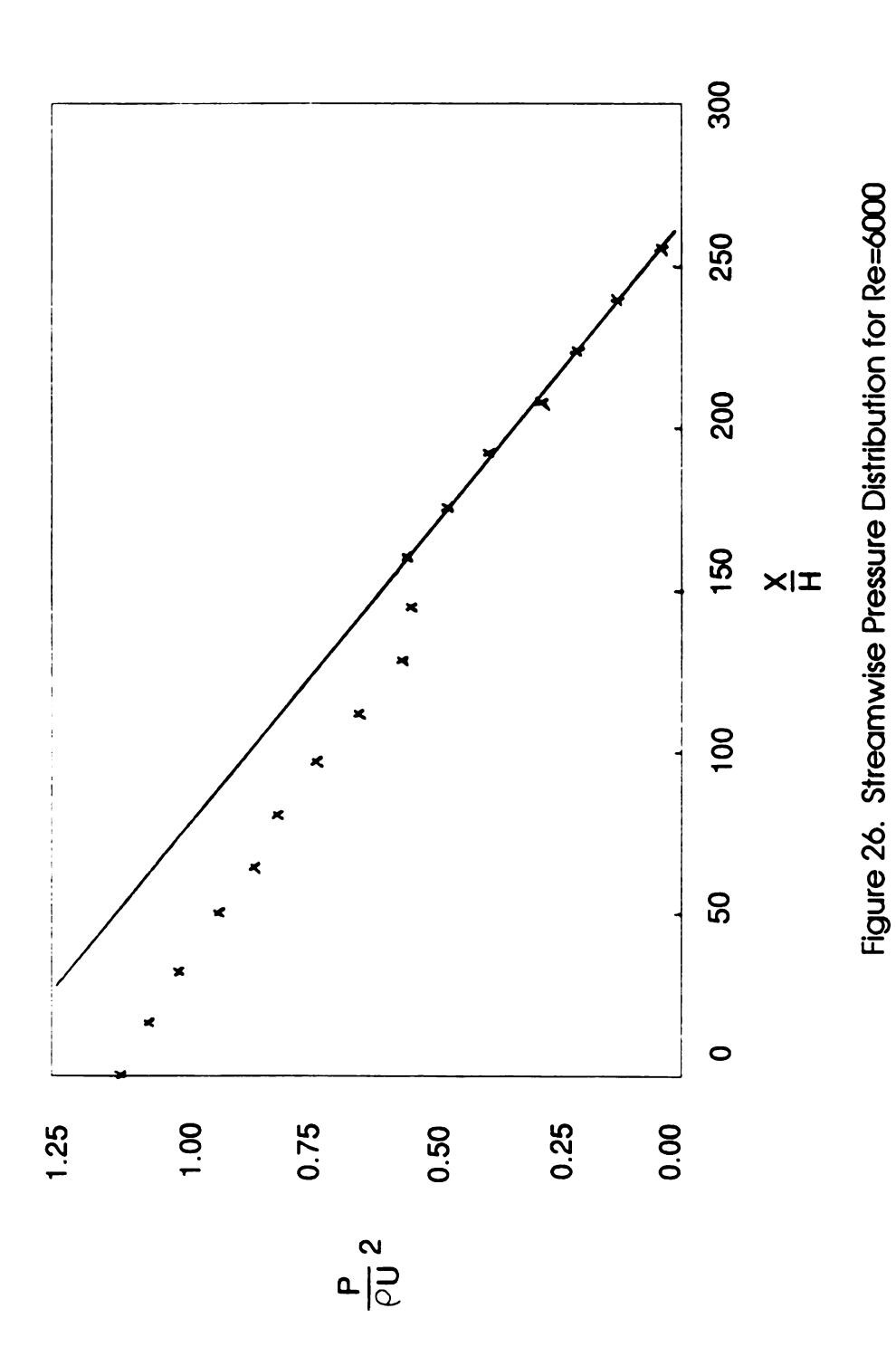


Figure 25. Streamwise Pressure Distribution for Re=4000



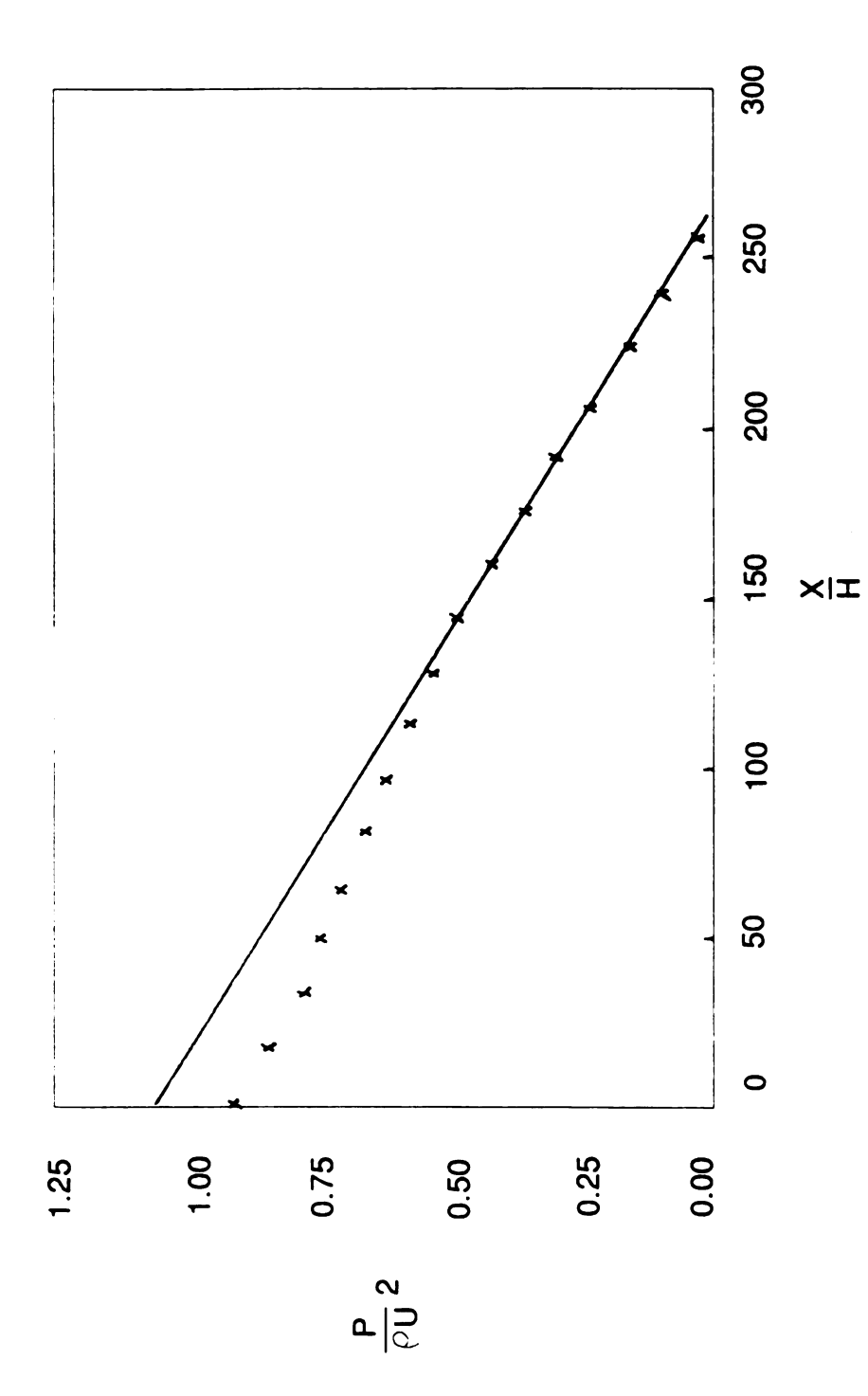


Figure 27. Streamwise Pressure Distribution for Re=8000

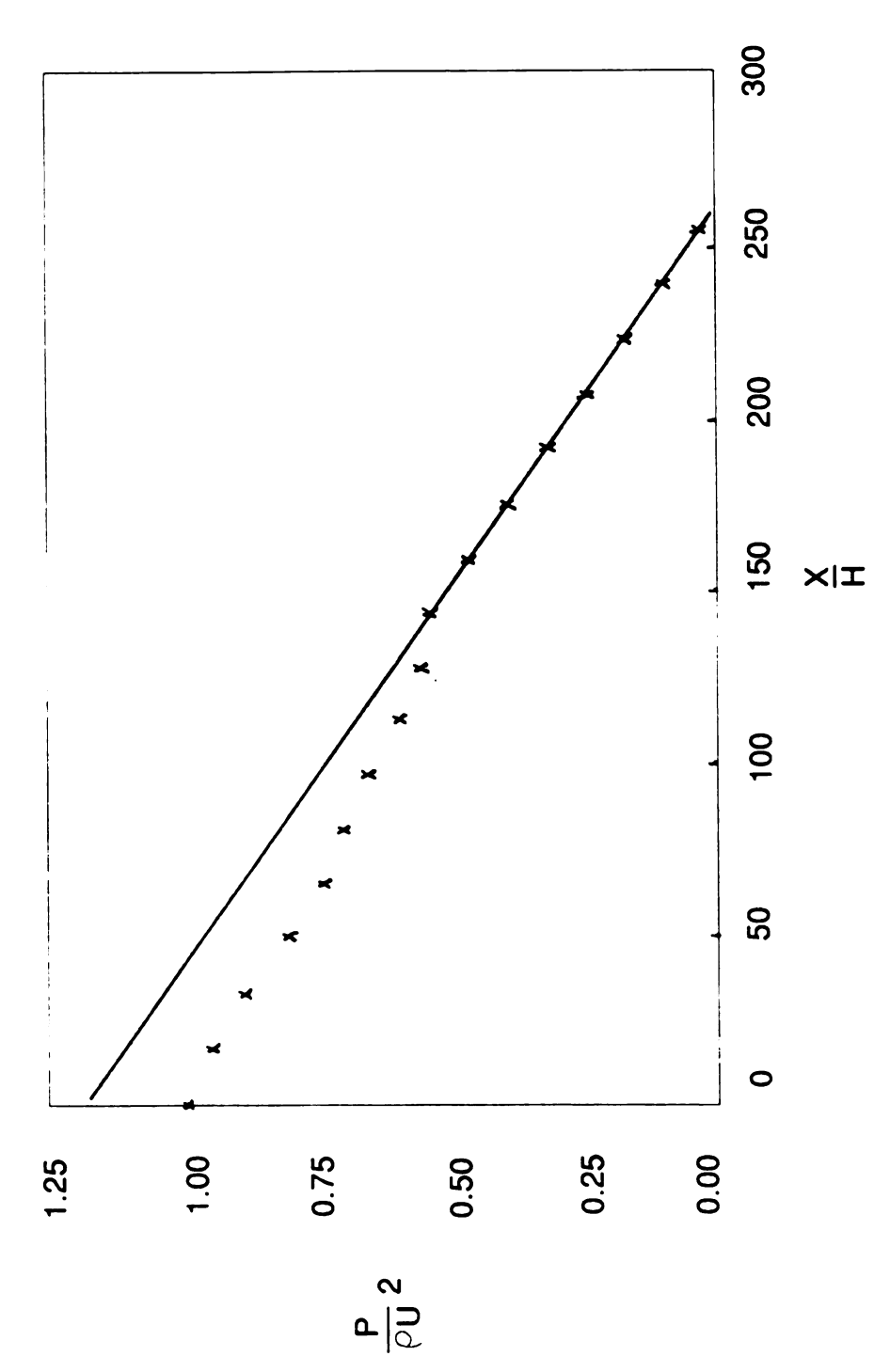


Figure 28. Streamwise Pressure Distribution for Re=10,000

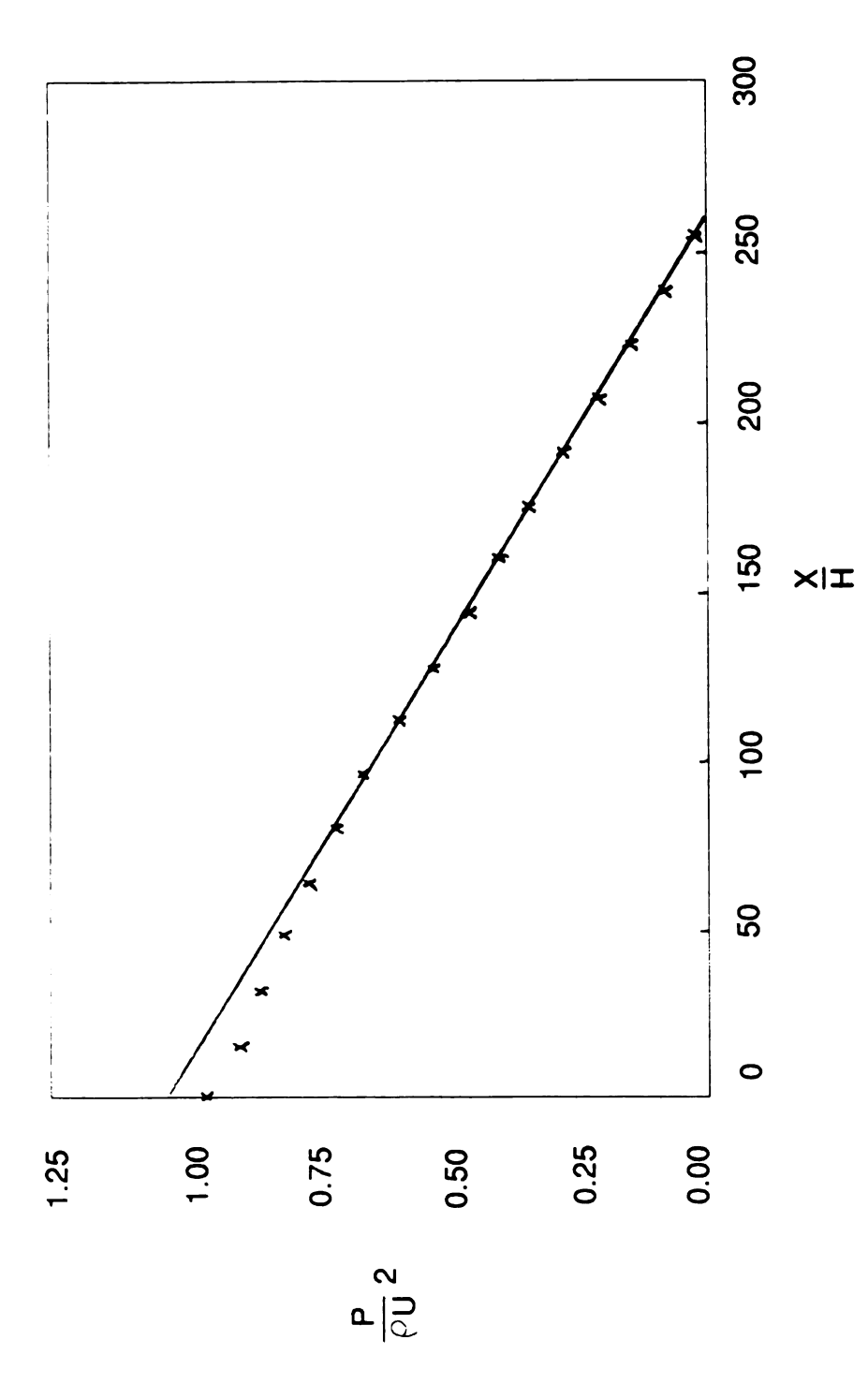


Figure 29. Streamwise Pressure Distribution for Re=12,000

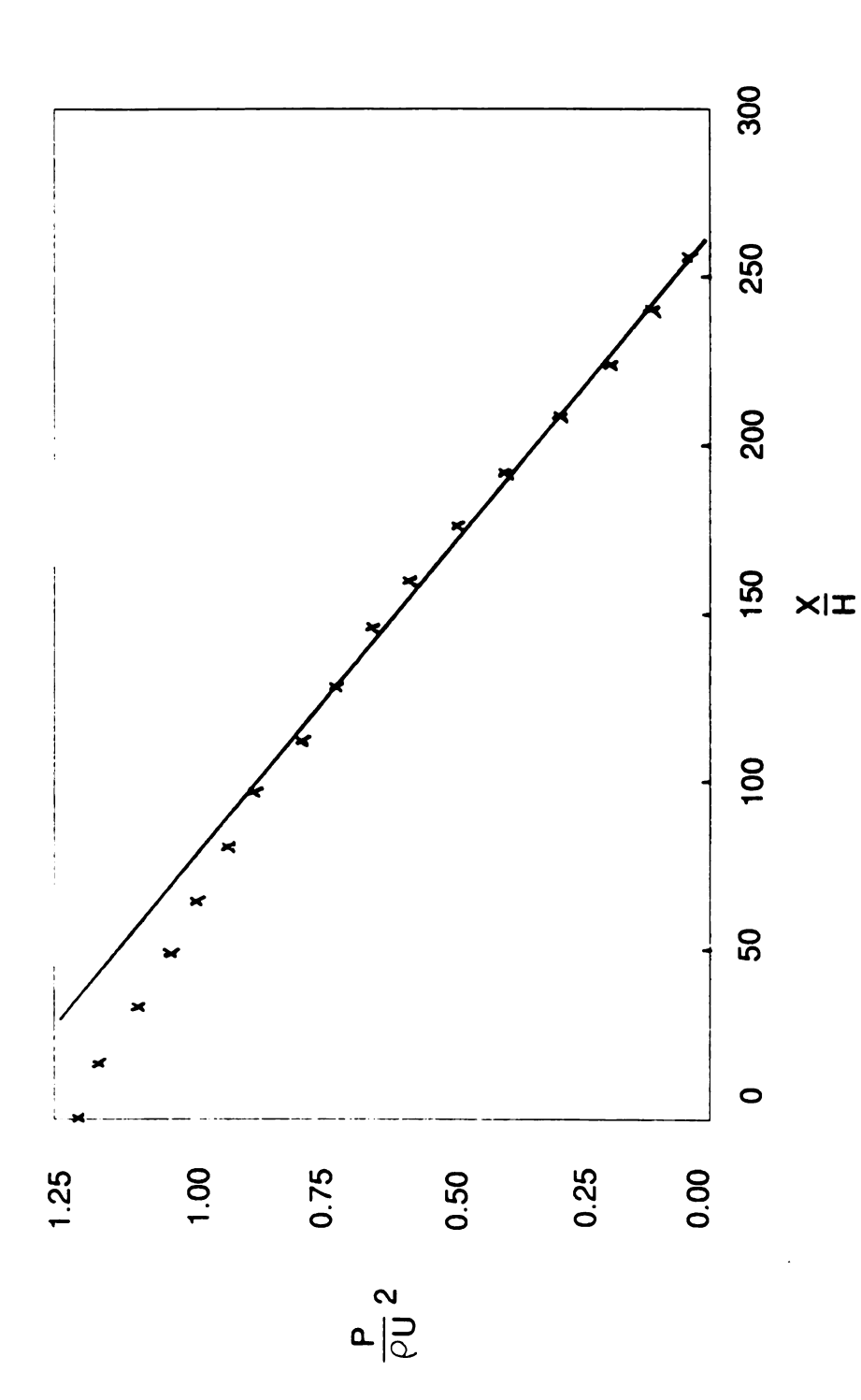


Figure 30. Streamwise Pressure Distribution for Re=14,000

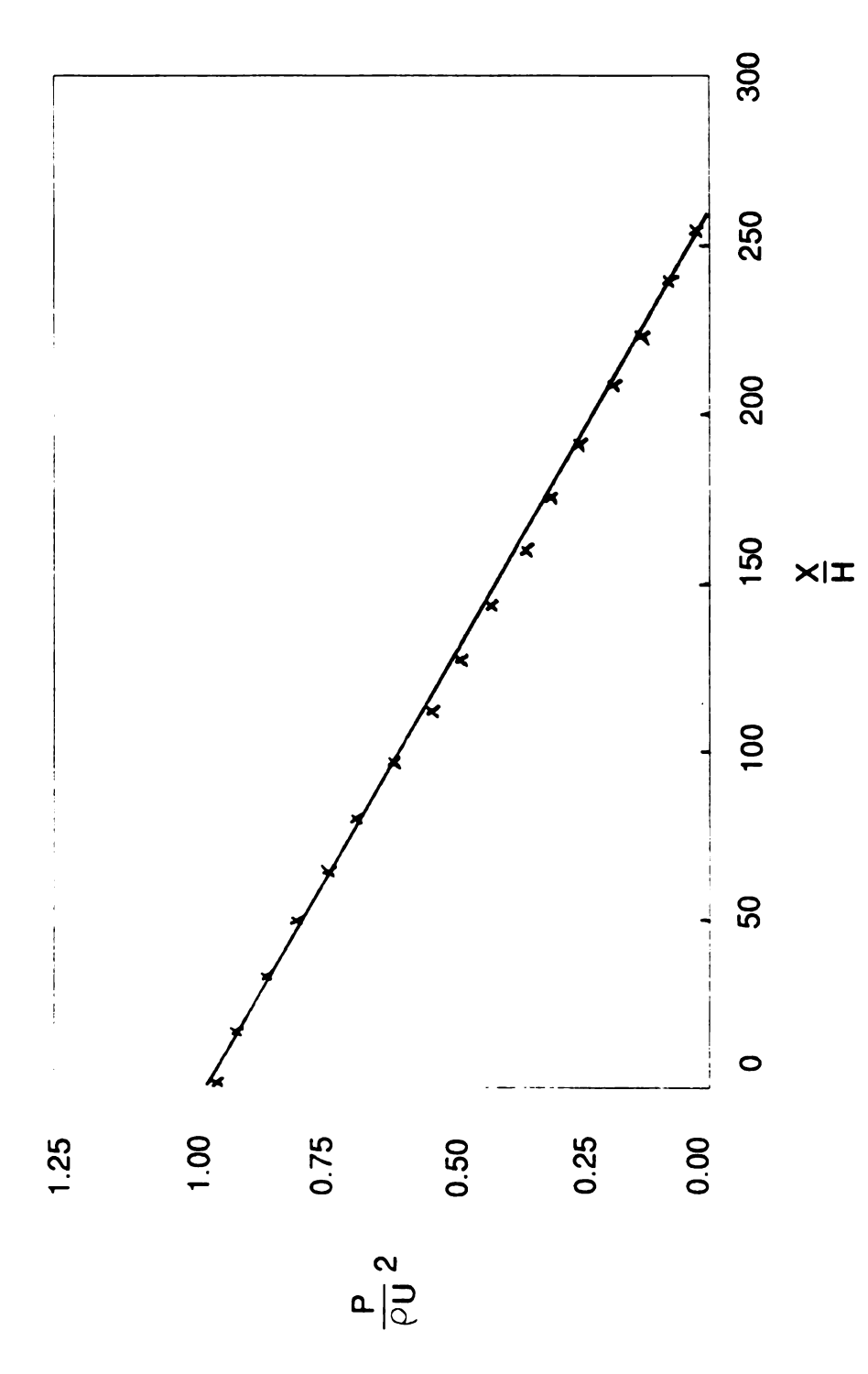


Figure 31. Streamwise Pressure Distribution for Re=16,000

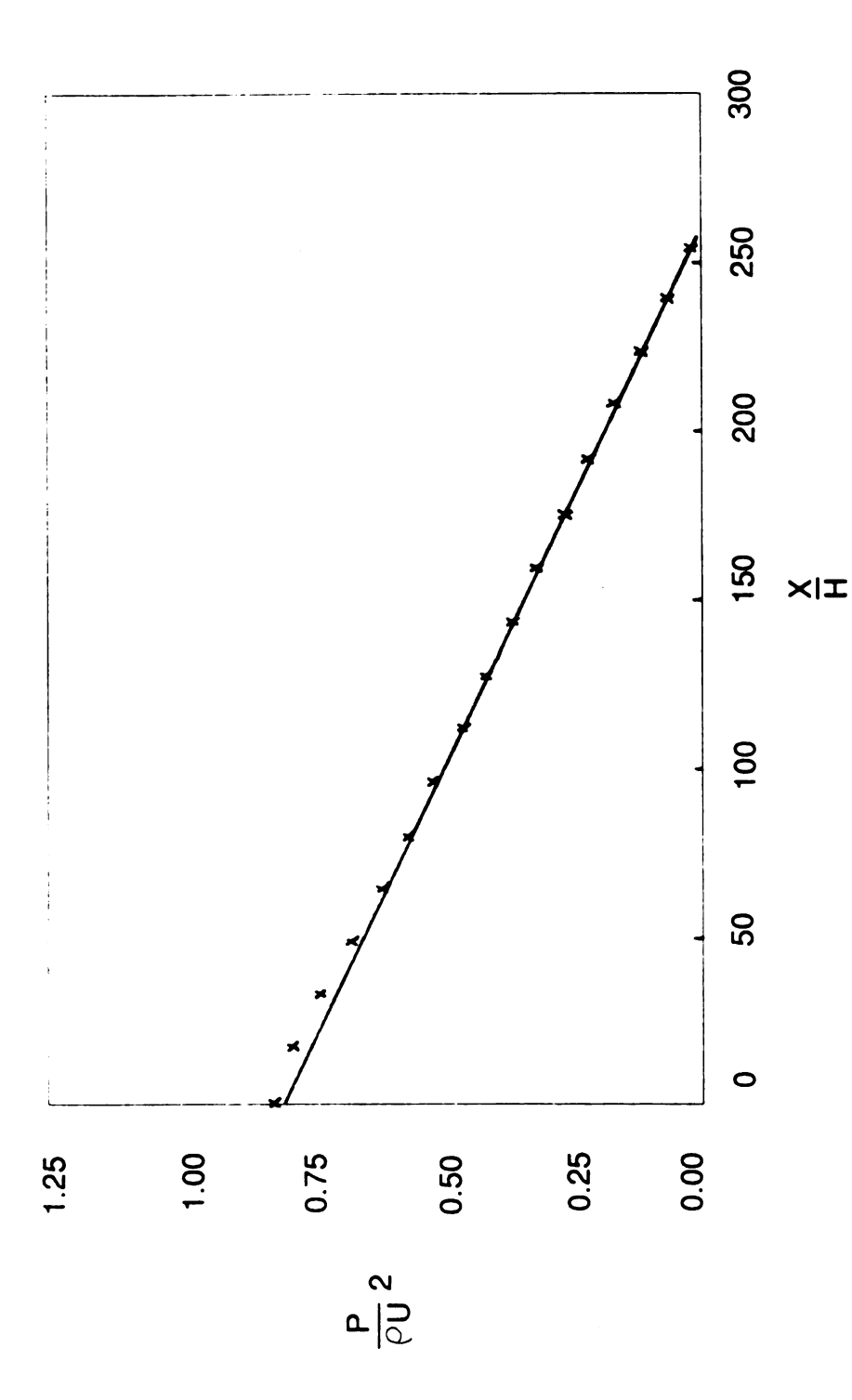
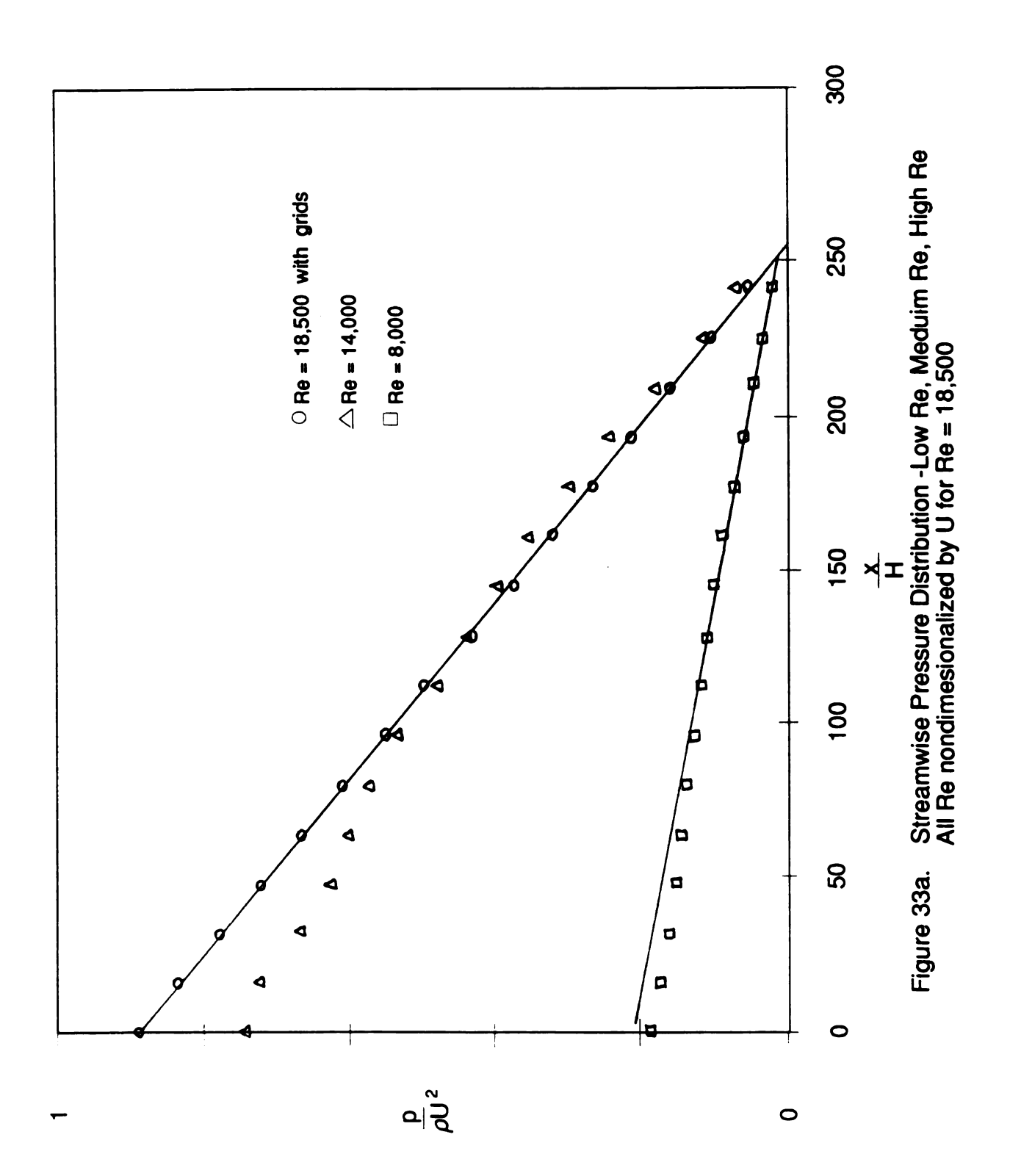


Figure 32. Streamwise Pressure Distribution for Re=18,000



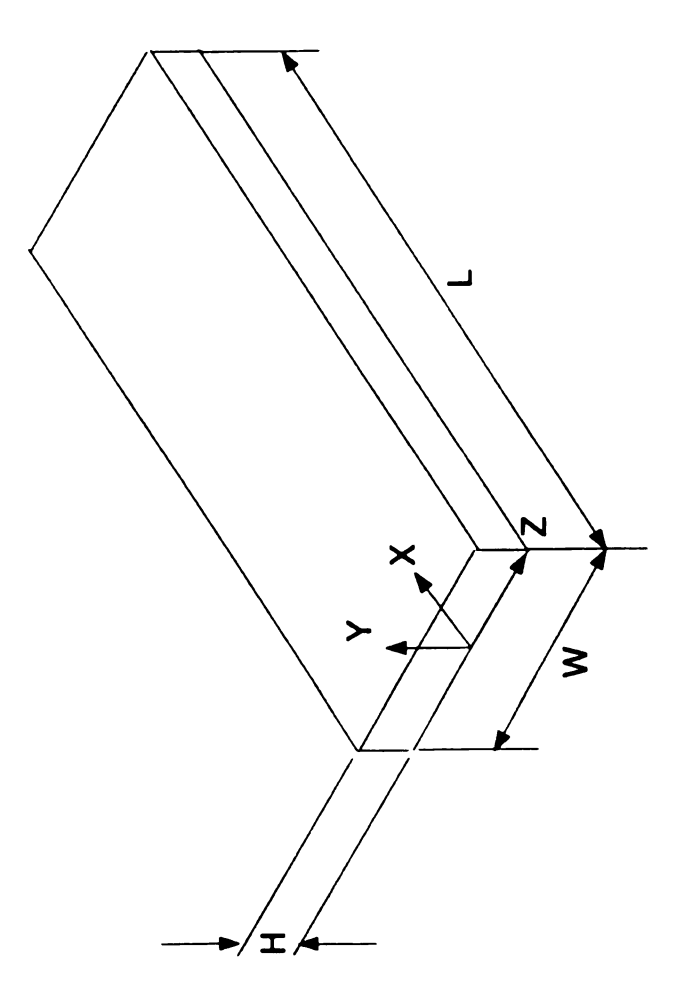


Figure 33. Experimental Channel 3-D View

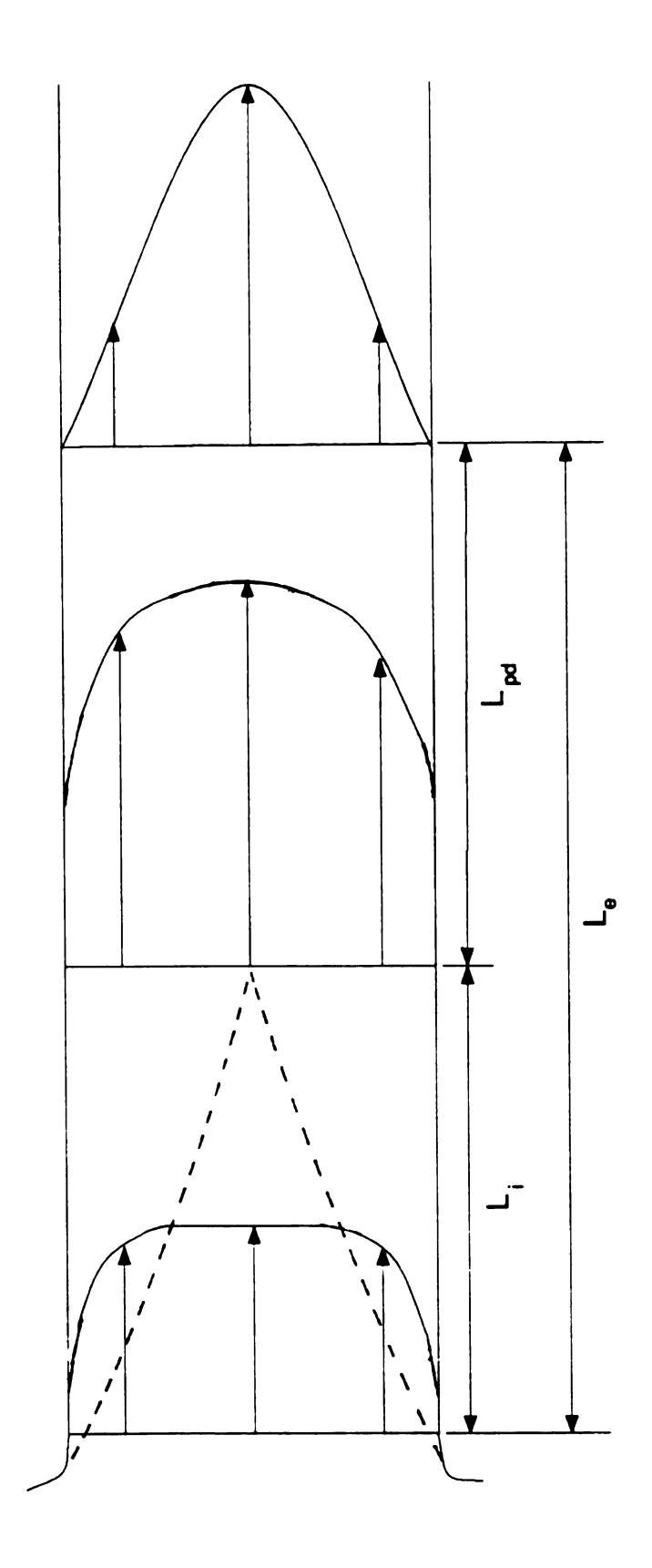
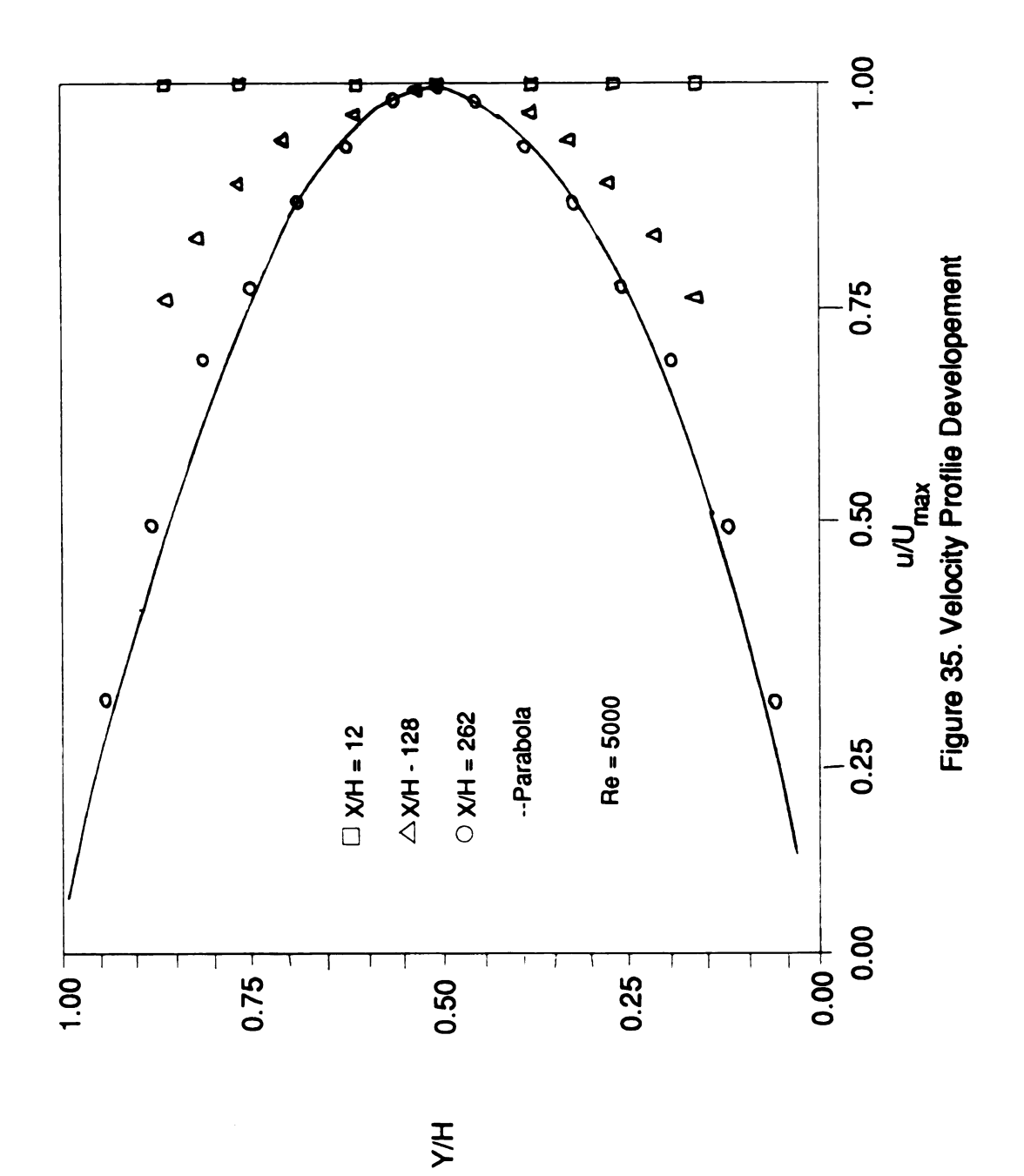


Figure 34. Laminar Flow Entrance Region.



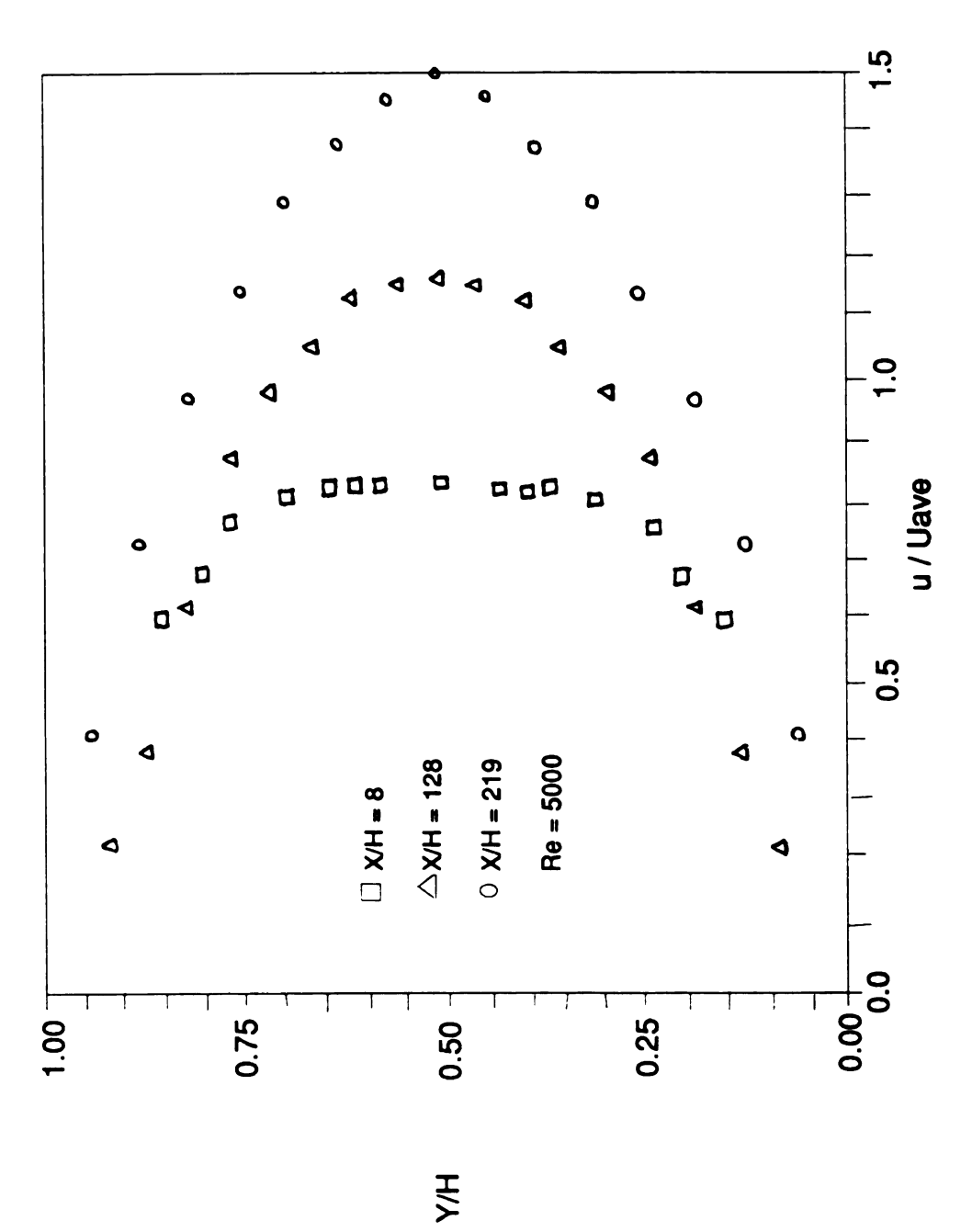
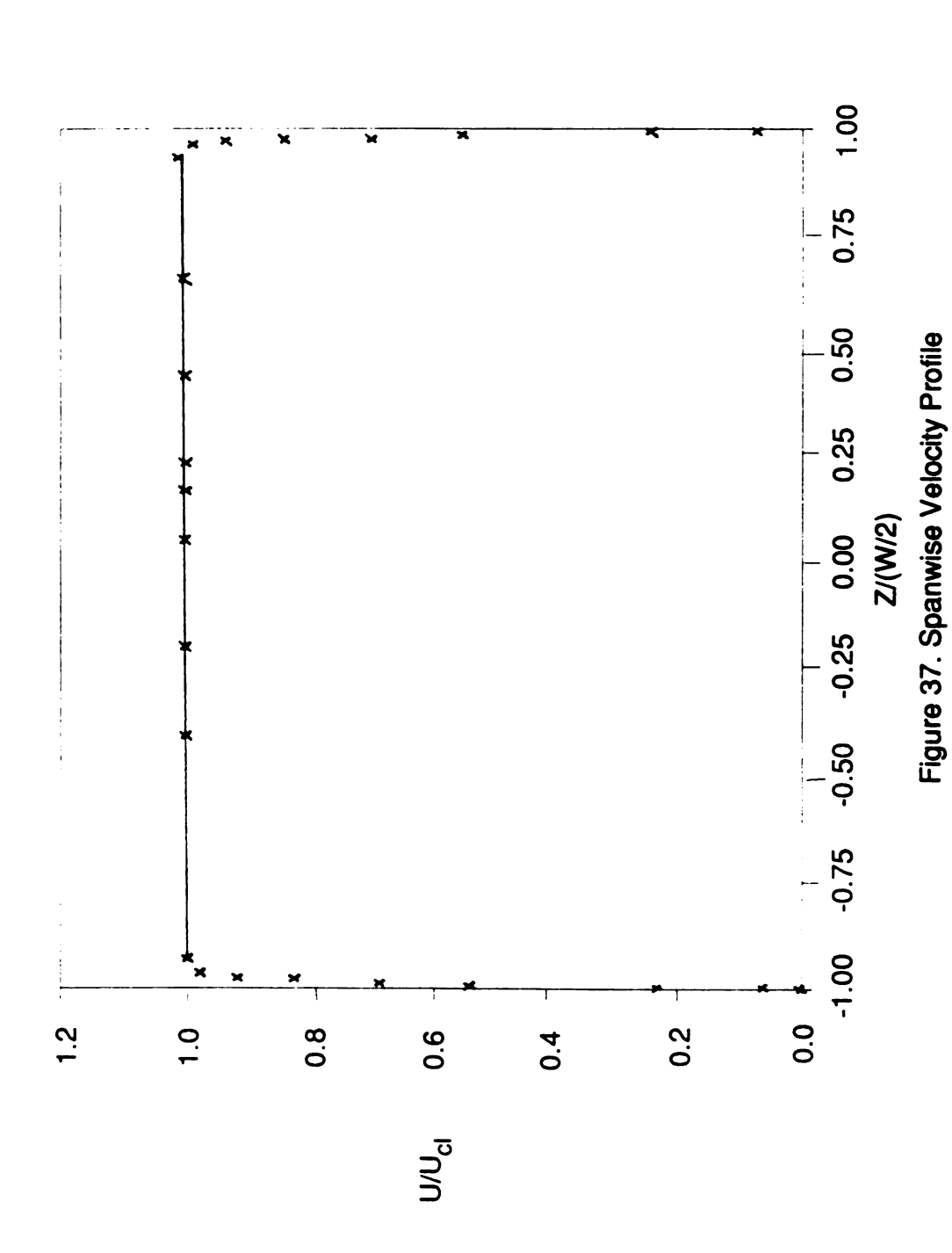


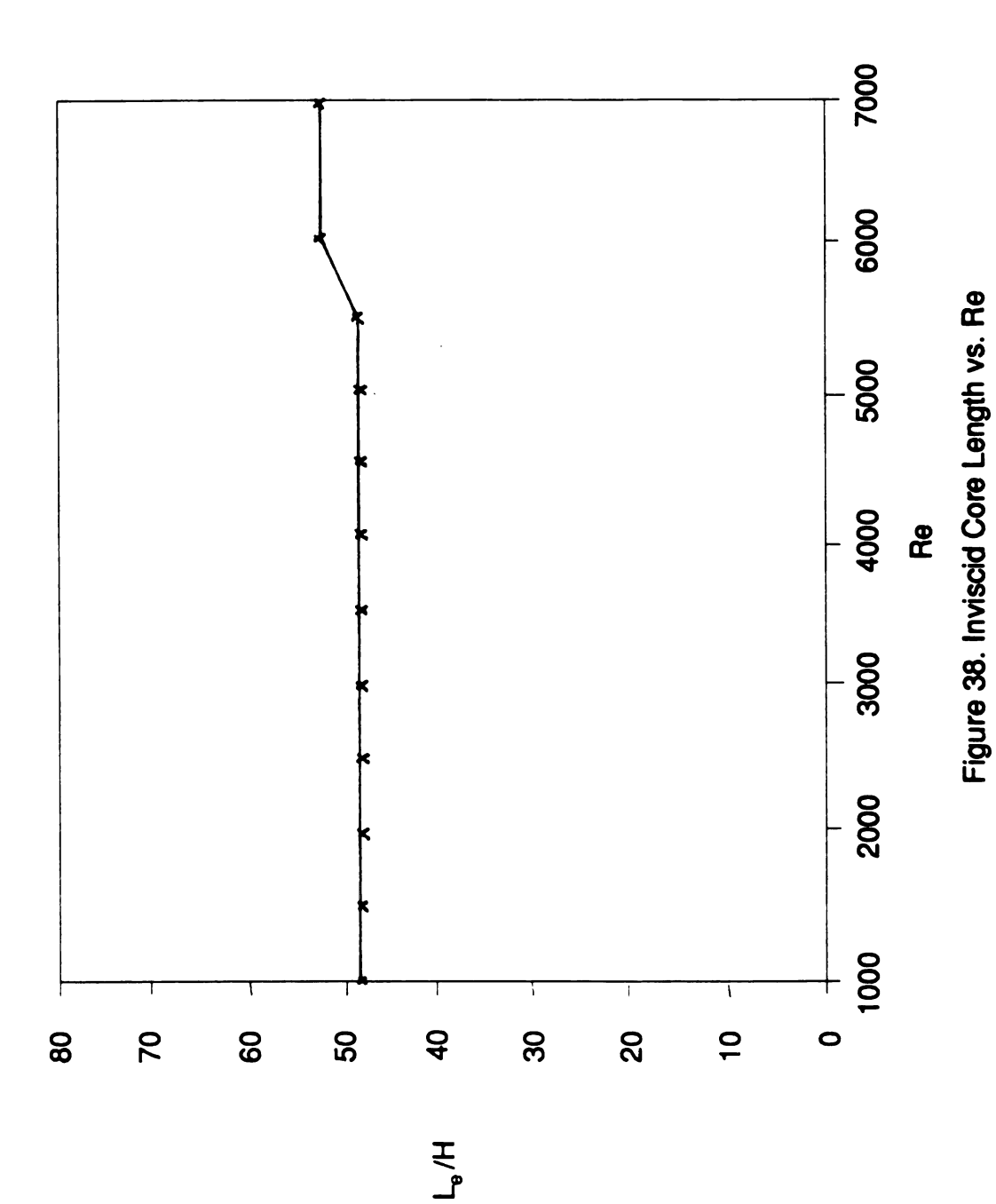
Figure 36. Velocity Proflie Developement

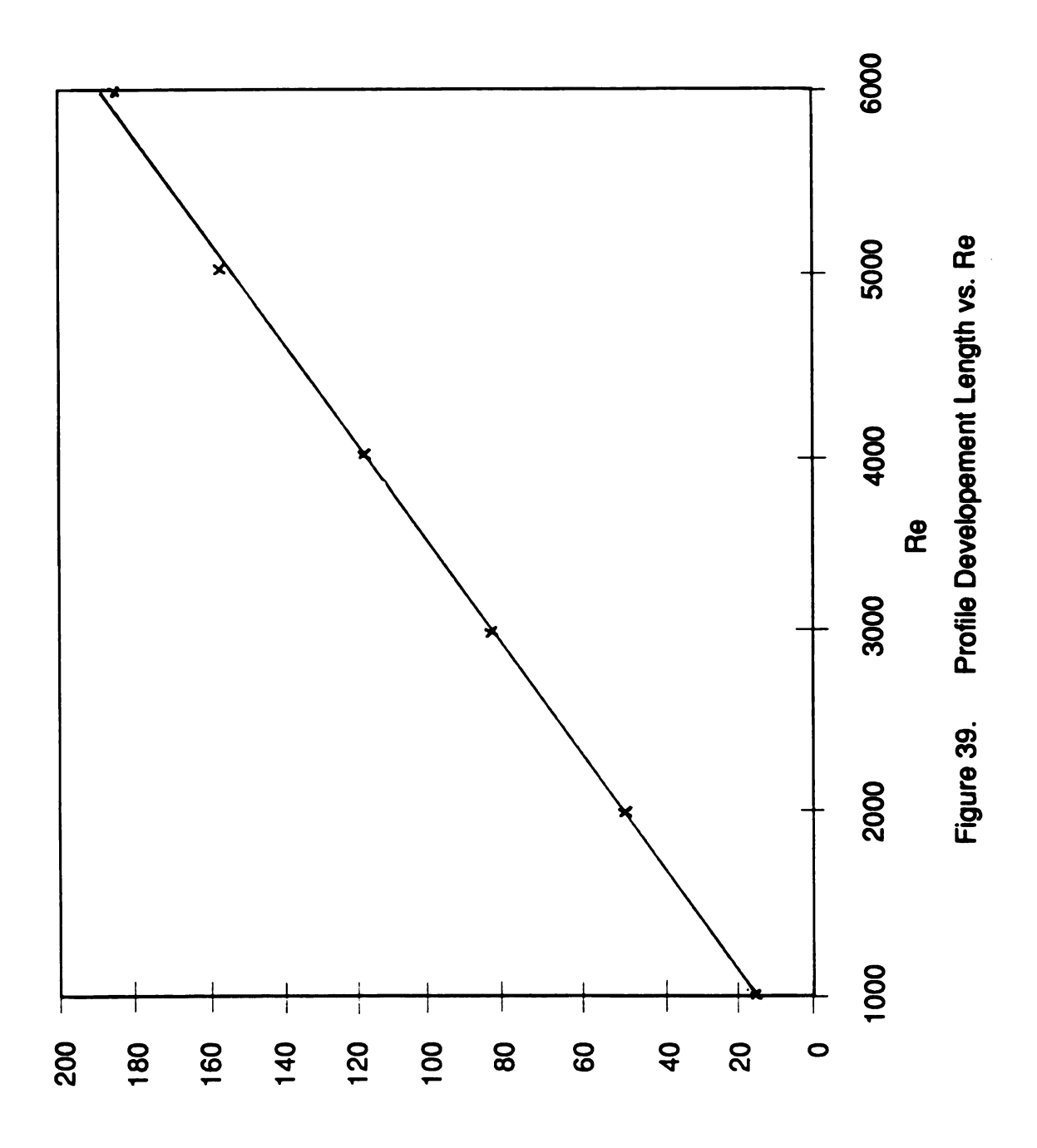
X/H = 262.4

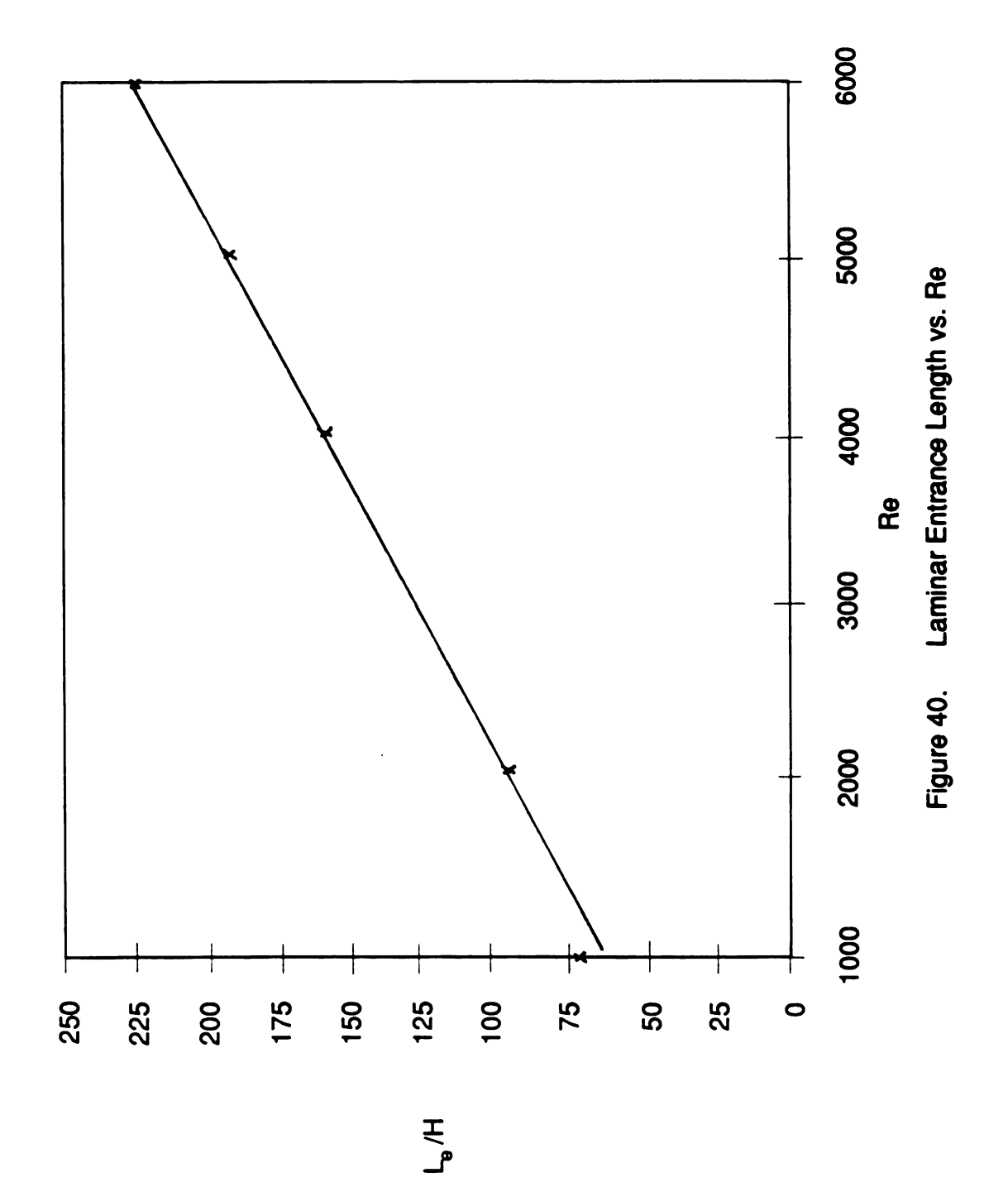
Y/H = 0

Re = 4000









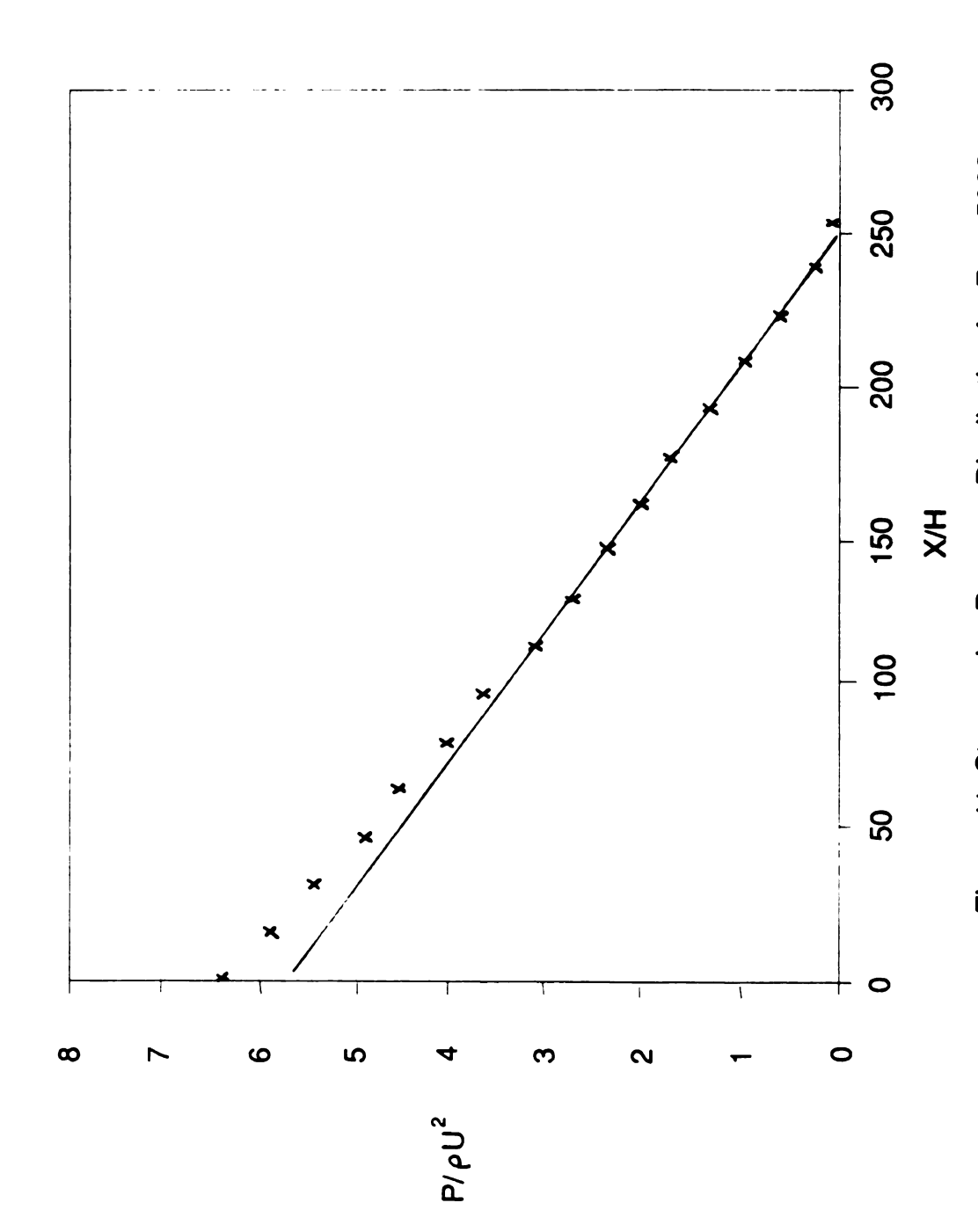


Figure 41. Streamwise Pressure Distribution for Re = 5000

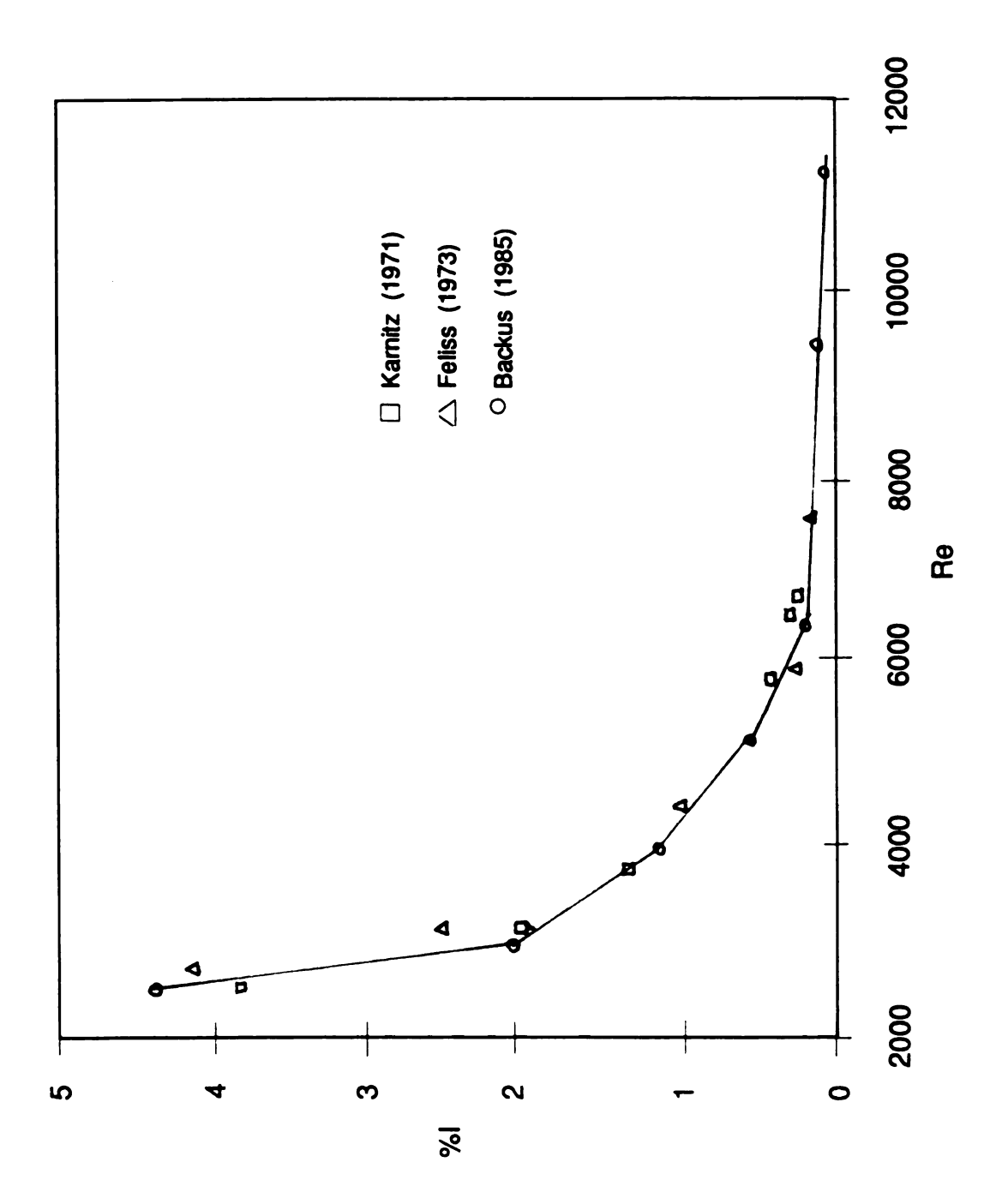
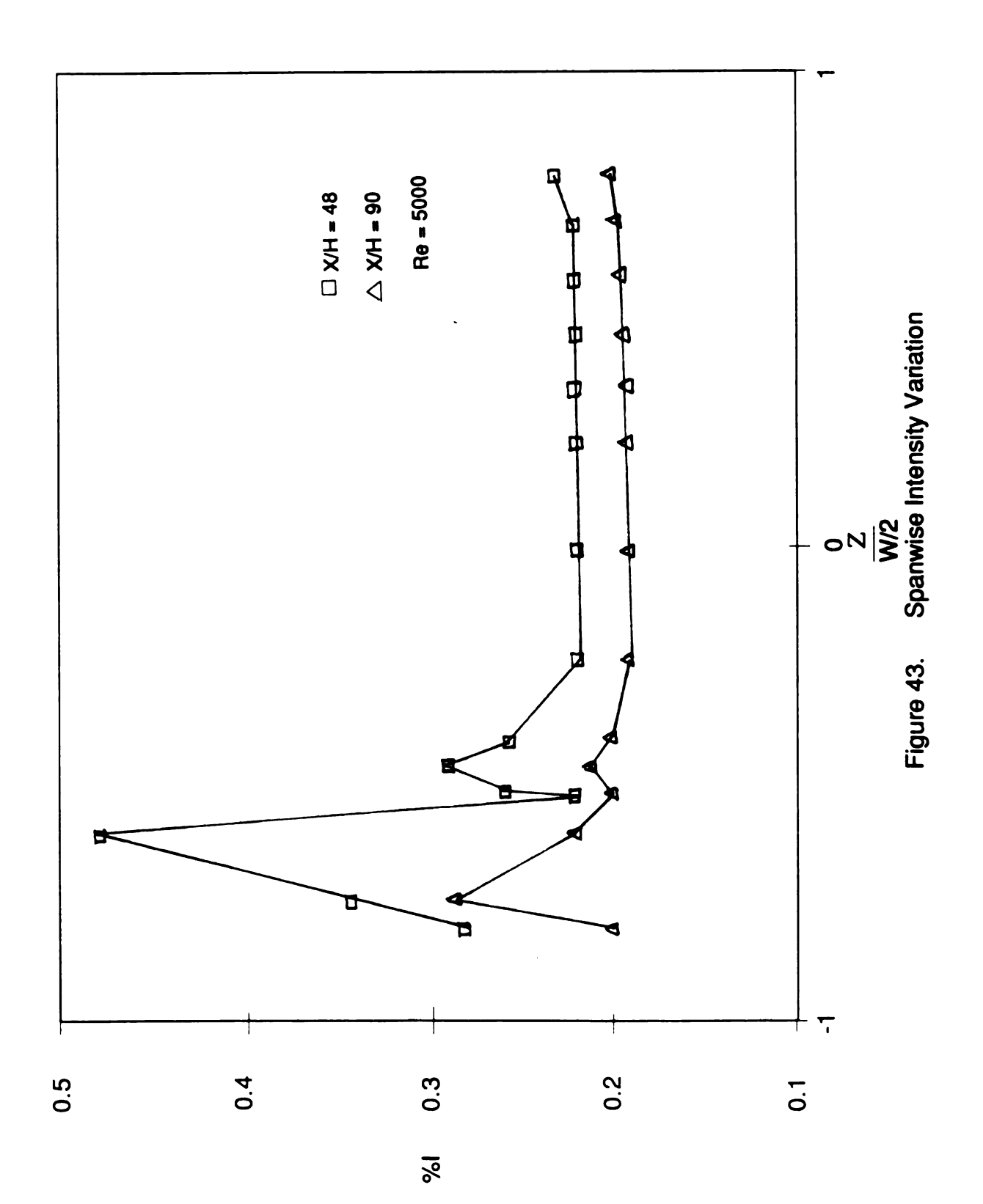
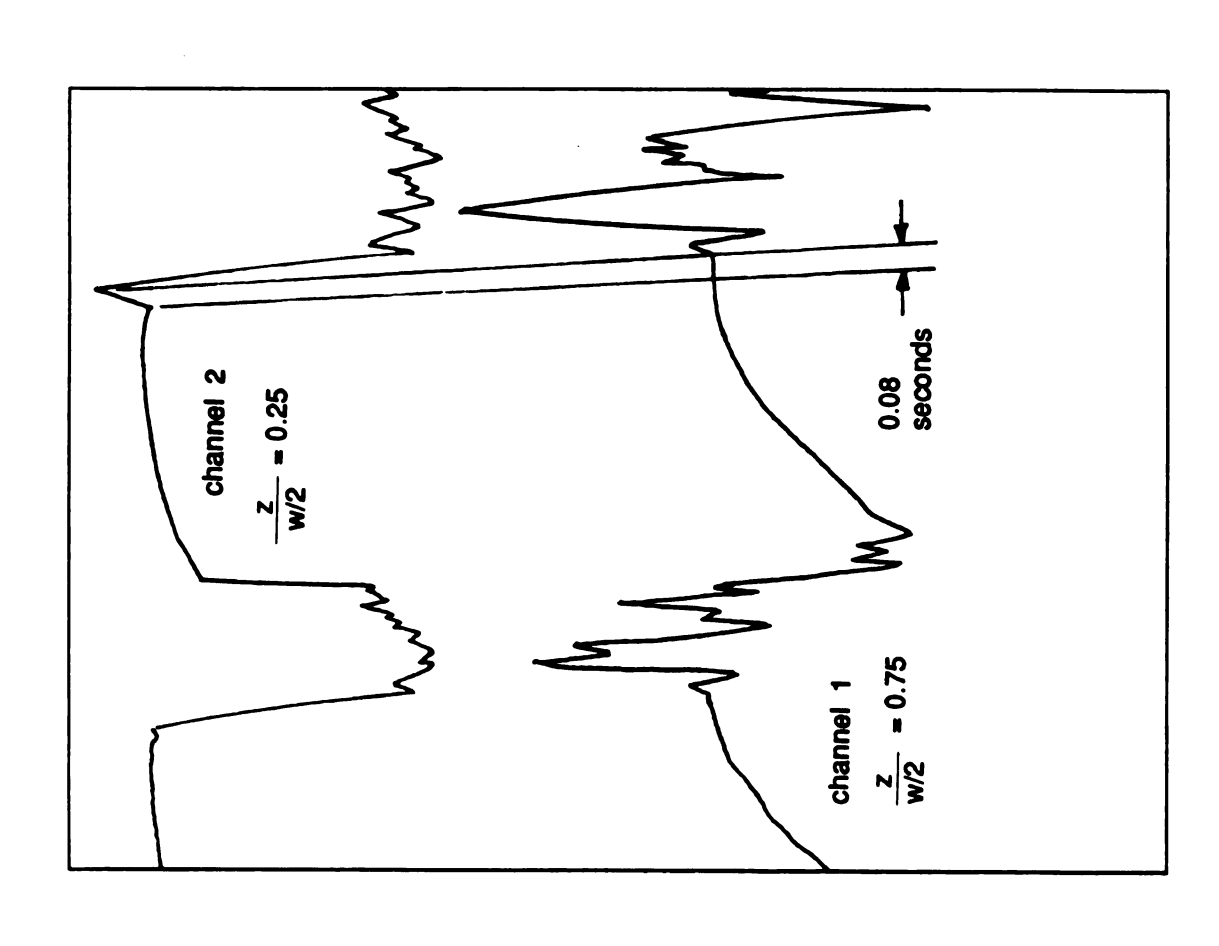


Figure 42. Percent Intensity vs. Critical Reynolds Number





E (volts)

Figure 44. Spanwise Variation of of Bursting

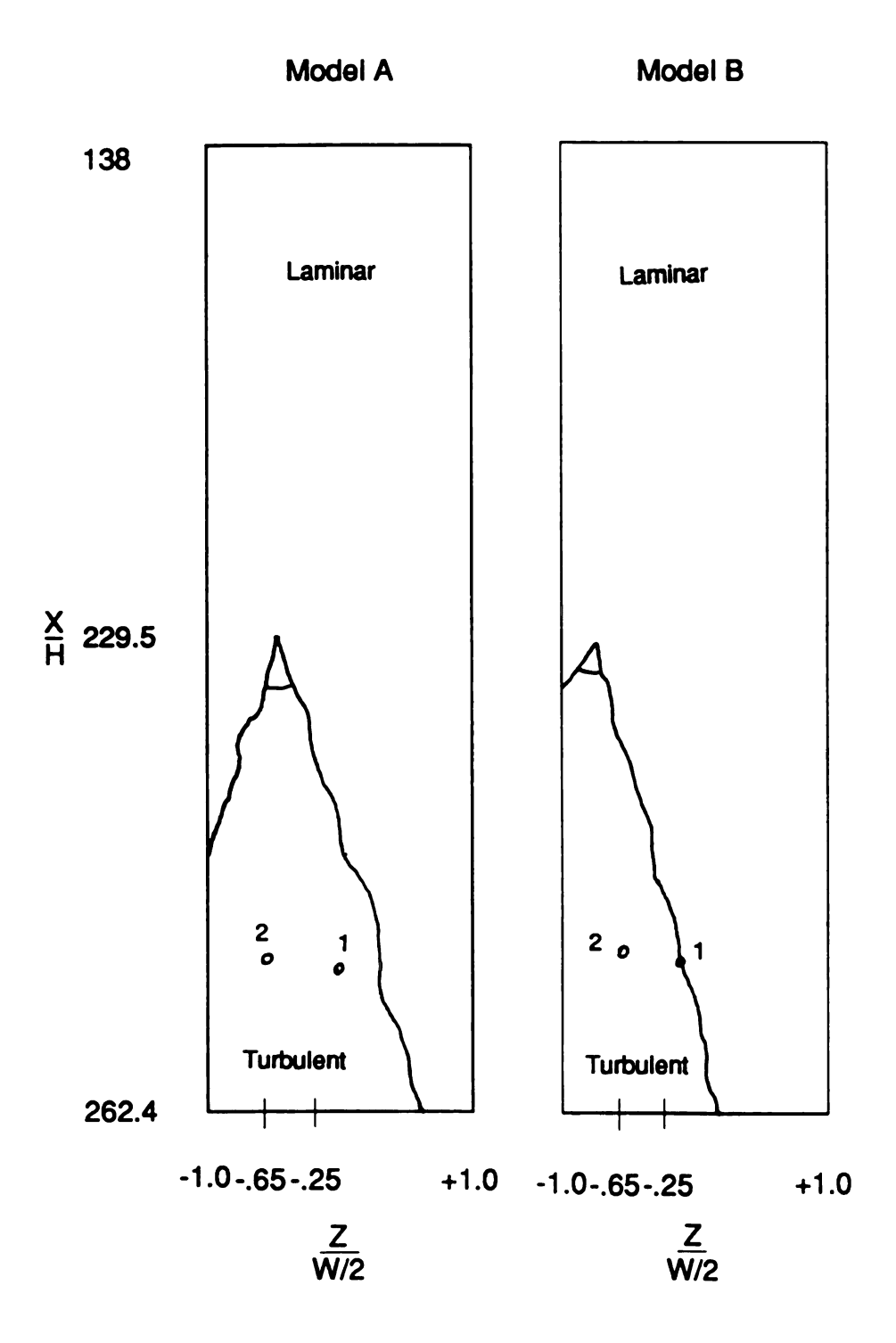


Figure 45. Possible Burst Model

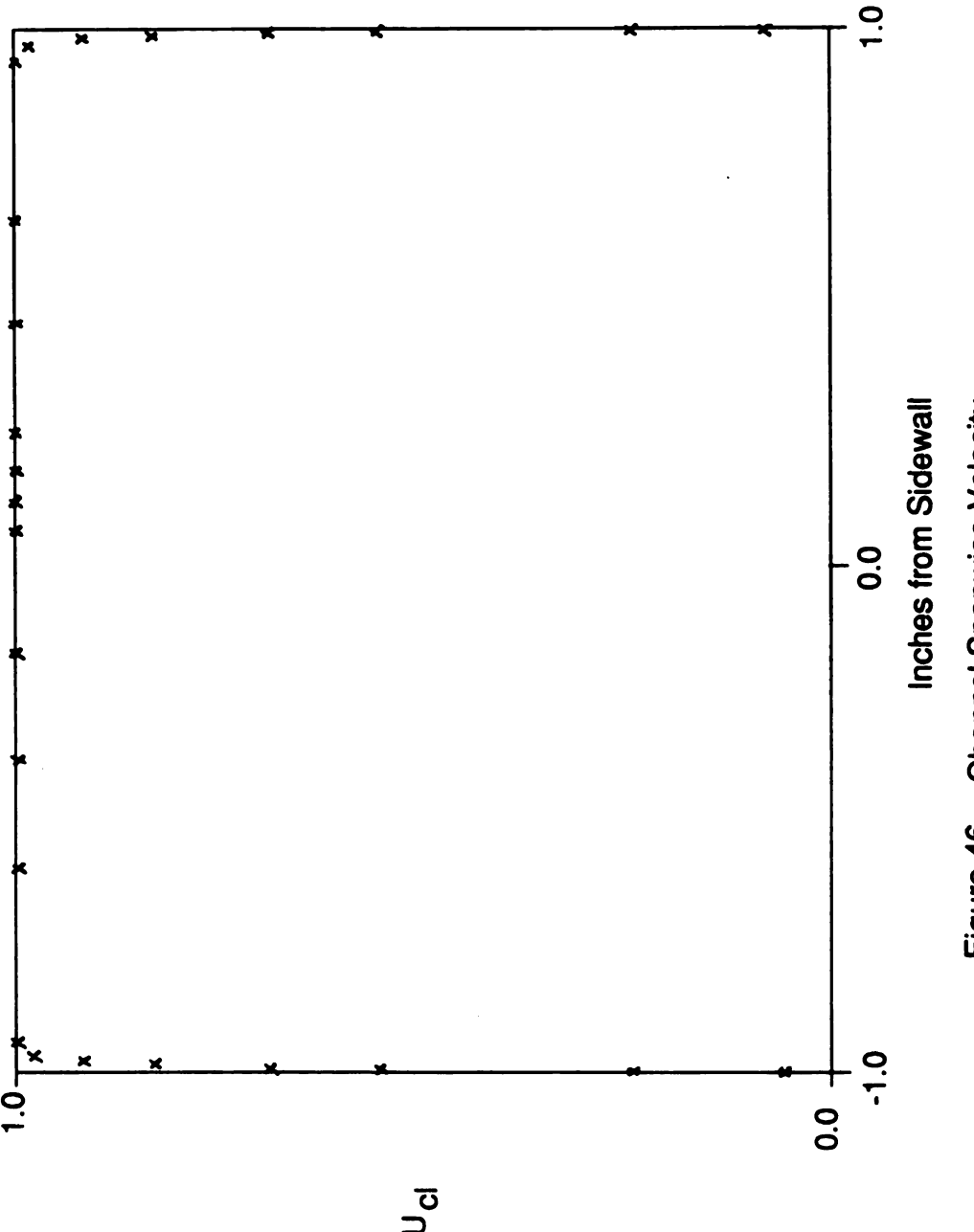
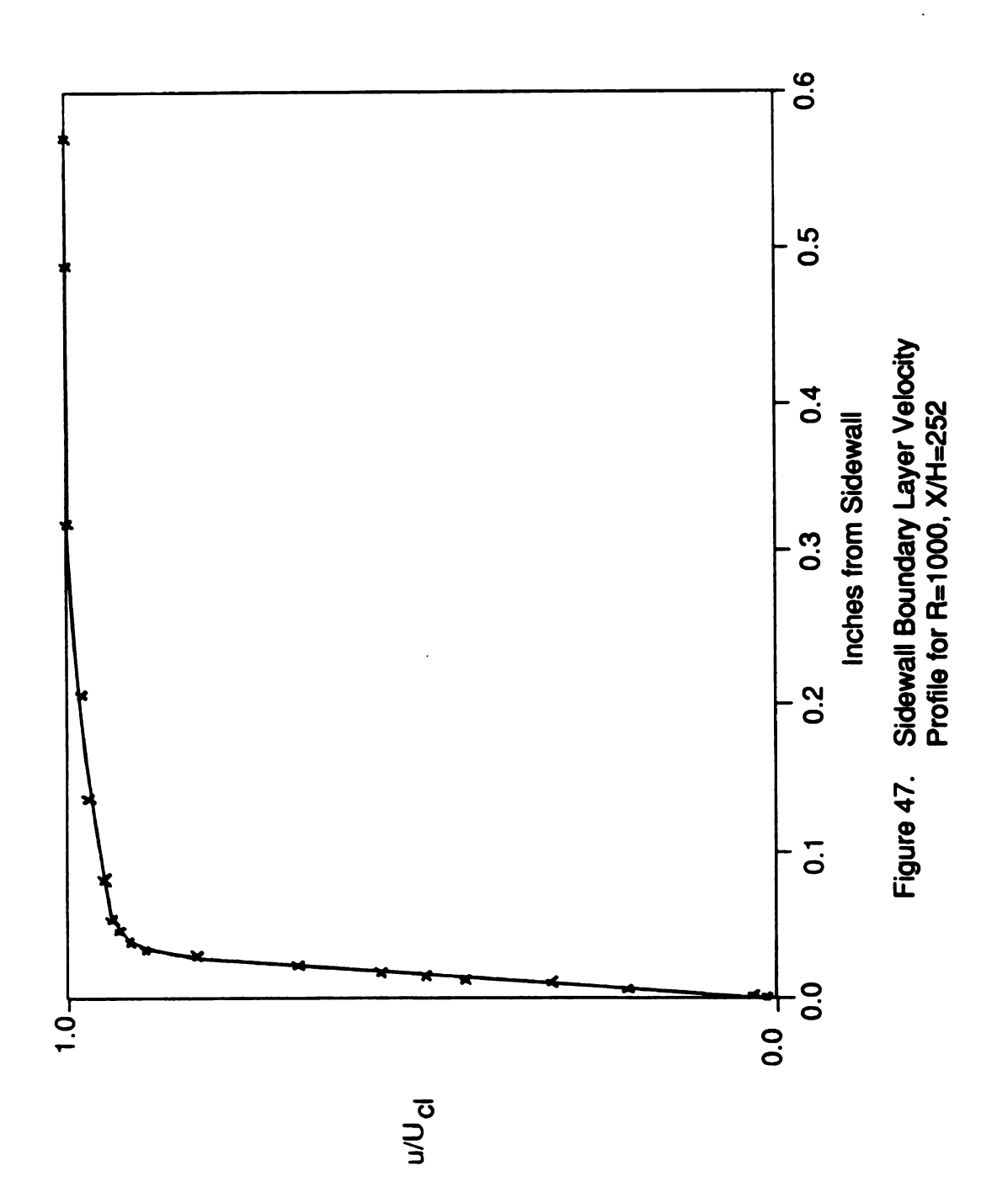
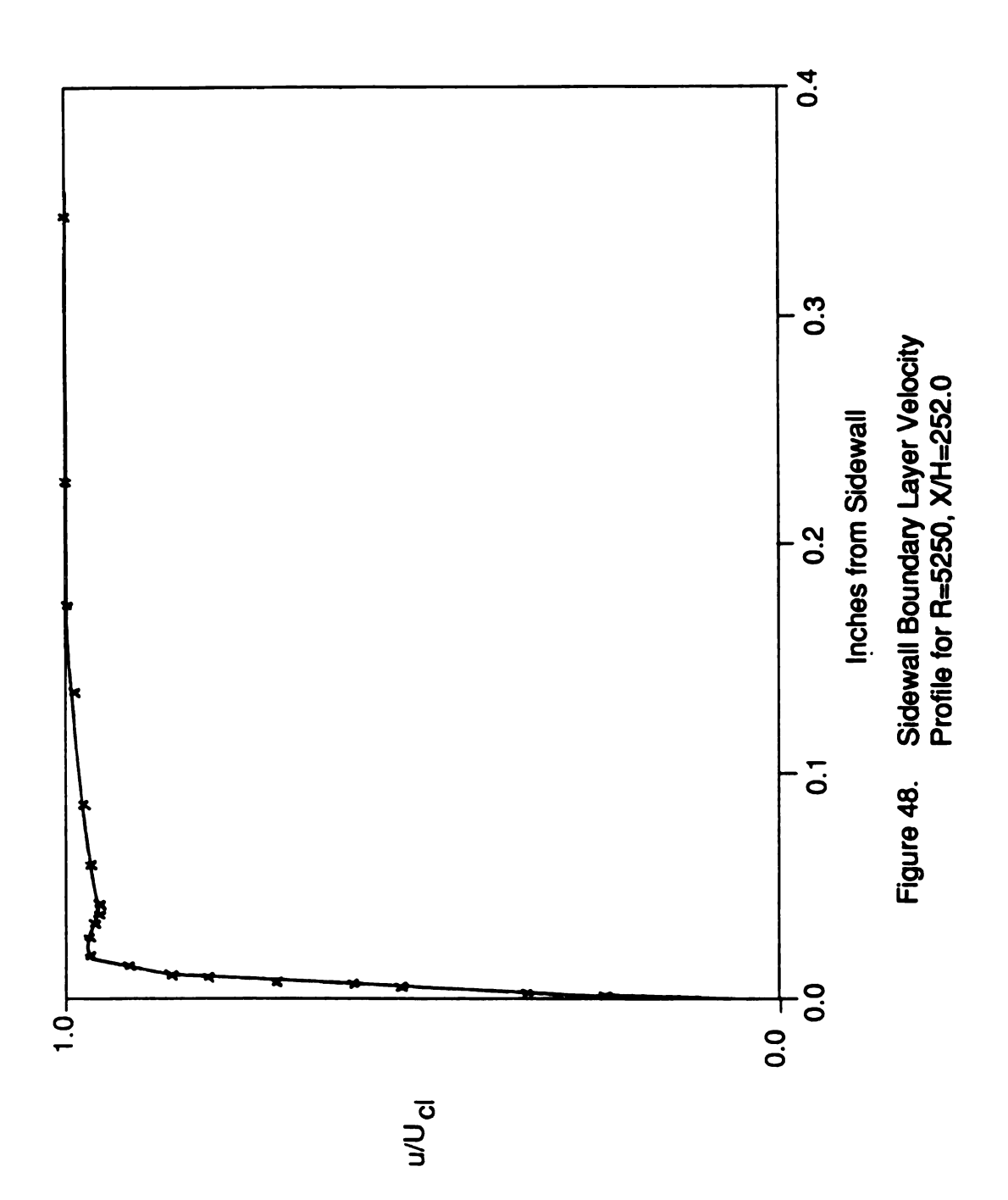
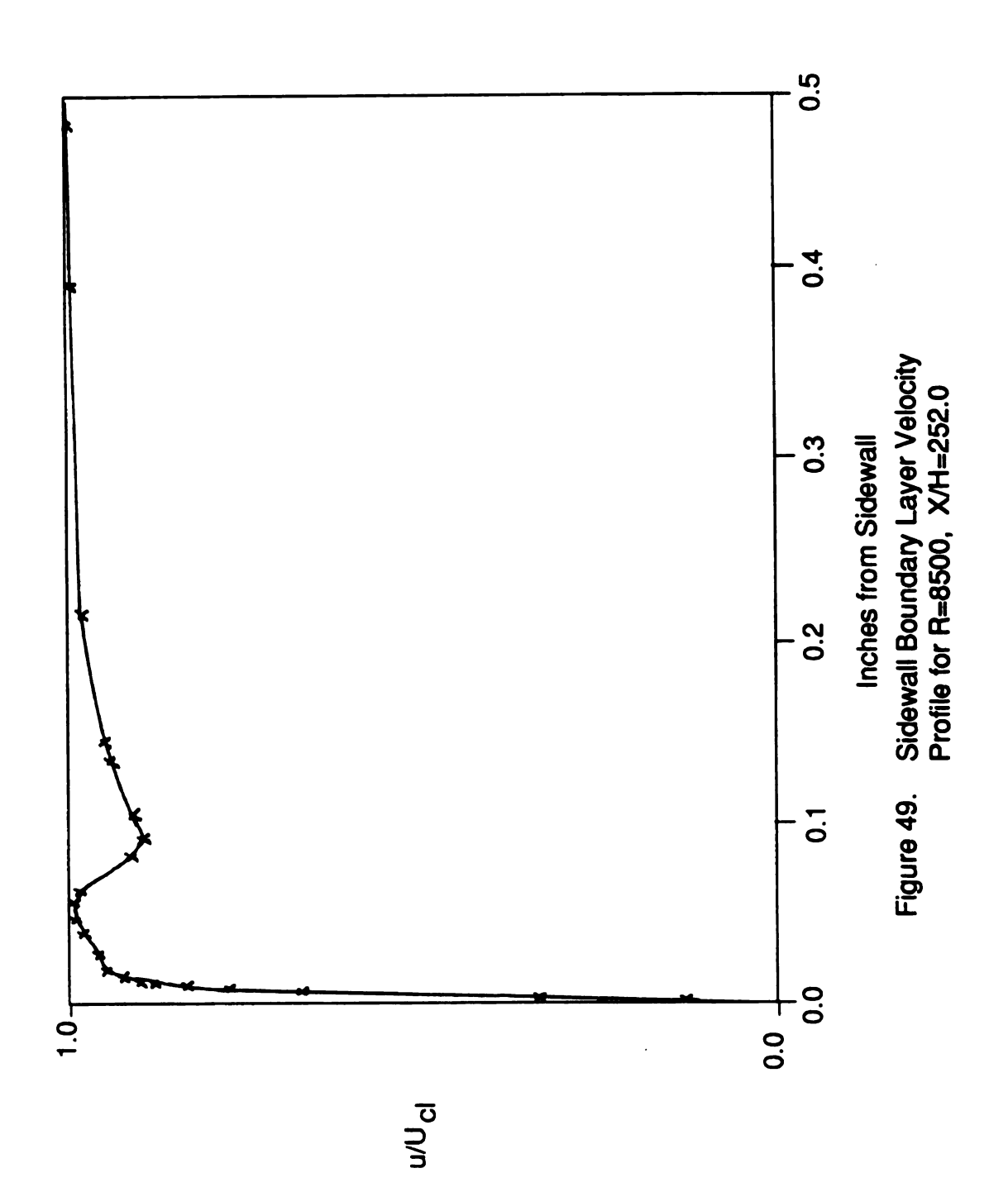
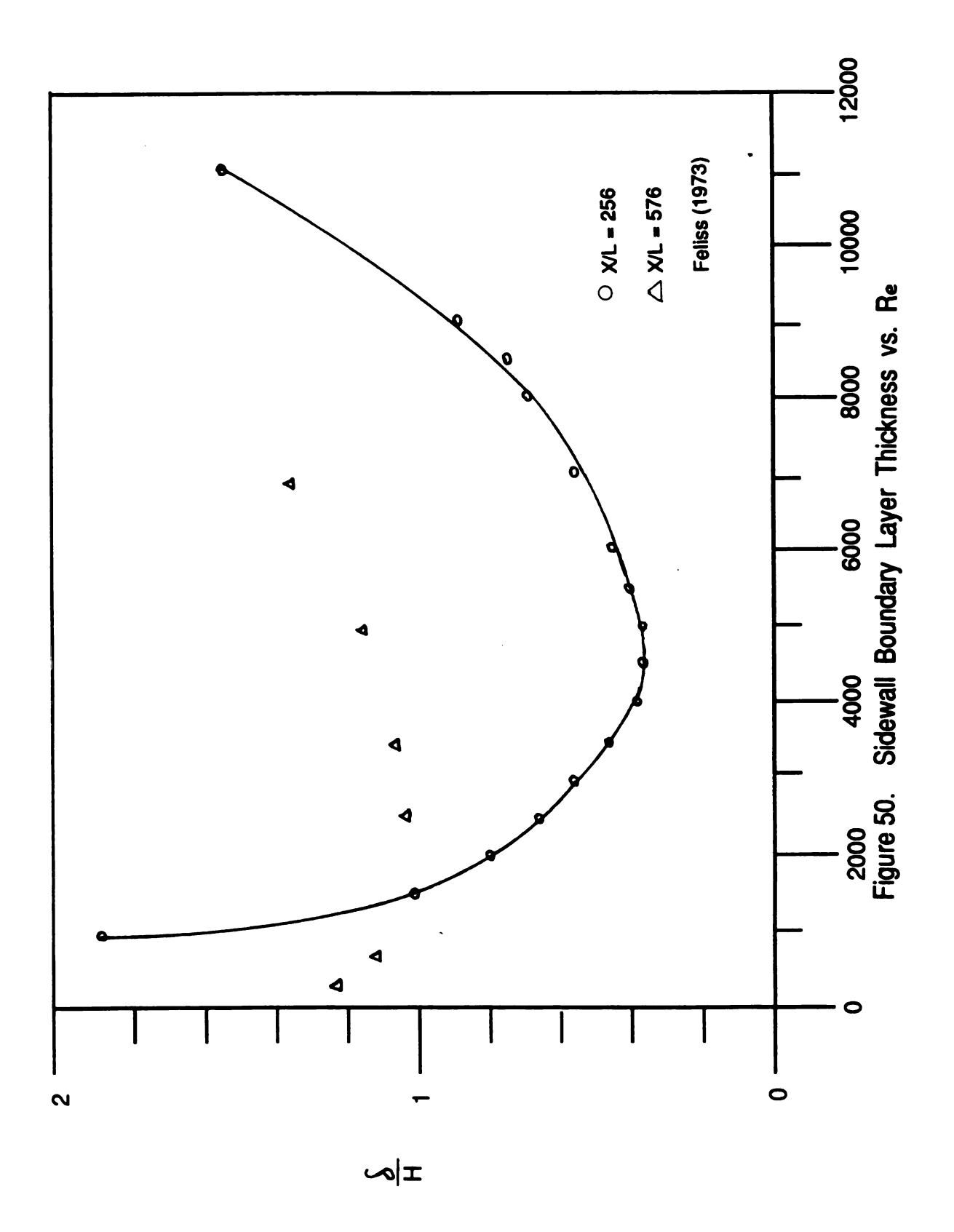


Figure 46. Channel Spanwise Velocity Profile for R=4000, X/H=262.4









MICHIGAN STATE UNIV. LIBRARIES
31293009087671